

AFAMRL-TR-83-078

8



AD A138254

**STUDIES TO IMPROVE ENVIRONMENTAL
ASSESSMENTS OF SONIC BOOMS PRODUCED
DURING AIR COMBAT MANEUVERING**

WILLIAM J. GALLOWAY

**BOLT BERANEK AND NEWMAN INC.
21120 VANOWEN ST.
CANOGA PARK, CALIFORNIA 91303**

OCTOBER 1983

**DTIC
ELECTE
FEB 24 1984**
S D
B

Approved for public release; distribution unlimited.

FILE COPY

**AIR FORCE AEROSPACE MEDICAL RESEARCH LABORATORY
AEROSPACE MEDICAL DIVISION
AIR FORCE SYSTEMS COMMAND
WRIGHT-PATTERSON AIR FORCE BASE, OHIO 45433**

84 02 21 104

NOTICES

When US Government drawings, specifications, or other data are used for any purpose other than a definitely related Government procurement operation, the Government thereby incurs no responsibility nor any obligation whatsoever, and the fact that the Government may have formulated, furnished, or in any way supplied the said drawings, specifications, or other data, is not to be regarded by implication or otherwise, as in any manner licensing the holder or any other person or corporation, or conveying any rights or permission to manufacture, use, or sell any patented invention that may in any way be related thereto.

Please do not request copies of this report from Air Force Aerospace Medical Research Laboratory. Additional copies may be purchased from:

National Technical Information Service
5285 Port Royal Road
Springfield, Virginia 22161

Federal Government agencies and their contractors registered with Defense Technical Information Center should direct requests for copies of this report to:

Defense Technical Information Center
Cameron Station
Alexandria, Virginia 22314

TECHNICAL REVIEW AND APPROVAL

AFAMRL-TR-83-078

This report has been reviewed by the Office of Public Affairs (PA) and is releasable to the National Technical Information Service (NTIS). At NTIS, it will be available to the general public, including foreign nations.

This technical report has been reviewed and is approved for publication.

FOR THE COMMANDER



HENNING E. VON GIERKE, Dr Ing
Director
Biodynamics and Bioengineering Division
Air Force Aerospace Medical Research Laboratory

operating areas associated with Luke and Nellis Air Force Bases. *Next;*

were
In a second part of these studies, a variety of pressure-time histories produced at ground microphone positions by sonic booms produced by an F-104 in a early NASA study ~~are~~ analyzed to obtain A-weighted and C-weighted sound levels. Particular attention was paid to the difference between peak unweighted overpressure, when expressed in decibels, and frequency-weighted sound exposure levels for sonic booms near a caustic produced by focusing during accelerated maneuvers, and as lateral cutoff conditions are approached.

A

PREFACE

This research was performed for the Aerospace Medical Research Laboratory at Wright-Patterson Air Force Base, Ohio, under Project/Task 723107, Technology to Define and Assess Environmental Quality of Noise From Air Force Operations. Technical monitor for this effort was Mr. Jerry D. Speakman of the Biodynamic Environment Branch, Biodynamics and Bioengineering-Division.

Acquisition of the flight data from range instrumentation was supervised by John F. Mills. Computer programs to process the flight data into usable form for this study were prepared by Richard D. Horonjeff, as he described in Appendix B. Analysis programs to obtain weighted sound levels from pressure-time traces of sonic booms were prepared by Michael P. Bucka, as he described in Appendix C. This work was performed under the overall contract technical direction of Dwight E. Bishop.

| | |
|------------------------------|-------------------------------------|
| Accession For | |
| NTIS GRA&I | <input checked="" type="checkbox"/> |
| DTIC TAB | <input type="checkbox"/> |
| Unannounced Justification | <input type="checkbox"/> |
| By _____ | |
| Distribution/ | |
| Availability Codes | |
| Dist | Avail and/or Special |
| A-1 | |



TABLE OF CONTENTS

| | | <u>Page</u> |
|-----|--|-------------|
| 1.0 | INTRODUCTION | 1 |
| | 1.1 Air Combat Maneuvering | 1 |
| | 1.2 Sound Exposure Levels for Sonic Booms | 3 |
| 2.0 | SUPERSONIC FLIGHT DATA OBTAINED FROM AIR COMBAT MANEUVERING INSTRUMENTATION | 7 |
| | 2.1 Air Combat Maneuvering Instrumentation (ACMI) | 7 |
| | 2.2 Construction of Flight Paths and Flight Parameter Statistics from ACMI Data | 7 |
| | 2.3 Data from Luke Air Force Base | 10 |
| | 2.4 Data from Nellis Air Force Base | 12 |
| 3.0 | RELATIONS BETWEEN PEAK OVERPRESSURE AND SOUND EXPOSURE LEVELS FOR SONIC BOOMS | 45 |
| | 3.1 Summary of Test Conditions | 45 |
| | 3.2 Nominal N-Waves | 47 |
| | 3.3 Focus Booms | 50 |
| | 3.4 Booms near Lateral Cutoff | 58 |
| 4.0 | IMPROVED MODELS FOR ASSESSING ENVIRONMENTAL IMPACT OF SONIC BOOMS PRODUCED DURING AIR COMBAT MANEUVERING | 70 |
| | 4.1 Sonic Boom Magnitudes | 71 |
| | 4.2 Fractions of Flight Time When Sonic Booms are Generated | 73 |
| | 4.3 Spatial Distribution of Sonic Booms | 73 |
| | 4.3.1 Rms Area and Sound Exposure Levels for Sonic Boom Carpets | 73 |
| | 4.3.2 Spatial Distribution of Flight Tracks | 75 |
| | 4.3.3 Spatial Distribution of Sonic Booms | 82 |

TABLE OF CONTENTS (continued)

| | <u>Page</u> |
|--|-------------|
| 4.3.4 Long-Term Average Sound Exposure Level | 86 |
| 4.3.5 Long-Term Average Sound Level | 86 |
| 4.3.6 Comparison to Previous Model | 87 |
| 5.0 RECOMMENDATIONS FOR FURTHER RESEARCH | 90 |
| 5.1 Operational Characteristics of ACM | 90 |
| 5.2 Sound Exposure Level Conversions | 91 |
| 5.3 Validation of Models | 91 |
| REFERENCES | 93 |
| APPENDIX A PREDICTION OF SONIC BOOM CHARACTERISTICS | |
| APPENDIX B AIRCRAFT FLIGHT DATA HANDLING AND ANALYSIS | |
| APPENDIX C PROCEDURES FOR OBTAINING SPECTRAL ANALYSIS OF SONIC BOOM PRESSURE-TIME TRACES | |
| APPENDIX D SUMMARY OF ANALYSES OF AIR COMBAT MANEUVERING INSTRUMENTATION DATA | |

LIST OF TABLES

| <u>Number</u> | | <u>Page</u> |
|---------------|--|-------------|
| 2.1 | Supersonic Flight Parameters and Sonic Boom Measures Sorted for Statistical Evaluation | 9 |
| 2.2 | Summary of 778 Supersonic Sorties from Luke AFB ACMI Data | 13 |
| 2.3 | Summary of 15 Supersonic Sorties from Nellis AFB ACMI Data | 14 |
| 3.1 | Summary of Representative Booms Analyzed | 47 |
| 3.2 | Sound Levels in Decibels Measured at Ground Positions for Nominal N-Wave - Pass 040, Ref. 6 . . . | 49 |
| 3.3 | Sound Levels in Decibels Measured at Ground Positions Down Track from a Caustic-Ground Intercept Pass 043, Ref. 6 | 53 |
| 3.4 | Sound Levels in Decibels Measured at Ground Positions on Which a Caustic-Ground Intercept is Superposed - Pass 045, Ref. 6 | 56 |
| 3.5 | Sound Levels in Decibels at Ground Positions on Which a Caustic-Ground Intercept is Superposed - Pass 046, Ref. 6 | 59 |
| 3.6 | Sound Levels in Decibels Measured at Ground Positions Just Prior to Lateral Cutoff Pass 029, Ref. 6 | 62 |
| 3.7 | Sound Levels in Decibels Measured at Ground Positions Near Lateral Cutoff Pass 030, Ref. 6 . . . | 65 |
| 3.8 | Sound Levels in Decibels Measured at Ground Positions Near Lateral Cutoff Pass 033, Ref. 6 . . . | 68 |
| 3.9 | Sound Levels in Decibels Measured at Ground Positions Near Lateral Cutoff Pass 035, Ref. 6 . . . | 69 |
| 4.1 | Parameters for Supersonic Flight That Represent RMS Values of Distributions | 72 |
| 4.2 | Dimensions of Ellipses Enclosing Specified Cumulative Fractions of Flight Tracks - All Aircraft Where $M > M_c$, Luke AFB | 79 |
| 4.3 | Dimensions of Ellipses Used to Determine Average Sound Level for Air Combat Maneuvering | 84 |

LIST OF FIGURES

| <u>Number</u> | | <u>Page</u> |
|---------------|--|-------------|
| 1.1 | Relation between Peak Sound Pressure Level and A-Weighted Sound Exposure Level for Sonic Booms with N-Durations of the Order of 100 ms (Young, 1975) . . | 5 |
| 2.1 | Flight Tracks for All Airplanes Exceeding Mach 1.0 Luke AFB | 15 |
| 2.2 | Flight Tracks for All Airplanes where $M > M_c$ Luke AFB | 16 |
| 2.3 | Flight Tracks for F-4 Airplanes Exceeding Mach 1.0 Luke AFB | 17 |
| 2.4 | Flight Tracks for F-4 Airplanes where $M > M_c$ Luke AFB | 18 |
| 2.5 | Flight Tracks for F-5 Airplanes Exceeding Mach 1.0 Luke AFB | 19 |
| 2.6 | Flight Tracks for F-5 Airplanes where $M > M_c$ Luke AFB | 20 |
| 2.7 | Flight Tracks for F-15 Airplanes Exceeding Mach 1.0 Luke AFB | 21 |
| 2.8 | Flight Tracks for F-15 Airplanes where $M > M_c$ Luke AFB | 22 |
| 2.9 | Flight Tracks for F-16 Airplanes Exceeding Mach 1.0 Luke AFB | 23 |
| 2.10 | Flight Tracks for F-16 Airplanes where $M > M_c$ Luke AFB | 24 |
| 2.11 | Height Distributions for 46 F-4 Supersonic Events - Determined at One-Second Intervals - Total Time 2291 Seconds - Luke AFB | 25 |
| 2.12 | Mach Number Distribution for F-4 Airplanes where $M > M_c$ - Luke AFB | 26 |
| 2.13 | Distribution of Peak Overpressures and C-Weighted Sound Exposure Levels Predicted for F-4 Airplanes where $M > M_c$ - Luke AFB | 27 |

LIST OF FIGURES (continued)

| <u>Number</u> | <u>Page</u> |
|--|-------------|
| 2.14 Height Distributions for 47 F-5 Supersonic Events - Determined at One-Second Intervals - Total Time 1204 Seconds - Luke AFB | 28 |
| 2.15 Mach Number Distribution for F-5 Airplanes where $M > M_c$ - Luke AFB | 29 |
| 2.16 Distribution of Peak Overpressures and C-Weighted Sound Exposure Levels Predicted for F-5 Airplanes where $M > M_c$ - Luke AFB | 30 |
| 2.17 Height Distributions for 133 F-15 Supersonic Events - Determined at One-Second Intervals - Total Time 4117 Seconds - Luke AFB | 31 |
| 2.18 Mach Number Distribution for F-15 Airplanes where $M > M_c$ - Luke AFB | 32 |
| 2.19 Distribution of Peak Overpressures and C-Weighted Sound Exposure Levels Predicted for F-15 Airplanes where $M > M_c$ - Luke AFB | 33 |
| 2.20 Height Distributions for 25 F-16 Supersonic Events - Determined at One-Second Intervals - Total Time 1151 Seconds - Luke AFB | 34 |
| 2.21 Mach Number Distribution for F-16 Airplanes where $M > M_c$ - Luke AFB | 35 |
| 2.22 Distribution of Peak Overpressures and C-Weighted Sound Exposure Levels Predicted for F-16 Airplanes where $M > M_c$ - Luke AFB | 36 |
| 2.23 Flight Tracks for All Airplanes Exceeding Mach 1.0 Nellis AFB | 37 |
| 2.24 Flight Tracks for All Airplanes where $M > M_c$ Nellis AFB | 38 |
| 2.25 Flight Tracks for F-4 Airplanes Exceeding Mach 1.0 Nellis AFB | 39 |
| 2.26 Flight Tracks for F-4 Airplanes where $M > M_c$ Nellis AFB | 40 |

LIST OF FIGURES (continued)

| <u>Number</u> | <u>Page</u> |
|--|-------------|
| 2.27 Flight Tracks for F-15 Airplanes Exceeding Mach 1.0 Nellis AFB | 41 |
| 2.28 Flight Tracks for F-15 Airplanes where $M > M_c$ Nellis AFB | 42 |
| 2.29 Flight Tracks for F-16 Airplanes Exceeding Mach 1.0 Nellis AFB | 43 |
| 2.30 Flight Tracks for F-16 Airplanes where $M > M_c$ Nellis AFB | 44 |
| 3.1 Ground Pressure Signatures Downtrack from Caustic-Ground Intersection - Pass 040, August 28, 1-3 - Ref. 4 | 48 |
| 3.2 Ground Pressure Signatures Just Downtrack of Caustic-Ground Intersection - Pass 043, August 28, 2-3 - Ref. 6 | 52 |
| 3.3 Ground Pressure Signatures near Caustic-Ground Intersection - Pass 045, August 28, 3-2 - Ref. 6 | 54 |
| 3.4 Ground Pressure Signatures near Caustic-Ground Intersection - Pass 046, August 28, 3-3 - Ref. 6 | 57 |
| 3.5 Ground Pressure Signatures before Lateral Cutoff - Pass 029, August 27, 1-1 - Ref. 6 | 61 |
| 3.6 Ground Pressure Signatures near Lateral Cutoff - Pass 030, August 27, 1-2 - Ref. 6 | 64 |
| 3.7 Ground Pressure Signatures near Lateral Cutoff - Pass 033, August 27, 2-2 - Ref. 6 | 66 |
| 3.8 Ground Pressure Signatures near Lateral Cutoff - Pass 035, August 27, 3-1 - Ref. 6 | 67 |

LIST OF FIGURES (continued)

| <u>Number</u> | | <u>Page</u> |
|---------------|--|-------------|
| 4.1 | Number of Seconds of Flight within 4 x 4 Mile Cells - All Aircraft where $M > M_c$ - Luke AFB | 77 |
| 4.2 | Spatial Density Distributions of Flight Tracks for All Aircraft where $M > M_c$ - Luke AFB | 80 |
| 4.3 | Area Enclosing Specified Percent of Flight Tracks for All Aircraft where $M > M_c$ - Luke AFB | 81 |
| 4.4 | Distribution of Regions where Booms Could Occur with Equal Probability to be Anywhere within an Annular Area | 83 |
| 4.5 | Template for Calculating Sound Exposure Level Contours, Luke AFB | 85 |

**STUDIES TO IMPROVE ENVIRONMENTAL
ASSESSMENTS OF SONIC BOOMS PRODUCED
DURING AIR COMBAT MANEUVERING**

1.0 INTRODUCTION

1.1 Air Combat Maneuvering

Modern fighter airplanes are designed to achieve their greatest tactical utility by using supersonic flight during portions of airplane-to-airplane combat. Pilots training to fly such airplanes, and trained pilots flying to maintain combat proficiency, must be able to operate supersonically at altitudes of less than 30,000 feet if they are to reach or maintain combat proficiency requirements. Supersonic flight over land at altitudes below 30,000 feet, in general, requires an environmental assessment before USAF approval.

Air combat maneuvering by one or more airplanes engaged against one or more opposing airplanes takes place within an airspace having the approximate shape of a right elliptical cylinder. The sides of the cylinder extend from the lowest height above terrain authorized for that particular airspace, up to a height of the order of 50,000 feet MSL. Airplanes maneuvering within this airspace can be at any point, at any time, at any airspeed within the airplane's operating envelope. They will typically be supersonic at higher altitudes on initial target acquisition, slow to subsonic conditions during combat maneuvering, then, after simulated weapon release, may make another supersonic dash for disengagement, starting from a lower altitude.

A simple statistical model, based on relatively limited aircraft data, has been developed for assessing environmental impact from supersonic air combat maneuvering [1]. This model

was derived from data obtained by personnel from the Environmental Planning Division, Headquarters, Tactical Air Command, from the Air Combat Maneuvering instrumentation (ACMI) installation at Langley AFB which is associated with the offshore Oceana Military Operating Area. Data were obtained from 21 sorties of F-15 airplanes, during which 56 supersonic flight segments occurred. The data consisted of hand traced flight tracks (horizontal projections to the ground of actual flight paths), with an average height and average Mach number assigned to each supersonic flight segment.

Use of the Oceana ACMI data provided a major first step towards understanding those aspects of supersonic flight during air combat maneuvering that are important for environmental assessments. The limited set of data, however, raises a number of questions regarding its generality for extrapolation to other locations or airplane types. Do the same statistical descriptions of flight parameters such as Mach number, altitude, fraction of total time supersonic, and fraction of time above cutoff Mach number apply to F-15 operations at another location, let alone to other airplane types? How important is it to know pitch angle during a flight, since booms produced when an airplane is in a dive are much stronger at the same Mach number, than when in a climb? Is the spatial distribution of flight tracks observed at Oceana applicable elsewhere?

Section 2 of this report summarizes studies directed at improving the F-15 data base on the statistics of supersonic flight during air combat maneuvering, and extension of the data base to include F-4, F-5, and F-16 airplanes. These data were extracted from ACMI installations at Nellis AFB and Luke AFB.

Section 4 uses the results of the ACMI data studies to refine the sonic boom prediction model of Reference 1.

1.2 Sound Exposure Levels for Sonic Booms

Historically, the magnitudes of sonic booms have been expressed largely in terms of peak overpressures, Δp , or in terms of the time integral of overpressure during the positive phase of the boom, called the positive impulse, I_0 . These quantities are generally used in assessing the effect of a boom on building structures. In order to assess the effects of sonic booms on people various sound levels in decibels are of more utility [2]. Three such measures are of use: peak flat sound pressure level, C-weighted sound exposure level, and A-weighted sound exposure level. Although elaborate and detailed models and computer programs exist to predict the idealized pressure-time signatures of a sonic boom produced by any particular airplane, none exist to predict sound exposure levels directly. Sound exposure levels must therefore be obtained by conversion from overpressures or other sonic boom parameters.

Peak flat sound pressure level, abbreviated as PKT, symbolized as L_{pk} , is the magnitude of the peak overpressure stated in terms of sound pressure level in decibels. It may be calculated as:

$$L_{pk} = 10 \log_{10} (\Delta p)^2 + 127.6 \quad (1.1)$$

where Δp is expressed in pounds per square foot (psf).

C-weighted sound exposure level, abbreviated as CSEL, symbolized as L_{CE} , is recommended in Reference 2 and used by various Department of Defense agencies for describing the effect of individual sonic booms on human response. C-weighted sound exposure level is the time integral over the duration of the boom of C-weighted, squared sound pressure, expressed in decibels. C-weighting is a standardized frequency weighting specified for sound level meters [3].

Schomer [4] has analyzed tape recorded sonic booms from four F-104, four B-58, and three XB-70 overflights. Peak overpressures varied between 0.91 and 3.24 psf, or peak sound pressure levels between 126.8 and 137.8 decibels. Tabulation of the differences between peak overpressure in decibels and CSEL shows that CSEL averages 26.2 decibels lower than peak overpressure sound level, with a standard deviation of 1.5 decibels. The range of differences over the set of data reported by Schomer is 23.9 to 27.7 decibels.

A-weighted sound exposure level, abbreviated as ASEL and symbolized as L_{AE} , is the preferred measure for describing the magnitude of non-impulsive sounds as produced, for example, by the flyover of a subsonic airplane. Analogous to C-weighted sound exposure level, A-weighted sound exposure level is the time integral over the duration of an event of the A-weighted, squared sound pressure expressed in decibels, where A-weighting is a frequency weighting standardized in Ref. 3. A-weighting significantly suppresses low frequencies which contain the predominant energy in a sonic boom, placing more emphasis on mid and high frequencies that are significant for human audibility.

Young [5] provides the only reported data on the difference between peak flat sound pressure level and A-weighted sound exposure level. He analyzed 15 sonic booms having peak overpressures from approximately 0.4 to 6.6 psf, or 120 to 144 decibels. The difference between peak flat sound pressure level and A-weighted sound exposure level varies monotonically but not linearly from about 45 decibels for the lowest overpressures to about 32 decibels at the higher overpressures. A conversion chart based on Young's data is provided in Figure 1. We have fit an analytic expression to Young's data to obtain the following equation:

$$L_{AE} = 188.7 \ln L_{pk} - 825.6 \quad (1.2)$$

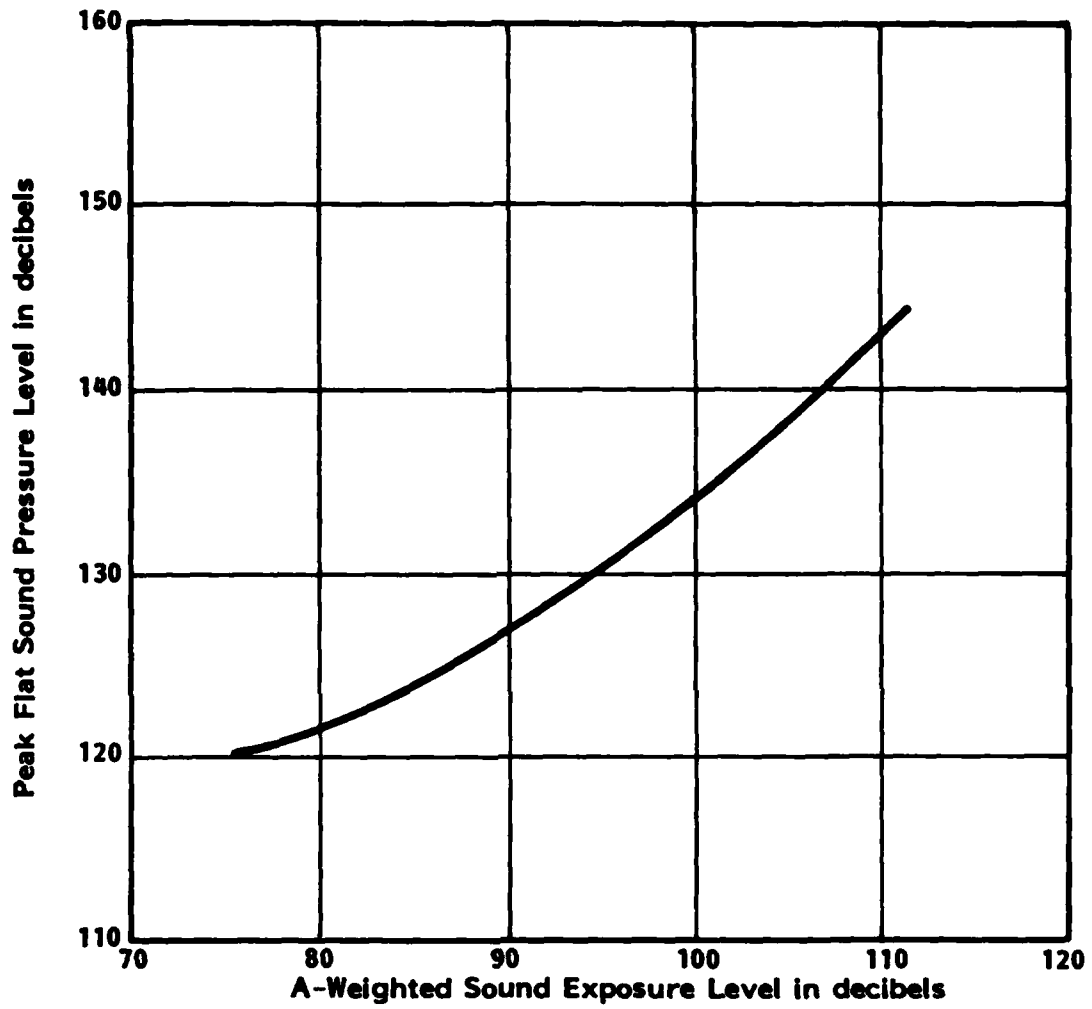


FIGURE 1.1 RELATION BETWEEN PEAK SOUND PRESSURE LEVEL AND A-WEIGHTED SOUND EXPOSURE LEVEL FOR SONIC BOOMS WITH N-DURATIONS OF THE ORDER OF 100 MS (YOUNG, 1975)

It is worth noting that Young reported that the computed difference between peak flat sound pressure level and A-weighted sound exposure level for an N-wave having a 3ms rise time and 100 ms duration is 50 decibels. The observed differences of between 45 and 32 decibels imply that distortion of the boom pressure-time signature greatly influences this difference in an unpredictable fashion.

In addition to the limited extent of both Schomer's and Young's data, nothing is known about the differences between sound exposure levels and boom pressures as the boom approaches either cutoff conditions or focusing conditions. As a boom signature departs more and more from an N-wave--that is, as high-frequency content is lost--one would expect that the differences between peak flat sound level and sound exposure level would vary substantially, at least for A-weighted sound levels. If a variety of tape recorded sonic booms were available, it would be relatively simple to evaluate the conversions. Unfortunately, of the thousands of sonic boom recordings that were made during the development studies for a supersonic transport, none seem to exist within NASA or the USAF, or at least be readily traceable.

Although the original recordings are not available, there are a number of published reports from the sonic boom programs of the 1960's and early 1970's. A variety of pressure-time signatures for various sonic boom propagation conditions are reproduced in these reports. The results of a study in which a number of these boom signatures were analyzed to obtain various sound level measures are described in Section 3 of this report. The data processing procedures by which the boom traces were digitized, spectrally analyzed by Fast Fourier procedures, and converted to weighted sound levels are described in Appendix C.

2.0 SUPERSONIC FLIGHT DATA OBTAINED FROM AIR COMBAT MANEUVERING INSTRUMENTION

2.1 Air Combat Maneuvering Instrumentation (ACMI)

A number of military training areas are equipped with instrumentation to provide real-time tracking of as many as eight airplanes engaged at one time in air combat maneuvering. One master and a number of slave receiver stations on the ground receive output signals from a transmitter on each airplane. When two or more ground stations receive signals from an airplane, the position of the airplane is tracked at a rate of 5 samples per second. The successive sets of position coordinates are used by the system's computer to obtain velocity and acceleration coordinates. The result, which is recorded on digital tape for subsequent playback in real time to pilots, is a complete picture of each airplane's flight trajectory, as well as other parameters related to weapons system functioning.

The existence of this instrumentation provides an ideal way to gather statistics on air combat maneuvering for the purpose of studying sonic boom environments. Arrangements were made in this project to examine records of ACM at Nellis Air Force Base and at Luke Air Force Base. Data were extracted from the ACMI tapes from 15 sorties, involving 30 supersonic events, at Nellis. Data from 78 sorties, involving 255 supersonic events, were obtained from Luke. Conflicting demands for range usage at Nellis, compared with the ease of access to data at Luke, led to considerably more data gathering at Luke.

2.2 Construction of Flight Paths and Flight Parameter Statistics from ACMI Data

Since the ACMI recorded data are on digital tape, in principle it would be straightforward to extract the data of interest

from the ACMI tapes. In practice, for the scope of this study, it was impractical to develop the computer programs required to perform the process. Instead, with the aid of a program flag that allowed easy identification of only the supersonic segments of each sortie, flight parameters of interest were extracted by inspection at selected times from each flight.

Rather than accumulate data for each time sample during which an airplane was supersonic, a much smaller set of samples was used. Data were extracted from the time interval where an airplane became initially supersonic, then at 0.05 increments in Mach number until a maximum was reached, at 0.05 increments as Mach number decreased, and at the point where the airplane ceased being supersonic. The number of samples thus varied from a minimum of 3 to as many as 16 per supersonic interval. Each time an airplane became supersonic during a sortie was treated as a separate supersonic event.

After visual screening of the individual data samples for internal consistency, the data were keypunched and assembled into digital files on magnetic tape. The first step in the analysis was to reconstruct the flight trajectories by linear interpolation, at one second time intervals, between successive ACMI samples. Since the initial selection of ACM samples were taken at equal Mach number intervals, rather than time intervals, the distance between actual sample points varies for each event. This variation is not considered significant for this analysis.

The reconstructed flight trajectories were used for two purposes. Drawing lines connecting each pair of x-y coordinates for the segments of each supersonic flight provides the projection to the ground of each flight path, i.e. the flight track. The set of these flight paths yields the geographic distribution of flights.

The second use of the data was to develop frequency distribution functions of various parameters such as altitude, Mach number, cutoff* Mach number, predicted sonic boom overpressure, and predicted value of various sound level measures. The various calculated quantities were first obtained for each one-second time interval using the computational procedures described in Appendix A, derived from a sonic boom model by Carlson [6]. These data were then sorted into the number of seconds that a specified parameter fell within a given increment of that parameter, summing all operations by airplanes of the same type. Data were included only for those samples where Mach number exceeded cutoff, i.e. that a boom would be expected to have been produced on the ground. Table 2.1 lists the parameters of interest, and the cell size (increment) used in sorting the data. The sorted data are listed in Appendix D.

Table 2.1

Supersonic Flight Parameters and Sonic Boom
Measures Sorted For Statistical Evaluation

| <u>Parameter</u> | <u>Cell Size</u> |
|---|------------------|
| x,y coordinates--feet from range center | 5280 feet |
| z coordinate--feet above MSL | 1000 feet |
| Effective height--feet | 1000 feet |
| Mach number | 0.02 |
| Cutoff Mach number | 0.02 |
| Effective Mach number | 0.02 |
| Overpressure - psf | 0.25 |
| Peak flat sound level - dB | 0.5 dB |
| C-weighted sound exposure level - dB | 0.5 dB |
| A-weighted sound exposure level - dB | 0.5 dB |

*See Appendix A for definitions and computational procedures for various sonic boom parameters.

2.3 Data From Luke Air Force Base

The 78 sorties examined at Luke were composed of the following operations:

| <u>Airplane</u> | <u>No. of Sorties</u> | <u>No. of Events</u> | <u>Flight Time - Seconds</u> | |
|-----------------|---------------------------|--------------------------|------------------------------|-----------------------------|
| | | | <u>M > 1</u> | <u>M > M_c</u> |
| F-4 | 8 | 46 | 2291 | 1237 |
| F-5 | 20 | 47 | 1204 | 368 |
| F-14 | 3 | 4 | 52 | 18 |
| F-15 | 41 | 133 | 4117 | 1048 |
| F-16 | 6 | 25 | 1151 | 170 |
| Total | 78 | 255 | 8815 | 2841 |

Flight tracks for these operations are shown in Figures 2.1 to 2.10. Flight paths for all airplanes in supersonic flight, regardless of type, are shown in Figure 2.1. The tracks produced only when cutoff Mach number was exceeded are shown in Figure 2.2. Successive figures show the same pair of conditions, by type, for F-4, F-5, F-15, and F-16 airplanes. The sample size for the F-14 was too small to be worth reproducing.

It is worth noting that the predominant direction of the flight paths, turns and crossed paths notwithstanding, is along a northwesterly-southeasterly direction. This alignment is the general direction of the Mohawk and Growler mountain ranges that lie more or less on each side of the active flight area, providing strong visual cues for orientation.

For a specified airplane type, Mach number, altitude, pitch angle, and ground elevation uniquely determine sonic boom overpressures and durations in Carlson's model (at least for a perfectly quiescent, standard atmosphere). Descriptions of the

statistical distributions of these parameters are thus fundamental to the development of models for predicting sonic boom environments produced during air combat maneuvering. The aggregated data obtained from the ACMI system, sorted as described above, provides the bases for such statistical descriptions.

Figures 2.11 to 2.22 provide frequency polygons for altitude, effective height, Mach number, predicted overpressure, and predicted CSEL for F-4, F-5, F-15, and F-16 airplanes. Effective height (see Appendix A) is that height above ground at which an airplane not in level flight will produce a boom of the same overpressure as an airplane in level flight at the same Mach number and same actual altitude. Airplanes having positive pitch angles, i.e., in a climb, have effective heights greater than their actual heights above ground; airplanes in a dive have effective heights less than their actual heights above ground.

Although the figures are largely self-explanatory, several general features may be observed. The effective height distribution peaks at lower heights than the actual height above ground, in all cases, indicating that the airplane is most likely to be in a shallow dive when it is supersonic. While there are usually several peaks in the altitude distributions, the predominant occurrences are usually at altitudes below 15,000 feet (except for the F-16's). The predominant Mach numbers are all at low supersonic values, comparable in many cases to cutoff Mach numbers at moderately low altitudes. The broad distribution of heights results in a range of approximately 20 decibels in CSEL.

A number of numerical values for use in developing incremental noise models can be extracted from the ACMI data. Those considered of interest to the author are listed in Table 2.2. Although most of the quantities are obvious, attention is called to the root-mean-square (rms) values for certain items-- Mach number, CSEL, and derivation of supersonic events. These values

are used in Section 4 of this report to specify statistical models for predicting mean-square sound levels and C-weighted day-night average sound levels. For example, the mean-square (or "energy") average CSEL for the distribution of operations by a specified airplane type can be calculated from an rms value of Mach number and single values of altitude and effective height.

2.4 Data From Nellis Air Force Base

The more limited data obtained at Nellis AFB may be treated in the same manner as above. Flight tracks are shown in Figures 2.23 to 2.30, for all aircraft together, and then separately for F-4, F-15, and F-16. Again separate figures show the tracks whenever supersonic, and then only for the portion where Mach number was above cutoff.

Frequency polygons for altitude, effective height, overpressure and CSEL have the same general characteristics as those from the Luke data, and are not repeated here. Parallel to the Luke analyses, various quantities of use in constructing environmental noise measures are summarized for each airplane type in Table 2.3.

In comparing the Luke and Nellis data one should be aware that the average ground elevation is 750 feet above mean sea level at the Luke range, and 4000 feet at the Nellis range.

Table 2.2
Summary of 78 Supersonic Sorties
from Luke AFB ACMI Data

| | | F-4 | F-5 | F-14 | F-15 | F-16 |
|--|----------|--------|--------|-------|--------|--------|
| No. of sorties | | 8 | 20 | 3 | 41 | 6 |
| No. of supersonic events per sortie | avg. | 5.8 | 2.3 | 1.3 | 3.2 | 4.2 |
| | std.dev. | 2.5 | 1.5 | 1.0 | 2.3 | 2.5 |
| Duration on range per sortie - min. | avg. | 21.6 | 32.6 | 31.7 | 28.5 | 19.5 |
| | std.dev. | 5.7 | 7.6 | | 9.3 | 10.1 |
| Fraction of duration while supersonic | avg. | 0.251 | 0.036 | 0.021 | 0.067 | 0.121 |
| | std.dev. | 0.075 | 0.027 | | 0.046 | 0.078 |
| Fraction of range duration where $M > M_c$ | avg. | 0.134 | 0.011 | 0.008 | 0.017 | 0.018 |
| | std.dev. | 0.044 | 0.008 | | 0.012 | 0.011 |
| Fraction of supersonic where $M > M_c$ | | 0.540 | 0.308 | 0.346 | 0.255 | 0.146 |
| Duration of Supersonic events - sec. | avg. | 56.5 | 33.0 | 23.8 | 32.6 | 43.1 |
| | rms | 71.7 | 42.9 | 28.5 | 44.8 | 52.9 |
| | std.dev. | 44.6 | 27.7 | 18.1 | 30.6 | 31.2 |
| Rms Mach no. | | 1.110 | 1.090 | 1.04 | 1.090 | 1.212 |
| Effective height-ft. | | 17,000 | 10,750 | 2,500 | 11,750 | 27,000 |
| Altitude, MSL - ft. | | 18,500 | 15,000 | 8,000 | 14,500 | 30,000 |
| Rms CSEL - dB | | 111.0 | 111.8 | 124.9 | 114.7 | 105.4 |
| $d_{y,c}$ - 1000 ft. | | 22.1 | 18.3 | 6.7 | 18.7 | 43.4 |
| Overpressure - psf | median | 2.9 | 3.1 | 14.5 | 3.5 | 1.3 |
| | 10% | 3.6 | 6.3 | 16.2 | 6.2 | 1.7 |
| | 1% | 5.5 | 6.9 | 17.0 | 8.7 | 3.9 |
| | max. | 9.3 | 7.1 | 17.1 | 10.1 | 4.1 |

Average ground elevation: 750 ft. above MSL

Table. 2.3

Summary of 15 Supersonic Sorties
from Nellis AFB ACMI Data

| | | F-4 | F-15 | F-16 |
|---|----------|--------|--------|--------|
| No. of Sorties | | 6 | 6 | 6 |
| No. of supersonic events per sortie | avg. | 1.7 | 3.0 | 1.8 |
| | std.dev. | 0.9 | 2.0 | 0.8 |
| Duration on range per sortie - min. | avg. | 22.0 | 28.5 | 20.0 |
| Fraction supersonic | avg. | 0.063 | 0.022 | 0.034 |
| | std.dev. | 0.047 | 0.021 | 0.028 |
| Fraction of sortie duration where $M > M_c$ | avg. | 0.036 | 0.006 | 0.021 |
| | dev. | 0.033 | 0.006 | 0.612 |
| Duration of supersonic events - sec. | mean | 44.5 | 37.0 | 22.0 |
| | rms | 62.2 | 50.2 | 31.2 |
| | std.dev. | 45.7 | 36.0 | 23.2 |
| Rms Mach No. | | 1.088 | 1.167 | 1.181 |
| Effective height - ft. | | 9,000 | 15,000 | 9,500 |
| Altitude - MSL - ft. | | 13,000 | 19,500 | 16,000 |
| Rms CSEL - dB | | 115.7 | 112.4 | 114.2 |
| $d_{y,c}$ - 1000 ft. | | 13.8 | 29.3 | 28.7 |
| Overpressure - psf | median | 5.1 | 3.3 | 3.7 |
| | 10% | 6.2 | 5.0 | 5.9 |
| | 1% | 7.3 | 5.4 | 12.6 |
| | max. | 7.9 | 5.4 | 13.1 |

Average ground elevation: 4000 ft. above MSL



Scale: 1:500,000

**FIGURE 2.1 FLIGHT TRACKS FOR ALL AIRPLANES EXCEEDING MACH 1.0
LUKE AFB**



Scale: 1:500,000

**FIGURE 2.2 FLIGHT TRACKS FOR ALL AIRPLANES WHERE $M > M_c$
LUKE AFB**



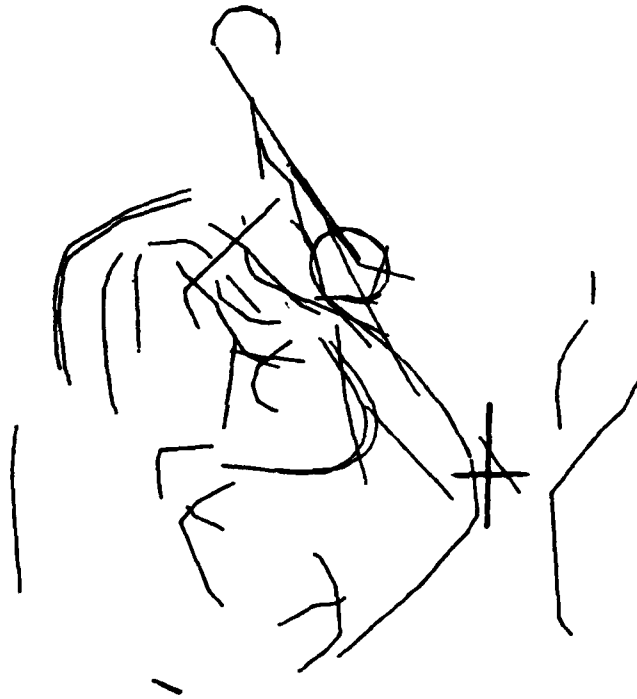
Scale: 1:500,000

**FIGURE 2.3 FLIGHT TRACKS FOR F-4 AIRPLANES EXCEEDING MACH 1.0
LUKE AFB**



Scale: 1:500,000

FIGURE 2.4 FLIGHT TRACKS FOR F-4 AIRPLANES WHERE $M > M_c$
LUKE AFB



Scale: 1:500,000

**FIGURE 2.5 FLIGHT TRACKS FOR F-5 AIRPLANES EXCEEDING MACH 1.0
LUKE AFB**



Scale: 1:500,000

**FIGURE 2.6 FLIGHT TRACKS FOR F-5 AIRPLANES WHERE $M > M_c$
LUKE AFB**



Scale 1:500,000

**FIGURE 2.7 FLIGHT TRACKS FOR F-15 AIRPLANES EXCEEDING MACH 1.0
LUKE AFB**



**FIGURE 2.8 FLIGHT TRACKS FOR F-15 AIRPLANES WHERE $M > M_c$
LUKE AFB**



Scale: 1:500,000

**FIGURE 2.9 FLIGHT TRACKS FOR F-16 AIRPLANES EXCEEDING MACH 1.0
LUKE AFB**



Scale: 1:500,000

**FIGURE 2.10 FLIGHT TRACKS FOR F-16 AIRPLANES WHERE $M > M_c$
LUKE AFB**

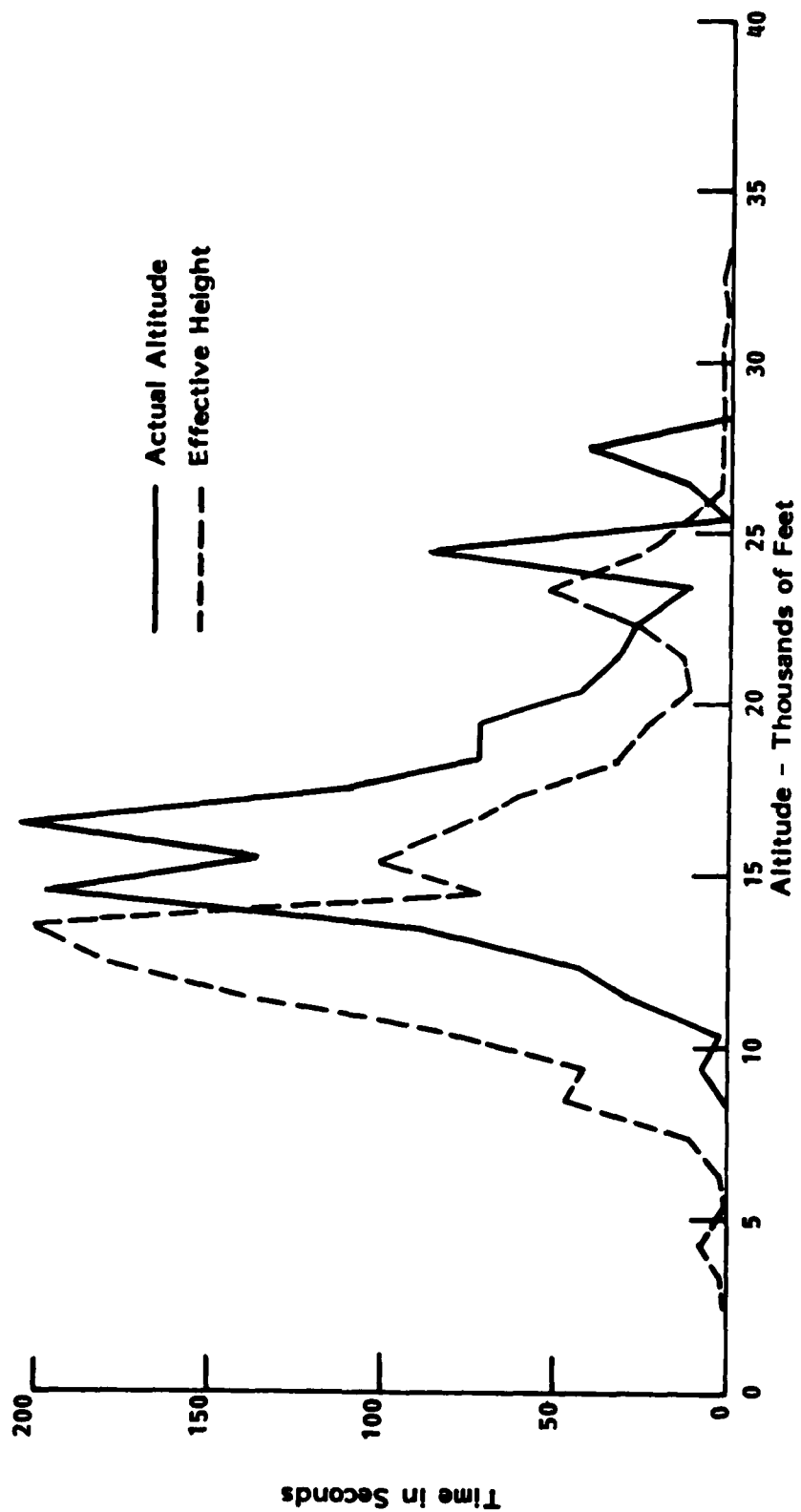


FIGURE 2.11 HEIGHT DISTRIBUTIONS FOR 46 F-4 SUPERSONIC EVENTS - DETERMINED AT ONE-SECOND INTERVALS - TOTAL TIME 2291 SECONDS - LUKE AFB

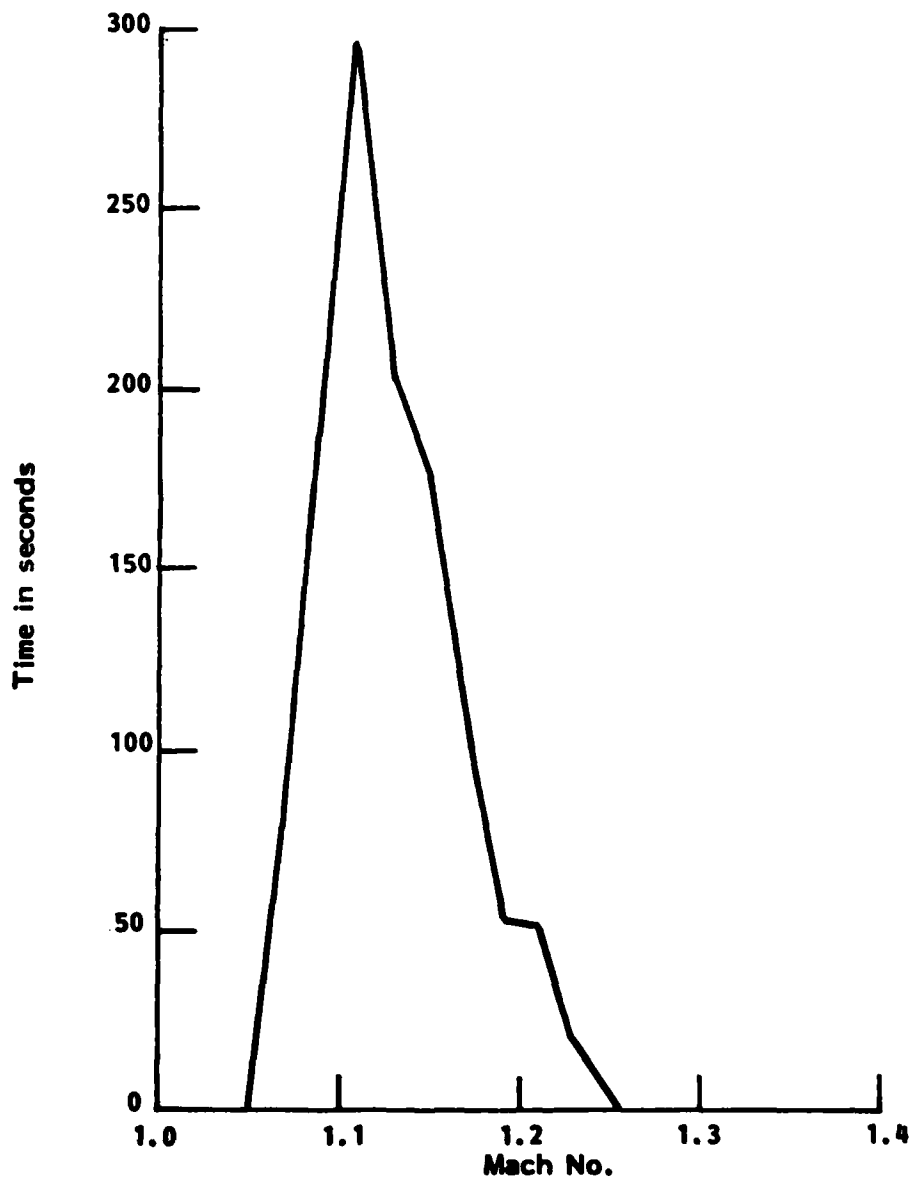


FIGURE 2.12 MACH NUMBER DISTRIBUTION FOR F-4 AIRPLANES WHERE $M > M_c$ - LUKE AFB

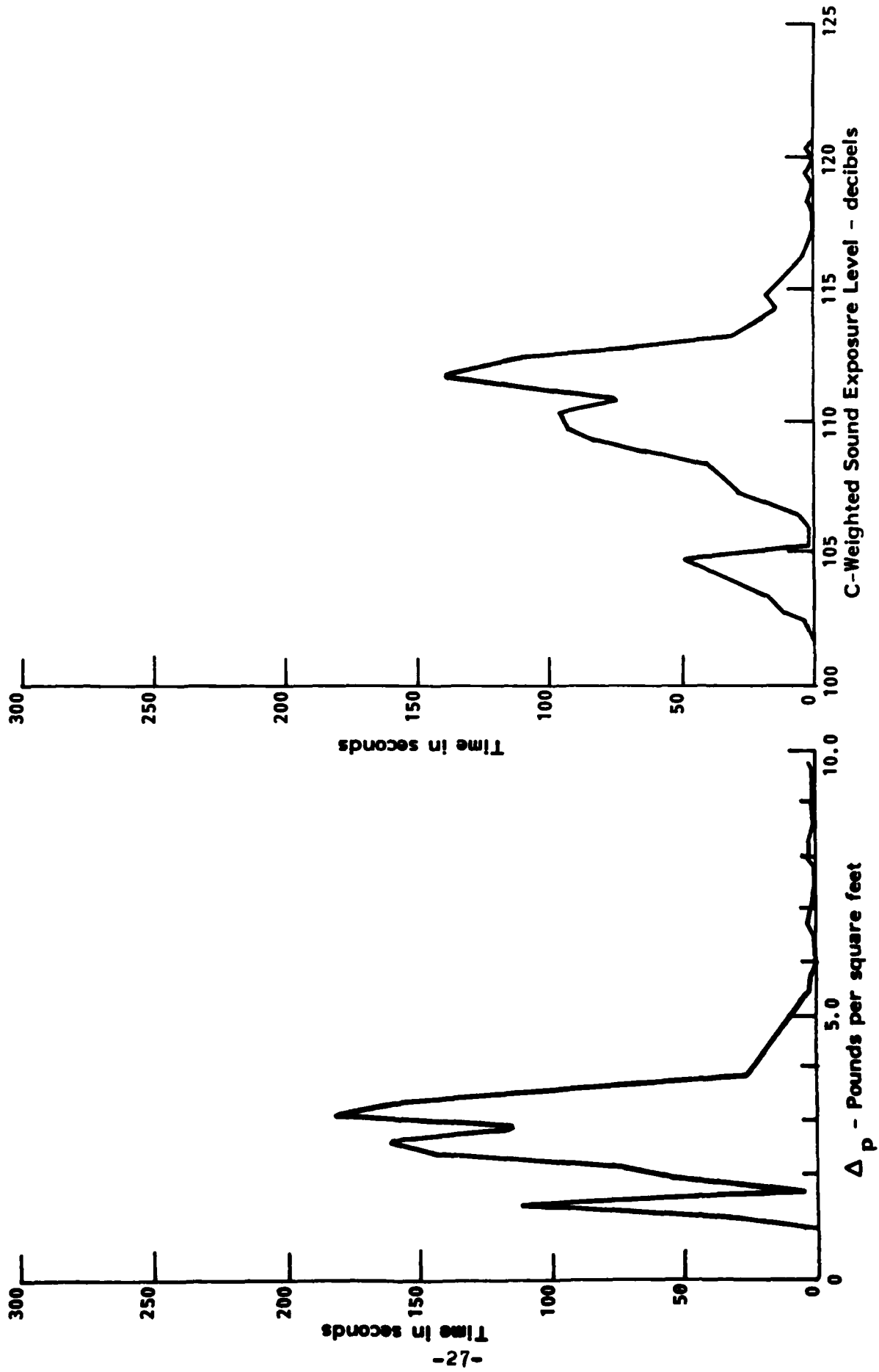


FIGURE 2.13 DISTRIBUTION OF PEAK OVERPRESSURES AND C-WEIGHTED SOUND EXPOSURE LEVELS PREDICTED FOR F-4 AIRPLANES WHERE $M > M_c$ - LUKE AFB

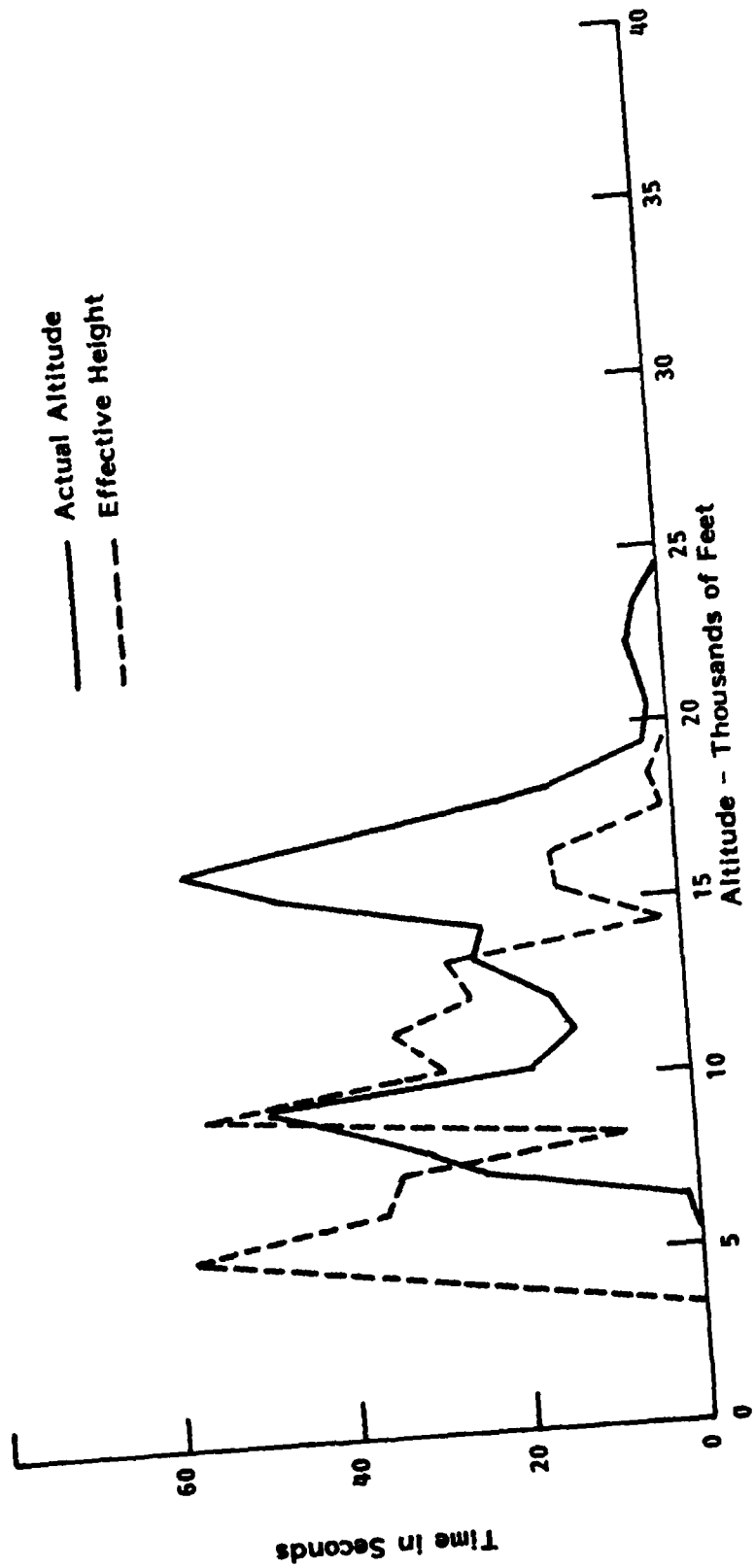


FIGURE 2.14 HEIGHT DISTRIBUTIONS FOR 47 F-5 SUPERSONIC EVENTS - DETERMINED AT ONE-SECOND INTERVALS - TOTAL TIME 1204 SECONDS - LUKE AFB

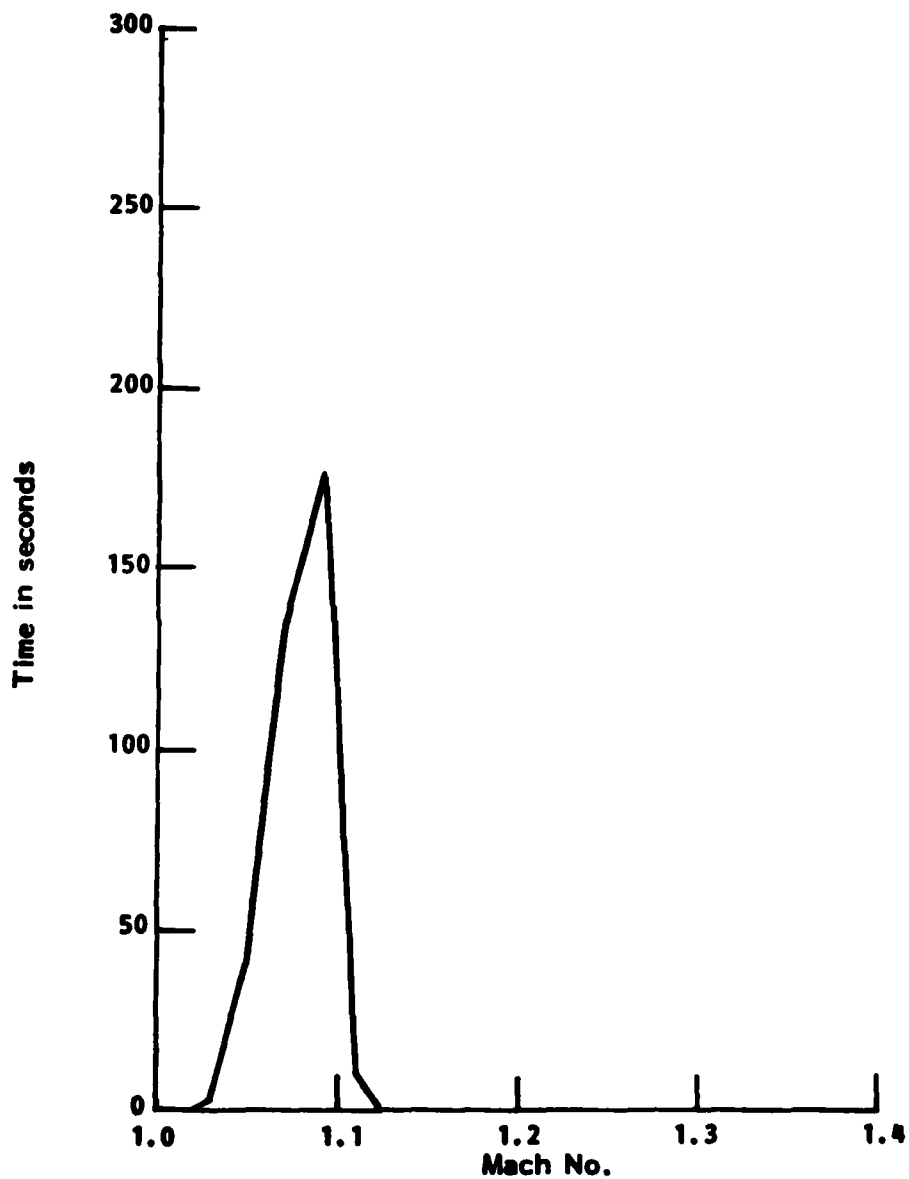


FIGURE 2.15 MACH NUMBER DISTRIBUTION FOR F-5 AIRPLANES WHERE $M > M_c$ - LUKE AFB

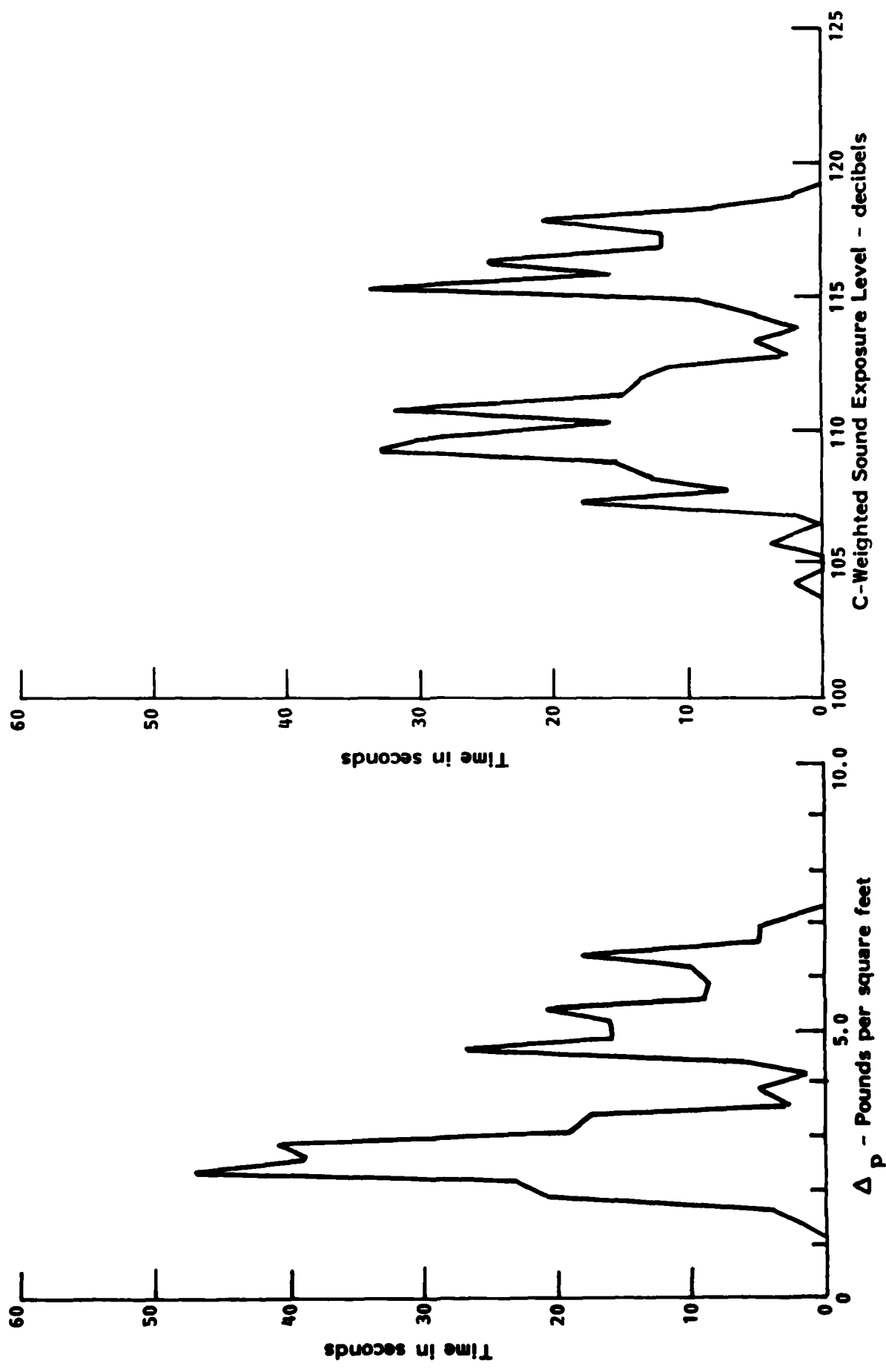


FIGURE 2.16 DISTRIBUTION OF PEAK OVERPRESSURES AND C-WEIGHTED SOUND EXPOSURE LEVELS PREDICTED FOR F-5 AIRPLANES WHERE $M > M_c$ - LUKE AFB

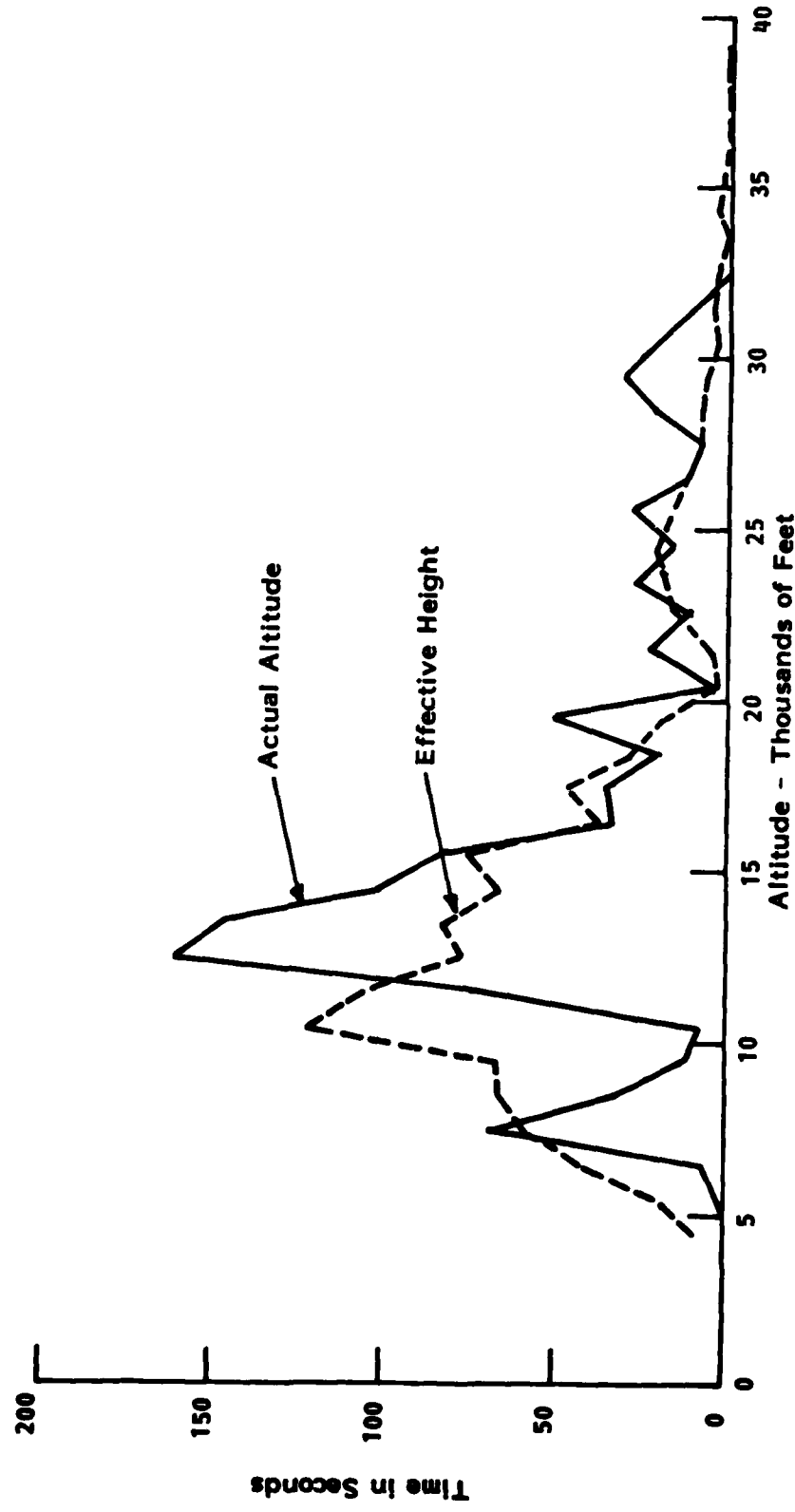
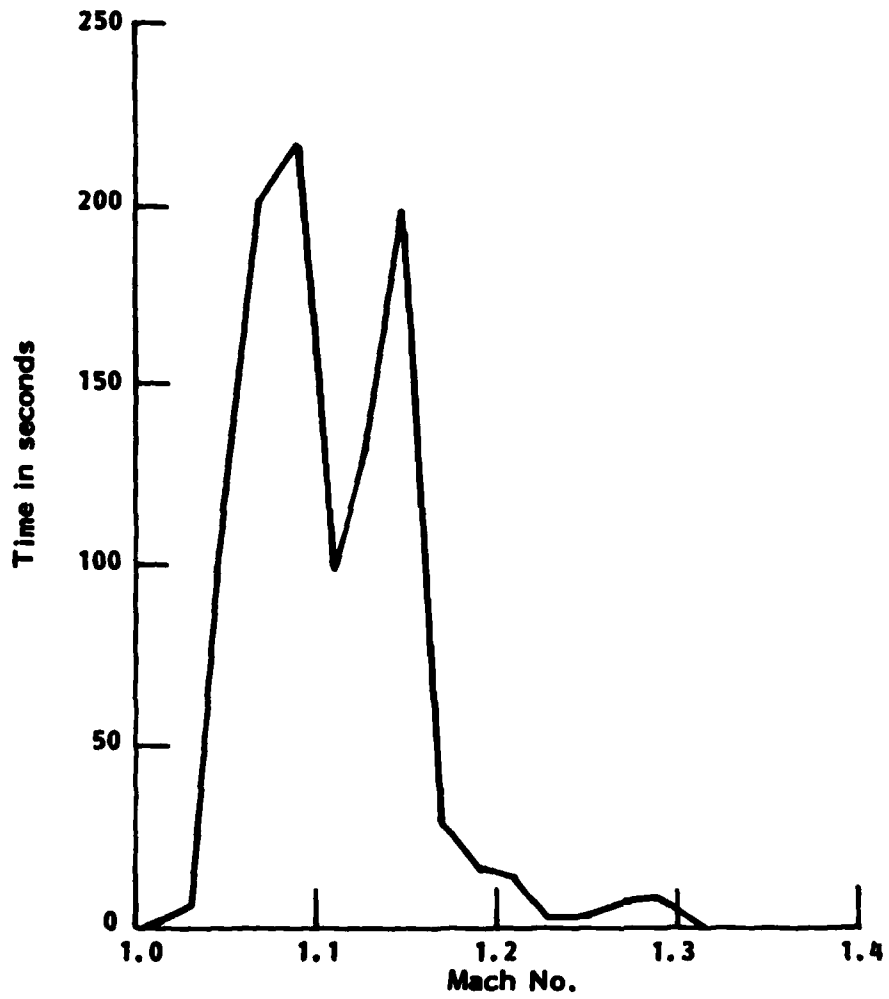


FIGURE 2.17 HEIGHT DISTRIBUTIONS FOR 133 F-15 SUPERSONIC EVENTS - DETERMINED AT ONE SECOND INTERVALS - TOTAL TIME 4117 SECONDS - LUKE AFB



**FIGURE 2.18 MACH NUMBER DISTRIBUTION FOR F-15 AIRPLANES
WHERE $M > M_c$ - LUKE AFB**

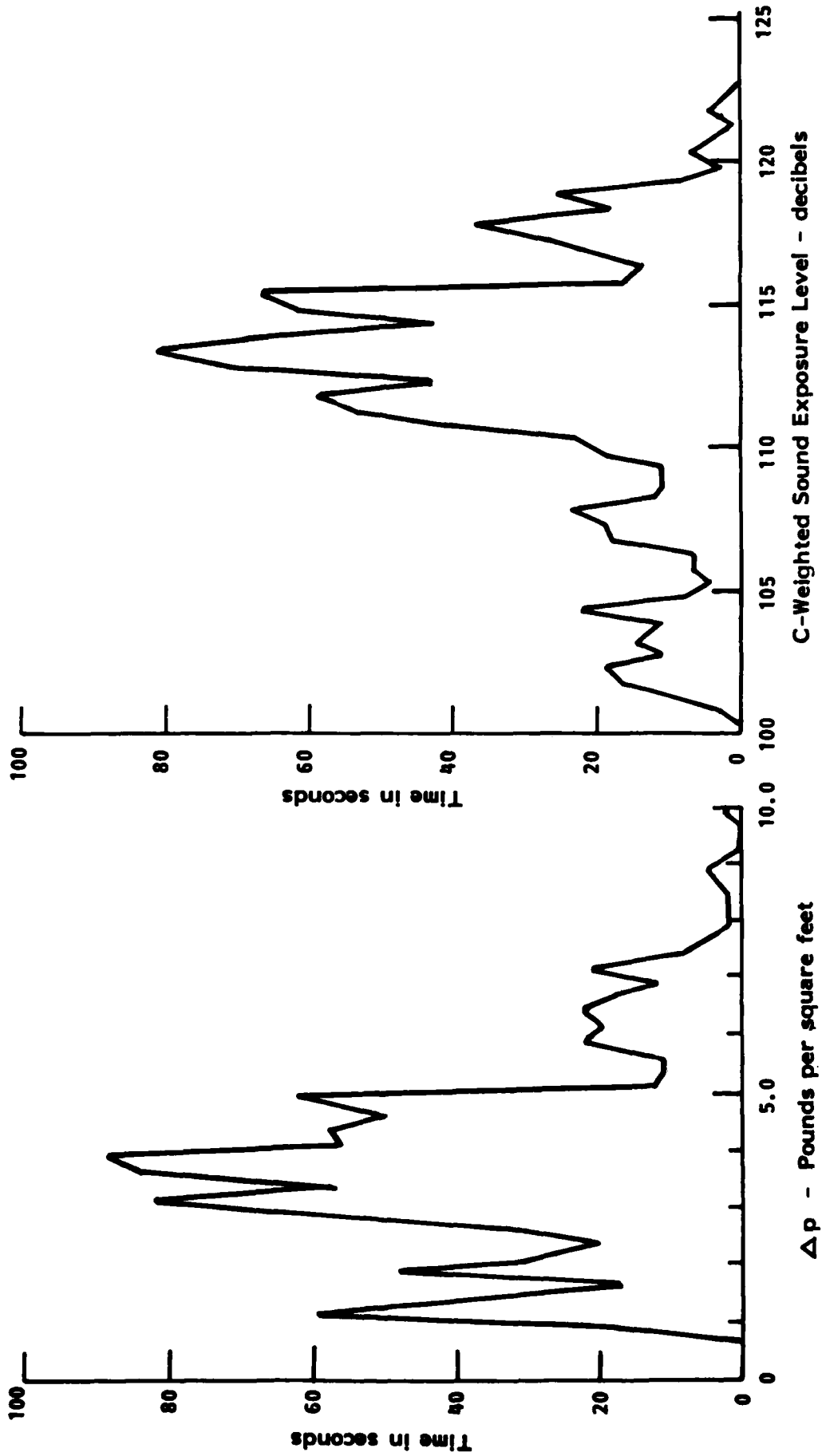


FIGURE 2.19 DISTRIBUTION OF PEAK OVERPRESSURES AND C-WEIGHTED SOUND EXPOSURE LEVELS PREDICTED FOR F-15 AIRPLANES WHERE $M > M_c$ - LUKE AFB

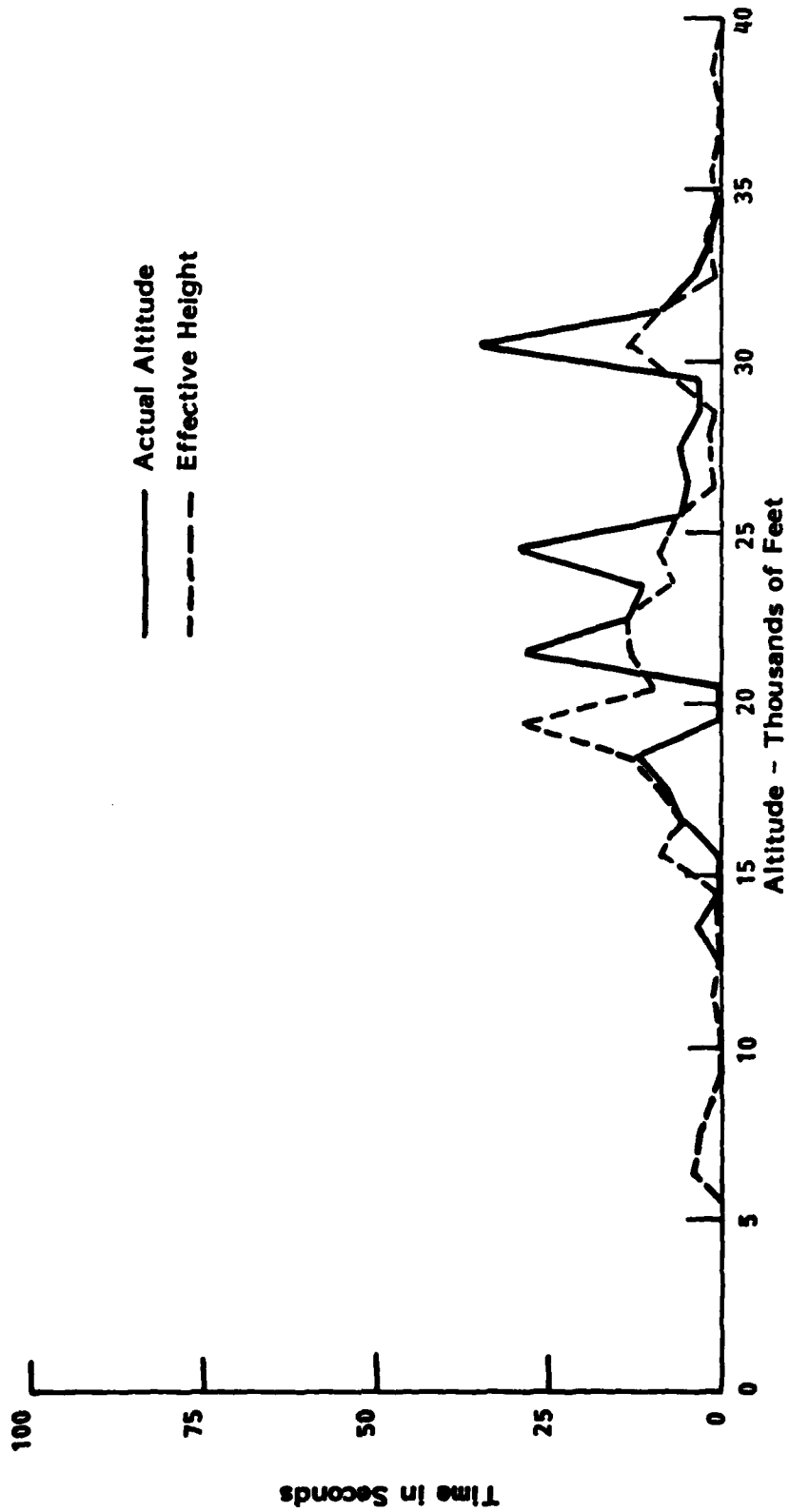


FIGURE 2.20 HEIGHT DISTRIBUTIONS FOR 25 F-16 SUPERSONIC EVENTS - DETERMINED AT ONE-SECOND INTERVALS - TOTAL TIME 1151 SECONDS - LUKE AFB

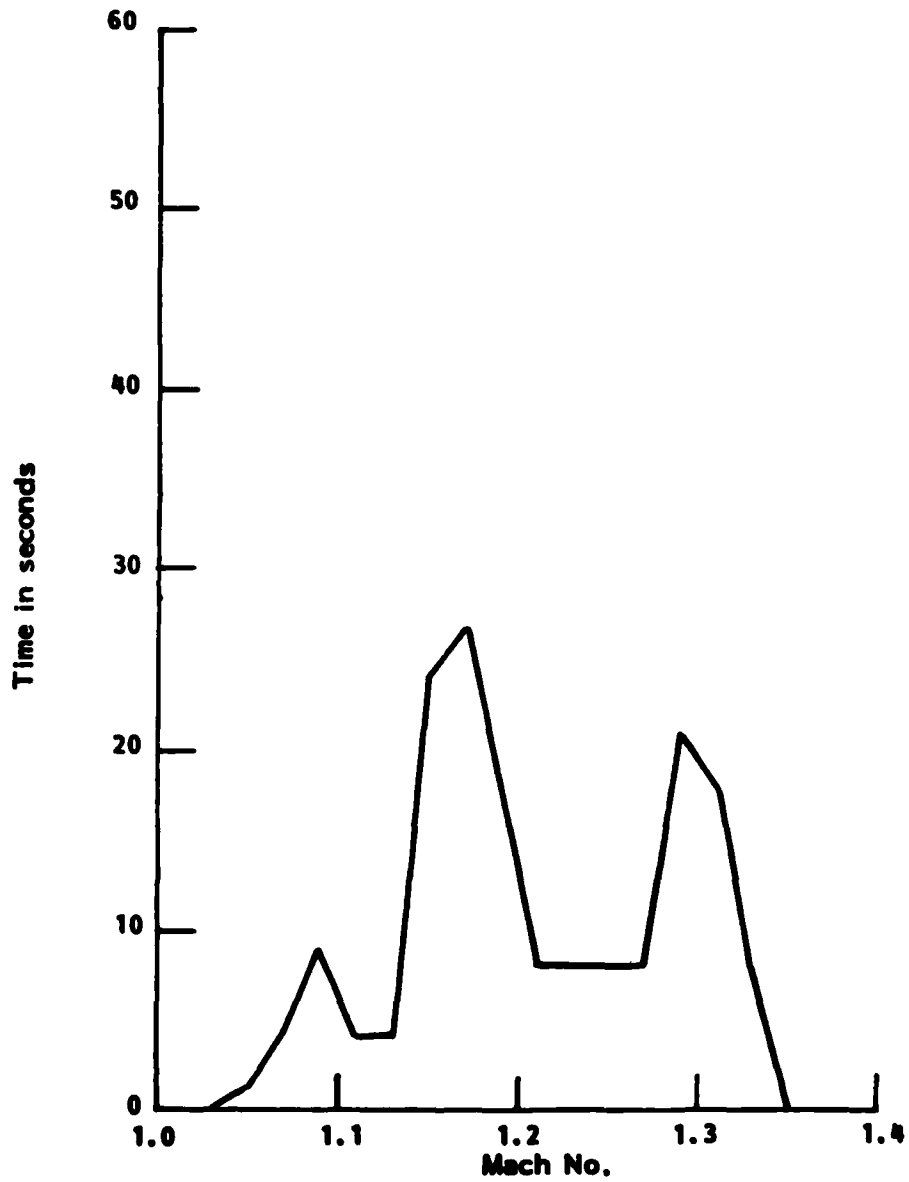


FIGURE 2.21 MACH NUMBER DISTRIBUTION FOR F-16 AIRPLANES WHERE $M > M_c$ - LUKE AFB

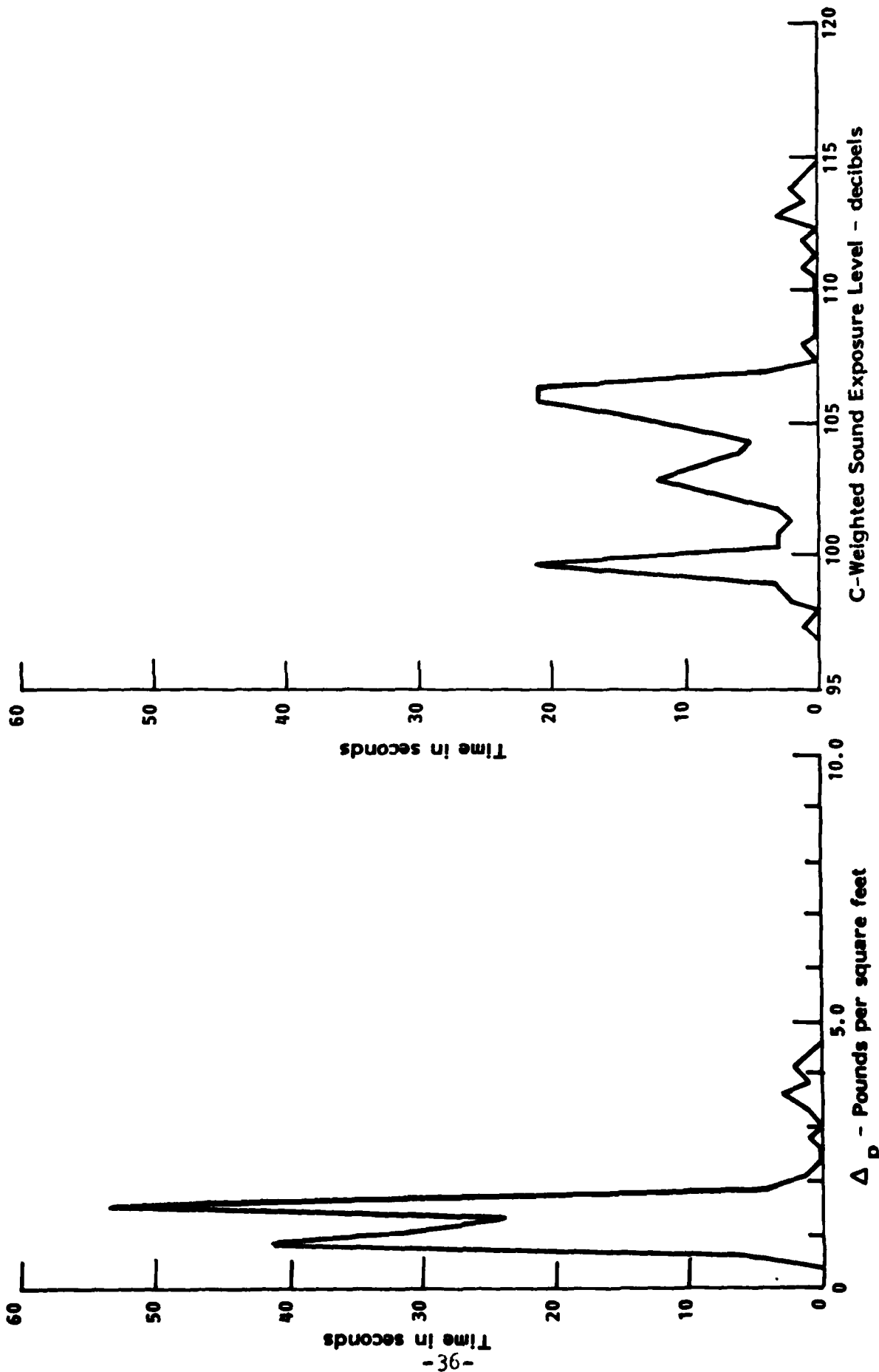
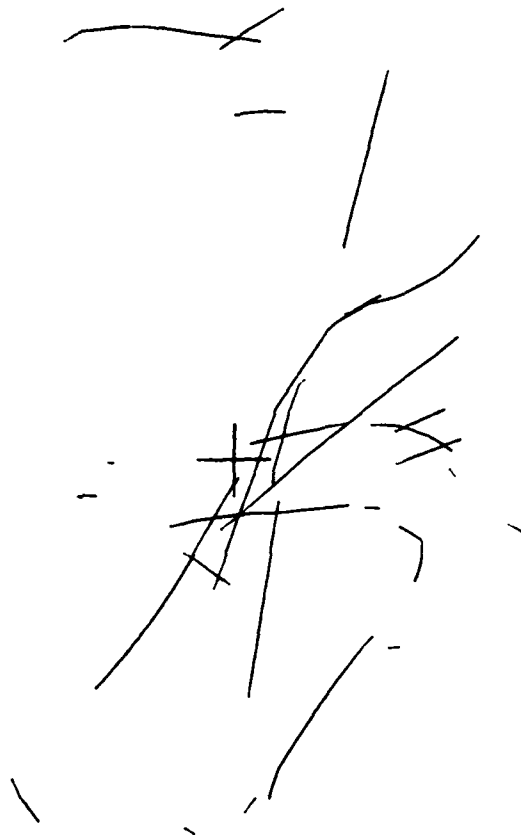


FIGURE 2.22 DISTRIBUTION OF PEAK OVERPRESSURES AND C-WEIGHTED SOUND EXPOSURE LEVELS PREDICTED FOR F-16 AIRPLANES WHERE $M > M_c$ - LUKE AFB



Scale: 1:500,000

**FIGURE 2.23 FLIGHT TRACKS FOR ALL AIRPLANES EXCEEDING MACH 1.0
NELLIS AFB**



Scale: 1:500,000

**FIGURE 2.24 FLIGHT TRACKS FOR ALL AIRPLANES WHERE $M > M_c$
NELLIS AFB**



**FIGURE 2.25 FLIGHT TRACKS FOR F-4 AIRPLANES EXCEEDING MACH 1.0
NELLIS AFB**



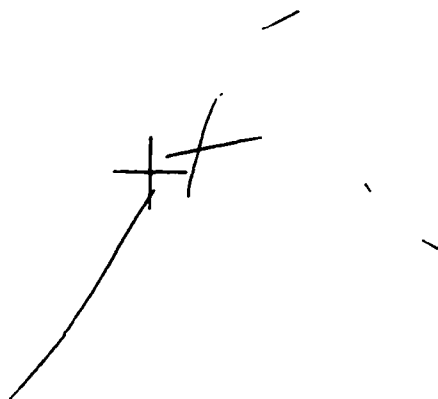
Scale: 1:500,000

FIGURE 2.26 FLIGHT TRACKS FOR F-4 AIRPLANES WHERE $M > M_c$
NELLIS AFB



Scale: 1: 500,000

**FIGURE 2.27 FLIGHT TRACKS FOR F-15 AIRPLANES EXCEEDING MACH 1.0
NELLIS AFB**



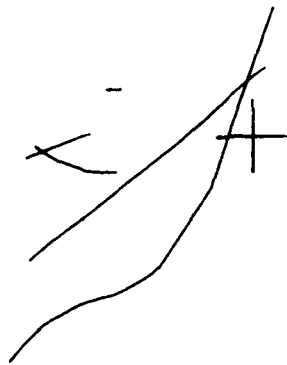
Scale: 1: 500,000

FIGURE 2.28 FLIGHT TRACKS FOR F-15 AIRPLANES WHERE $M > M_c$
NELLIS AFB



Scale: 1:500,000

**FIGURE 2.29 FLIGHT TRACKS FOR F-16 AIRPLANES EXCEEDING MACH 1.0
NELLIS AFB**



Scale: 1:500,000

**FIGURE 2.30 FLIGHT TRACKS FOR F-16 AIRPLANES WHERE $M > M_c$
NELLIS AFB**

3.0 RELATIONS BETWEEN PEAK OVERPRESSURE AND SOUND EXPOSURE LEVELS FOR SONIC BOOMS

The published differences between peak overpressure and C-weighted sound exposure level (CSEL) or A-weighted sound exposure level (ASEL) reviewed in Section 1.2 were restricted to sonic booms having more or less classical N-wave pressure-time signatures. In these cases there was an almost constant 26 decibel difference between peak overpressure and CSEL. On the other hand, the difference between peak overpressure and ASEL appeared to be inversely, but non-linearly related to the magnitude of the overpressure.

The analyses reported here explore the relations between sonic boom overpressure and various sound level measures for different classes of sonic booms. In addition to classical N-waves, focus booms and booms near cutoff conditions, the two extremes on either side of an N-wave, are of primary interest.

The results obtained in this study are based on frequency and time domain computations of the characteristics of published pressure-time signatures for sonic booms. The general procedure was first to digitize the graphical representation of the sonic boom signature, then to compute a pressure spectrum by Fourier analysis. Various frequency weightings could then be applied to these spectra, from which the time-integrated measures and sound exposure levels could then be computed. Analysis procedures for these computations are described in Appendix C.

3.1 Summary of Test Conditions

Pressure time traces of sonic booms under known aircraft flight conditions were processed using the Appendix C procedures. For the most part, these traces were taken from Reference 6. Sonic booms from F-104 aircraft were recorded in this NASA study

at 16 flush-mounted ground microphone locations and 15 tower microphone locations. Ground microphones 1-14 were placed in a line with a nominal separation of 200 feet. Microphones 15 and 16 were located 1800 feet from either side of the center point of the line. In this way, 16 sonic booms from each passby were recorded on the ground.

Ground microphone data from three classes of booms were analyzed:

- (1) "Normal" Booms - exhibiting the classical N-wave shape,
- (2) Focusbooms - experienced at the caustic-ground intersection (focus), due to aircraft longitudinal acceleration,
- (3) Lateral Cutoff booms - commonly heard as a low frequency rumble at ground locations near the edges of the boom "carpet".

Of particular interest to community noise analysis are the category (2) and (3) booms, for which the relationships between peak overpressure and A-weighted and C-weighted sound exposure levels are not well known. Table 3.1 summarizes the runs representative of the 3 categories that were analyzed in this study. The booms corresponding to categories (1) and (2) occurred with aircraft longitudinal accelerations between about 3.7 to 5.1 ft/sec², (0.11 to 0.16 g) with the aircraft nearly overhead, traveling parallel to the ground microphone array at constant altitude. For the category (3) runs the aircraft flew perpendicular to the array at the displacement specified at constant (supersonic) speed.

Table.3.1
Summary of Representative Booms Analyzed

| <u>Category</u> | <u>Pass</u> | <u>Altitude ft.</u> | <u>Lateral Distance miles</u> | <u>Aircraft Mach No.</u> | <u>Subjective* Boom Character</u> |
|-----------------|-------------|-------------------------|---------------------------------------|------------------------------|---------------------------------------|
| (1) | 040 | 33,700 | 0 | 0.95-1.3 | Sharp double boom |
| (2) | 043 | 33,700 | 0 | 0.95-1.3 | Near Superboom |
| | 045 | 33,700 | 0 | 0.95-1.3 | Superboom |
| | 046 | 33,700 | 0 | 0.95-1.3 | Superboom |
| (3) | 029 | 32,600 | 11.4 | 1.3 | Low boom-rumble |
| | 030 | 32,600 | 14.0 | 1.3 | Very light dble boom-rumble |
| | 033 | 32,900 | 12.8 | 1.3 | Low boom-rumble |
| | 035 | 32,650 | 12.3 | 1.3 | light boom-rumble |

*quoted from Ref. 6

3.2 Nominal N-Waves

Pass 040 provided a set of sonic boom measurements well past the ground location where a caustic was produced during acceleration to supersonic conditions. The resulting pressure-time signatures are representative of nominal N-wave conditions and provide insight on the variability of a "constant" boom. Traces from the 16 ground microphones are shown in Figure 3.1. The irregularities in the leading edges and other parts of the traces are attributed in Reference 6 to aberrations produced by atmospheric fluctuations and are certainly not atypical.

Sound level measures computed from the pressure time traces of Figure 3.1 are listed in Table 3.2. Differences between peak overpressure in decibels and the different frequency weighted sound exposure levels are also listed. Note that the average difference between CSEL and peak overpressure is 25.3 decibels, with a standard deviation of 0.7 decibels, very comparable to

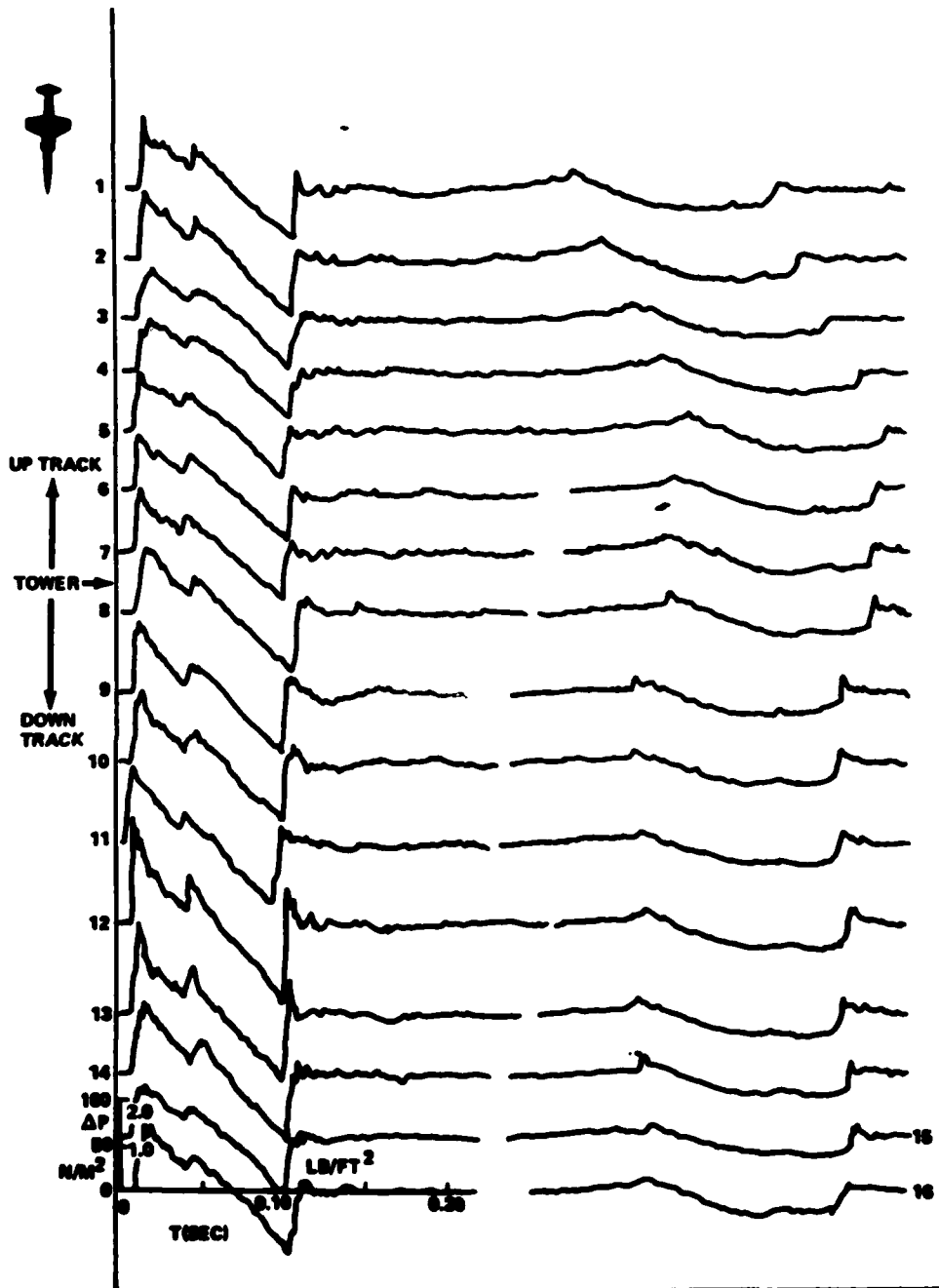


FIGURE 3.1 GROUND PRESSURE SIGNATURES DOWNTRACK FROM CAUSTIC-GROUND INTERSECTION- PASS 040, AUGUST 28, 1-3 - REF. 6

Table 3.2

Sound Levels in Decibels Measured at Ground
Positions For Nominal N-Wave - Pass 040, Ref. 6

| Position | L_{pk} | L_E | L_{AE} | L_{CE} | L_{pk}^- L_E | L_{pk}^- L_{AE} | L_{pk}^- L_{CE} |
|----------|----------|-------|----------|----------|---------------------|------------------------|------------------------|
| 1 | 130.4 | 114.0 | 87.8 | 104.4 | 16.4 | 42.6 | 26.0 |
| 2 | 131.7 | 115.5 | 85.6 | 105.9 | 15.7 | 45.6 | 25.2 |
| 3 | 128.0 | 113.3 | 75.7 | 102.8 | 14.7 | 52.3 | 25.2 |
| 4 | 129.1 | 113.7 | 80.1 | 102.8 | 15.4 | 49.0 | 26.3 |
| 5 | 127.8 | 113.5 | 79.7 | 103.0 | 14.3 | 48.1 | 24.7 |
| 6 | 128.5 | 113.2 | 85.0 | 104.1 | 15.3 | 43.6 | 24.5 |
| 7 | 131.0 | 113.5 | 85.6 | 104.0 | 17.5 | 45.4 | 27.0 |
| 8 | 130.5 | 114.9 | 87.5 | 105.5 | 15.6 | 42.9 | 25.0 |
| 9 | 131.1 | 114.7 | 88.2 | 106.4 | 16.3 | 42.8 | 24.7 |
| 10 | 131.9 | 114.9 | 89.9 | 106.2 | 17.0 | 42.0 | 25.7 |
| 11 | 131.4 | 115.4 | 81.2 | 105.8 | 16.0 | 50.2 | 25.6 |
| 12 | 135.7 | 117.5 | 94.3 | 110.4 | 18.1 | 41.4 | 25.3 |
| 13 | 133.5 | 116.3 | 91.6 | 107.6 | 17.2 | 41.9 | 25.9 |
| 14 | 131.2 | 116.4 | 89.8 | 106.7 | 14.9 | 41.4 | 24.6 |
| 15 | 128.0 | 113.8 | 81.8 | 103.9 | 14.2 | 46.2 | 24.2 |
| 16 | 131.3 | 115.8 | 85.2 | 105.9 | 15.6 | 46.1 | 25.4 |
| Avg. | 130.7 | 114.8 | 85.6 | 105.3 | 15.9 | 45.1 | 25.3 |
| Std.Dev. | 1.1 | 1.3 | 4.9 | 2.0 | 2.1 | 3.4 | 0.7 |

L_{pk} peak flat sound level
 L_E flat sound exposure level
 L_{AE} A-weighted sound exposure level
 L_{CE} C-weighted sound exposure level

the 26 decibel average previously obtained in Reference 4. In contrast, the difference between peak level and ASEL has an average of 45.1 decibels, with a standard deviation of 3.4 decibels. This difference is to be compared with the 36.5 decibels that would be predicted from Young's data in Reference 5. The regression equation obtained in Appendix A from this data would predict an average ASEL of 93.9 decibels rather than the 85.6 decibels obtained here. Despite the large range of ASEL values, compared to the range of peak levels (standard deviation of 4.9 for ASEL and 1.1 for peak level), ASEL is reasonably well correlated (R^2 of 0.688) with peak level, yielding a regression equation of:

$$L_{AE} = 251.2 \ln L_{pk} - 1138.5 \quad (3.1)$$

For prediction purposes Carlson's model is used to Estimate overpressures, from which the various sound levels are then derived. The Carlson model predicts a peak flat sound level of 131.5 decibels for these flight conditions, compared to the measured average value of 130.7 decibels with standard deviation of 1.1 decibels.

3.3 Focus Booms

Airplane maneuvers that involve acceleration at supersonic speeds change the shock wave front propagation angles in such a way that wave fronts coalesce to form a caustic. These maneuver, or focus booms are produced within a narrow geographic region at a fixed location on the ground. Pressure-time signatures for these booms have sharp, spike-like initial and trailing overpressures, whose magnitudes may be up to five times that of a normal N-wave, although the initial overpressure peak decays more rapidly than for an N-wave. These characteristics imply that the high frequency content of maneuver booms should be substantially greater than for N-waves.

Ground microphone data for three focus booms reported in Ref. 6 were analyzed to obtain sound levels. On pass 043 the caustic intercepted the ground just before the first microphone, thus the spreading separation of leading and trailing shocks is observed in the ground microphone traces. During passes 045 and 046 the caustic intercepted the ground within the microphone array, providing a picture of the fine structure of focus booms.

Pressure-time traces obtained from Pass 043 at ground microphones are shown in Figure 3.2. The "spikey" nature of the focus shows clearly only at positions 1 and 2. Divergence of the leading and trailing shocks shows at positions 1 through 9, less clearly thereafter.

Sound level measures at representative microphone positions for Pass 043 are listed in Table 3.3. Recalling that the predicted overpressure has a peak flat sound level of 131.3, the excess pressure from the caustic shows up only at positions 1 and 2. As the leading and trailing shocks separate, the peak overpressures are several decibels lower than for a steady-state N-wave. The nominal 26 decibel difference between peak flat sound level and CSEL again appears here. The difference between peak sound level and ASEL is again much larger than would be predicted from Young's data. However, the regression equation obtained above in Section 3.2 predicted an ASEL of 79.3 decibels compared to the average 79.8 decibels listed in Table 3.3.

Passes 045 and 046 placed the ground intercepts of their caustics across the microphone array. The traces for Pass 045 shown in Figure 3.3 are probably the least distorted of all the data. The data at positions 1 to 6 for this pass show the acoustical "precursor" of the shock waves, with the focus effects clearly becoming apparent at position 8. Divergence of the leading and trailing shocks begins to show by position 11 and is clearly obvious at position 14.

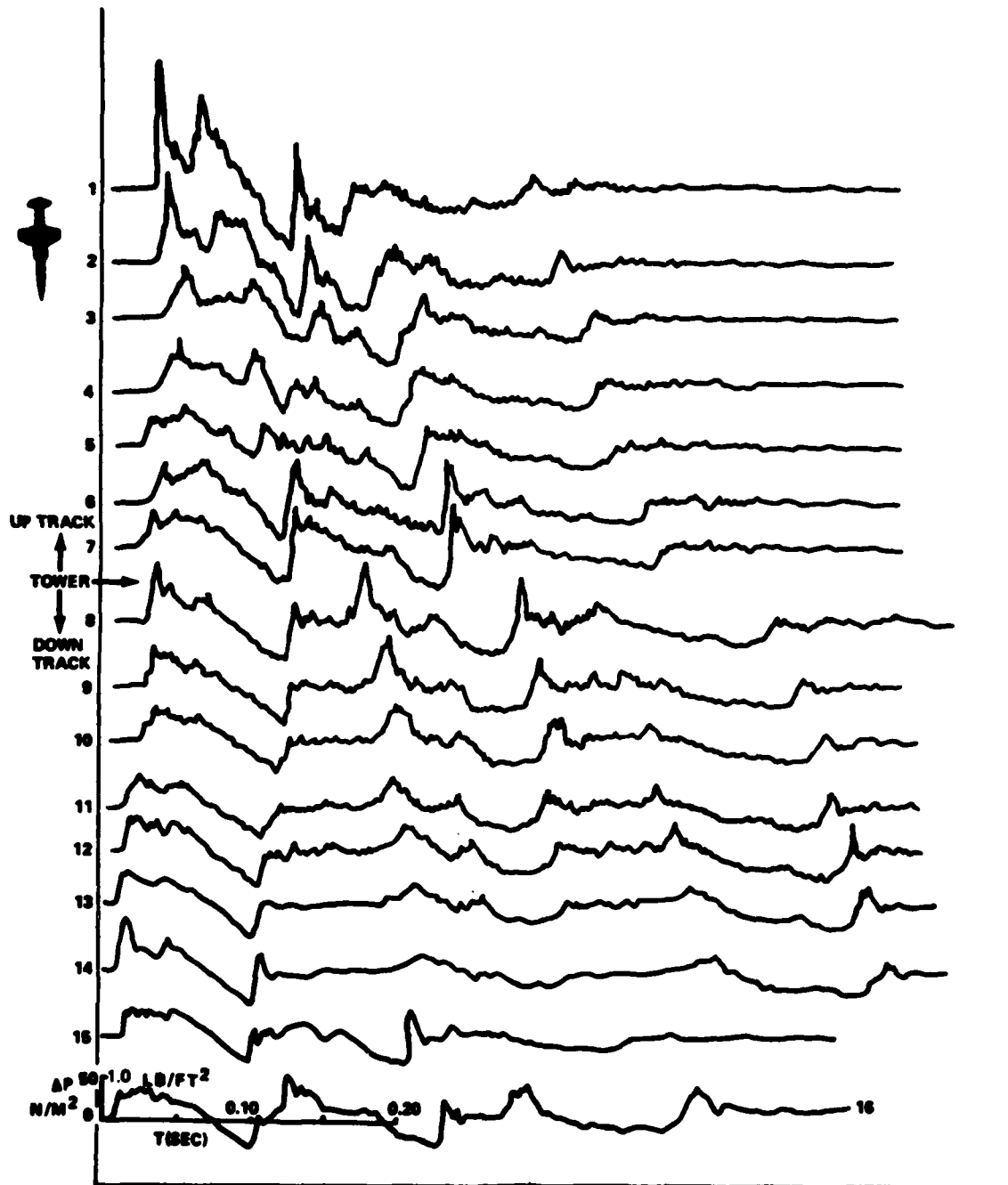


FIGURE 3.2 GROUND PRESSURE SIGNATURES JUST DOWNTRACK OF CAUSTIC-GROUND INTERSECTION—PASS 043, AUGUST 28, 2-3 - REF. 6

Table 3.3

Sound Levels in Decibels Measured at Ground
Positions Down Track from a Caustic-Ground Intercept
Pass 043, Ref. 6

| Position | L_{pk} | L_E | L_{AE} | L_{CE} | $L_{pk} - L_E$ | $L_{pk} - L_{AE}$ | $L_{pk} - L_{CE}$ |
|---------------|----------|-------|----------|----------|----------------|-------------------|-------------------|
| 1 | 136.7 | 118.4 | 99.9 | 111.1 | 18.4 | 36.8 | 25.6 |
| 2 | 133.7 | 117.0 | 87.3 | 108.3 | 16.8 | 46.5 | 25.4 |
| 3 | 128.5 | 113.9 | 80.1 | 104.0 | 14.6 | 48.5 | 24.6 |
| 5 | 126.0 | 110.0 | 84.4 | 96.6 | 16.0 | 41.5 | 29.4 |
| 7 | 125.5 | 112.0 | 78.8 | 99.8 | 13.5 | 46.7 | 25.7 |
| 8 | 130.4 | 112.6 | 82.4 | 103.6 | 17.8 | 48.0 | 26.8 |
| 10 | 124.8 | 110.3 | 80.7 | 98.7 | 14.5 | 44.1 | 26.1 |
| 11 | 125.8 | 110.6 | 73.9 | 98.8 | 15.2 | 52.0 | 27.1 |
| 12 | 125.6 | 112.0 | 75.1 | 100.2 | 13.7 | 50.5 | 25.4 |
| 13 | 125.0 | 110.8 | 74.7 | 100.2 | 14.1 | 50.3 | 24.7 |
| 14 | 129.1 | 111.6 | 78.9 | 103.6 | 17.5 | 50.2 | 25.5 |
| 16 | 128.3 | 113.6 | 81.4 | 101.8 | 14.8 | 47.0 | 26.5 |
| Position 1-2 | | | | | | | |
| Avg. | 135.2 | 117.7 | 93.6 | 109.6 | 17.6 | 41.7 | 25.5 |
| Position 3-16 | | | | | | | |
| Avg. | 126.9 | 111.7 | 79.0 | 100.7 | 15.2 | 47.9 | 26.2 |
| Std.Dev. | 2.0 | 1.4 | 3.5 | 2.5 | 1.5 | 3.2 | 1.4 |

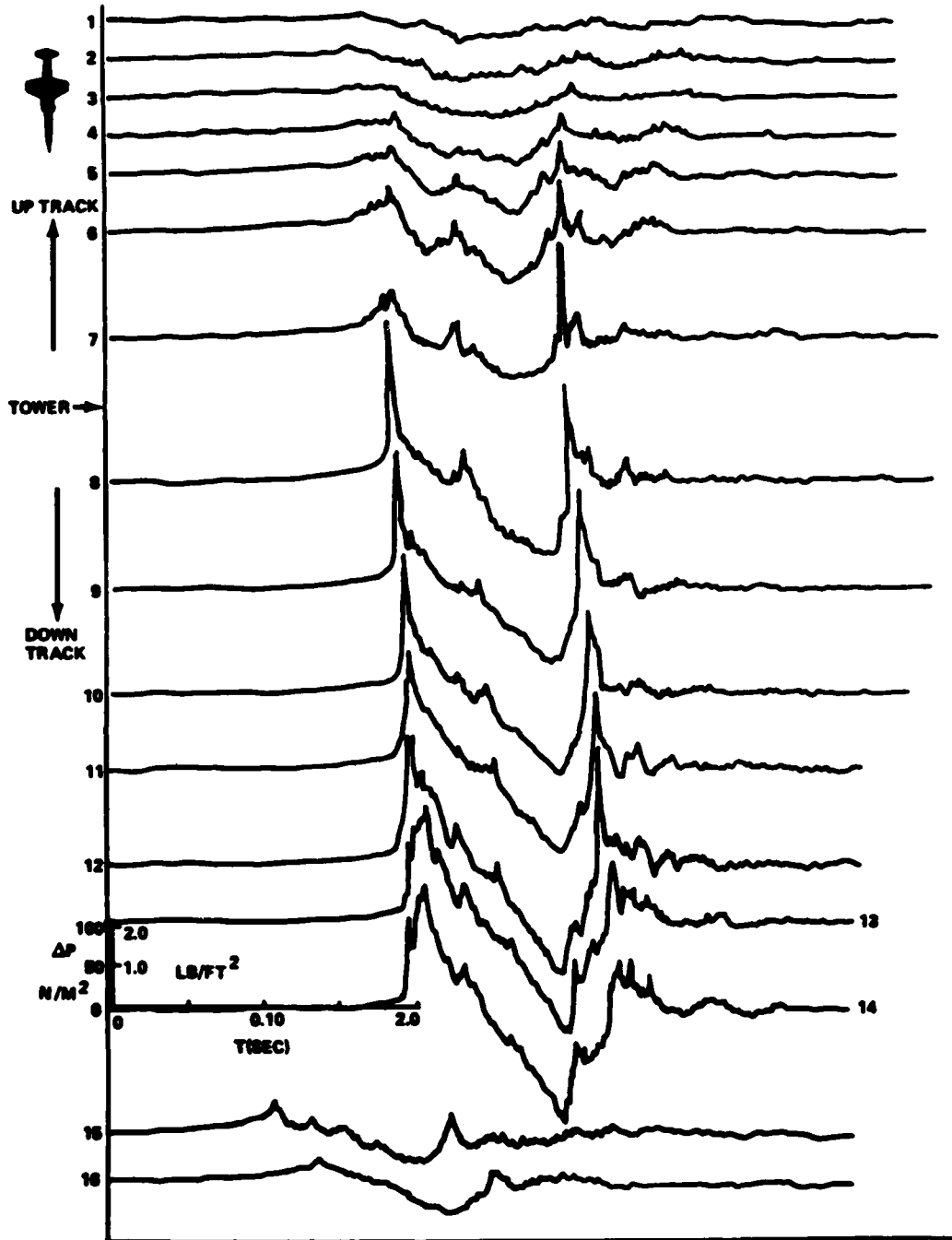


FIGURE 3.3 GROUND PRESSURE SIGNATURES NEAR CAUSTIC-GROUND INTERSECTION—PASS 045, AUGUST 28, 3-2 - REF. 6

Note that the traces at positions 15 and 16, which are 1800 feet offset on either side of the microphone array, midway between positions 7 and 8, show that the positions are outside the focus zone.

Sound level data for Pass 045 are listed in Table 3.4. Averages are listed only for data at positions 8 to 14, which represent the focus conditions. Peak flat sound levels at positions 7 to 14 are all in excess of the 131.5 decibel sound level expected for an N-wave. The highest value, at position 8, 138.6 decibels, represents a pressure amplification factor of 2.3 times the steady-state N-wave overpressure.

As expected, the high-frequency content in the focus boom signals changes the relations between peak flat sound level and CSEL or ASEL substantially as compared to N-waves. Although the average difference between peak sound level and CSEL is 23.3 decibels as compared with the 26 decibel average for N-waves, the dispersion is greater. Differences between peak sound level and ASEL are much more variable, ranging from a low of 21.3 to a high of 48.3 decibels, all for a range of peak sound levels of about 5 decibels. The regression equation for converting peak sound level to ASEL given in Section 3.2 is obviously of not much use here. For example, the equation would predict an ASEL of 100.3 decibels at position 8, as compared to the 113.3 measured, yet at position 10, 400 feet farther downtrack, the equation predicts 97.6 decibels as compared to the measured 88.8. Plus or minus 10 decibels or so is hardly a prediction of much use.

The data from Pass 046 were analyzed here because they had the highest peak overpressures observed during the tests. Pressure-time traces for the ground microphones are shown in Figure 3.4

Table 3.4

Sound Levels in Decibels Measured at Ground
Positions on Which a Caustic-Ground Intercept is
Superposed - Pass 045, Ref. 6

| Position | L_{pk} | L_E | L_{AE} | L_{CE} | L_{pk}^- L_E | L_{pk}^- L_{AE} | L_{pk}^- L_{CE} |
|----------|----------|-------|----------|----------|---------------------|------------------------|------------------------|
| 2 | 114.7 | 108.6 | 97.2 | 98.0 | 6.1 | 17.6 | 16.7 |
| 3 | 113.5 | 108.0 | 96.4 | 97.5 | 5.5 | 17.1 | 16.0 |
| 4 | 120.5 | 110.7 | 98.0 | 100.4 | 9.8 | 22.6 | 20.1 |
| 5 | 125.2 | 112.5 | 77.9 | 100.8 | 12.7 | 47.3 | 24.4 |
| 7 | 133.3 | 116.8 | 112.0 | 113.3 | 16.5 | 21.3 | 20.0 |
| 8 | 138.6 | 120.3 | 113.3 | 116.0 | 18.4 | 25.4 | 22.7 |
| 9 | 136.7 | 119.0 | 99.8 | 110.8 | 17.7 | 36.8 | 25.9 |
| 10 | 137.1 | 119.5 | 88.8 | 110.4 | 17.6 | 48.3 | 26.7 |
| 11 | 135.6 | 120.0 | 114.21 | 114.9 | 15.5 | 21.4 | 20.7 |
| 12 | 136.9 | 122.0 | 113.4 | 114.7 | 15.5 | 23.5 | 22.2 |
| 13 | 135.2 | 120.7 | 109.3 | 111.6 | 14.5 | 25.9 | 23.6 |
| 14 | 136.3 | 121.8 | 108.0 | 112.0 | 14.5 | 28.3 | 24.4 |
| 15 | 122.8 | 109.6 | 86.5 | 96.5 | 13.1 | 36.2 | 26.2 |
| 16 | 119.6 | 110.3 | 71.3 | 93.7 | 9.6 | 48.6 | 26.2 |
| Position | | | | | | | |
| 7-14 | | | | | | | |
| Avg. | 136.2 | 120.0 | 107.4 | 113.0 | 16.3 | 28.9 | 23.3 |
| Std.Dev. | 1.5 | 1.7 | 8.8 | 2.1 | 1.5 | 9.3 | 2.4 |

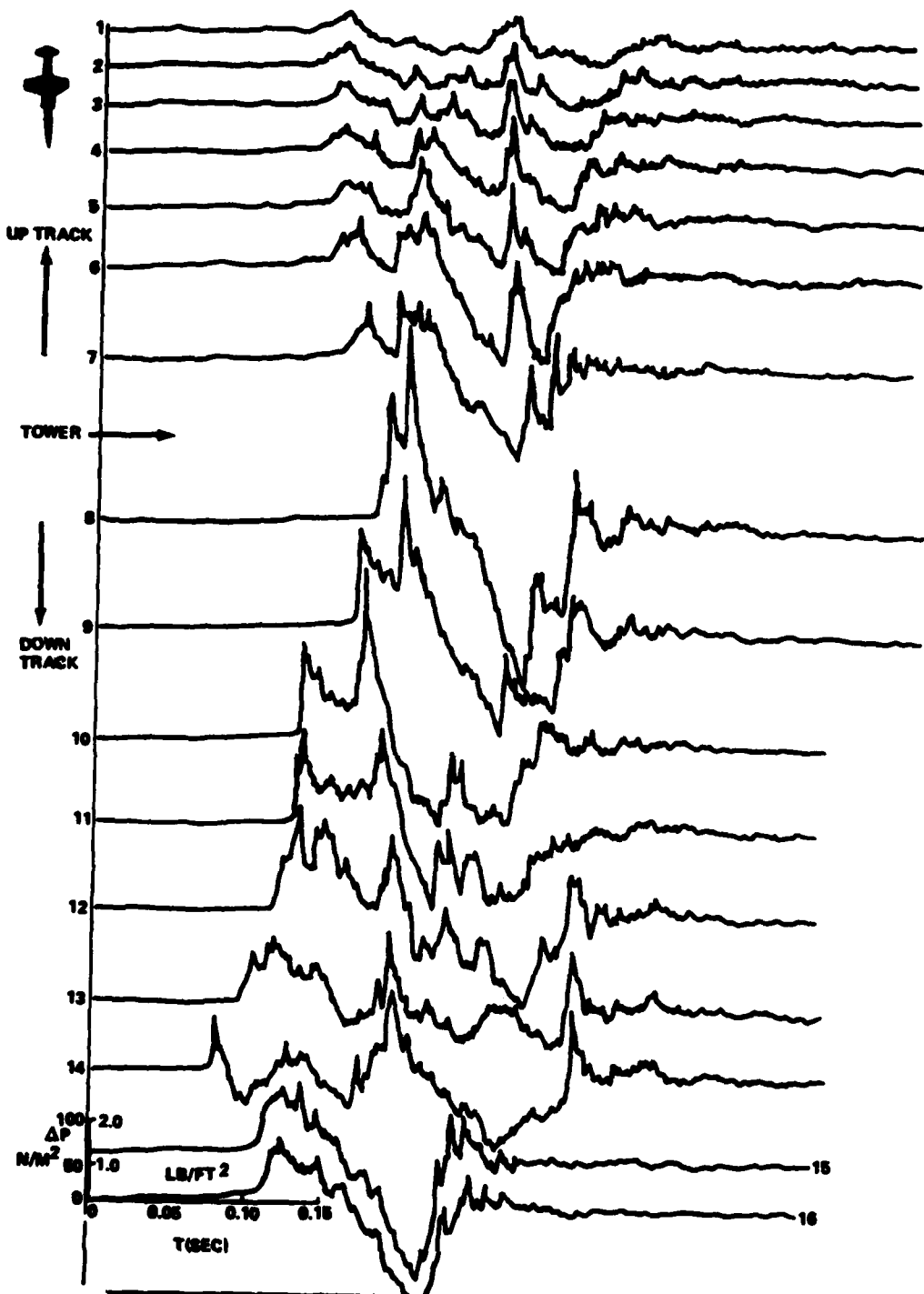


FIGURE 3.4 GROUND PRESSURE SIGNATURES NEAR CAUSTIC-GROUND INTERSECTION—PASS 046, AUGUST 28, 3-3 - REF. 6

and sound levels are listed in Table 3.5. The traces show that the caustic intercepts the ground very near to position 8, with the greatest overpressures at positions 8, 9, and 10. By position 11 the leading and trailing shocks are clearly diverging and peak pressures are dropping. The lateral positions, 15 and 16, show little of the focus effects, and have peak sound levels within one decibel of that for a normal N-wave at these flight conditions.

Selecting positions from which data averages are sensible is again quite arbitrary. Clearly, at positions 8, 9, and 10 the major focus effects are apparent. By position 11 the overpressure amplification of the focus is losing its effect, and by position 13 has essentially disappeared. Amplification at position 8 is 3.3 times the expected N-wave overpressure.

Differences between peak level and CSEL for Pass 046 are consistent with the previous data, but the differences between peak level and ASEL are not consistent with Pass 045 as described above. In this case the differences are consistently in the 43 to 45 decibel range irrespective of the signal conditions. The section 3.2 regression equation in this case predicts ASEL's that are from 5 to 8 decibels higher than measured. At least the 20 decibel swings in the conversion of peak level to ASEL are not present here.

3.4 Booms Near Lateral Cutoff

In a perfectly stable, standard atmosphere linear acoustical theory predicts that sonic boom wavefronts will curve along ray paths that eventually become tangent to the earth. At this point the wavefront is perpendicular to the earth. Beyond this distance the boom is refracted back up into the air, and no boom should be heard at greater distances. Linear theory also predicts that as the wave front approaches cutoff, a caustic is formed that increases the overpressure just before cutoff.

Table 3.5

Sound Levels in Decibels Measured at Ground
Positions on Which a Caustic-Ground Intercept is
Superposed - Pass 046, Ref. 6

| Position | L_{pk} | L_E | L_{AE} | L_{CE} | L_{pk}^- L_E | L_{pk}^- L_{AE} | L_{pk}^- L_{CE} |
|----------|----------|-------|----------|----------|---------------------|------------------------|------------------------|
| 1 | 124.9 | 110.8 | 79.7 | 100.7 | 14.1 | 45.3 | 24.3 |
| 2 | 125.6 | 111.9 | 81.1 | 103.2 | 13.7 | 44.6 | 22.5 |
| 3 | 127.5 | 113.1 | 82.8 | 104.9 | 14.4 | 44.7 | 22.6 |
| 4 | 127.9 | 115.1 | 86.5 | 107.0 | 12.8 | 41.4 | 21.0 |
| 5 | 130.3 | 116.6 | 85.0 | 107.1 | 13.7 | 45.3 | 23.2 |
| 6 | 130.9 | 120.2 | 94.1 | 110.4 | 10.7 | 36.8 | 20.5 |
| 7 | 131.8 | 119.7 | 92.6 | 109.4 | 12.1 | 39.2 | 22.4 |
| 8 | 141.9 | 125.3 | 100.2 | 114.8 | 16.6 | 41.7 | 27.1 |
| 9 | 138.8 | 122.4 | 95.6 | 111.5 | 16.4 | 43.3 | 27.3 |
| 10 | 140.3 | 122.9 | 97.3 | 112.6 | 17.4 | 43.0 | 27.7 |
| 11 | 135.3 | 121.1 | 93.0 | 110.0 | 14.2 | 42.3 | 25.3 |
| 12 | 134.6 | 122.1 | 88.2 | 111.3 | 12.6 | 46.5 | 23.3 |
| 13 | 132.1 | 117.3 | 85.6 | 109.2 | 14.7 | 46.5 | 22.9 |
| 14 | 133.4 | 119.4 | 87.7 | 109.9 | 14.0 | 45.7 | 23.5 |
| 15 | 132.8 | 121.8 | 91.2 | 109.7 | 11.0 | 41.6 | 23.1 |
| 16 | 131.8 | 120.9 | 83.7 | 107.3 | 11.0 | 48.1 | 24.6 |
| 8-10 | | | | | | | |
| Avg. | 140.3 | 123.5 | 97.7 | 113.0 | 16.8 | 42.7 | 27.4 |
| Std.Dev. | 1.6 | 1.6 | 2.3 | 1.7 | 0.5 | 0.9 | 0.3 |
| 11-14 | | | | | | | |
| Avg. | 133.9 | 120.0 | 88.6 | 110.1 | 13.7 | 45.1 | 23.8 |
| Std.Dev. | 1.4 | 2.1 | 3.1 | 0.9 | 1.9 | 0.7 | 1.1 |

In practice, under real atmospheric conditions, Maglieri [8] finds that linear theory predicts lateral propagation very well until the distance to the side is about 0.8 times the predicted lateral cutoff distance. Overpressures between this distance and the lateral cutoff distance appear to decrease by an order of magnitude. Nothing at all has been reported on the relations between peak overpressure and the various sound level measures.

The data of Ref. 6 provide a means for exploring the magnitude of peak overpressures near lateral cutoff and the associated sound levels. The four airplane passes examined here include one where cutoff occurs just beyond the microphone array, one which appears to be typical of conditions just after cutoff, and two that are at cutoff, showing the caustic-like characteristics predicted by theory.

Pressure-time traces for Pass 029 where cutoff occurs just beyond the microphone array are shown in Figure 3.5. Sound levels for these traces are listed in Table 3.6. As expected, the shock has degenerated to the shape of a distorted sine wave since much of the high frequency content of the original shock has been absorbed or scattered. If cutoff phenomena were not involved, the peak flat sound level at the lateral cutoff distance for these flight conditions would be 129.8 decibels. The measured average peak sound level is 15.3 decibels lower at 114.5 decibels.

The relation between peak overpressure and CSEL for this flight is essentially the 26 decibel difference obtained earlier for N-waves. The relation between peak sound level and ASEL is hardly correlated, with ASEL having a range of 52.3 to 90.0 decibels although the range of peak sound level is less than 6 decibels.

Data for Pass 030 are characteristic of signals produced in the vicinity of cutoff, but not exactly at the point where a

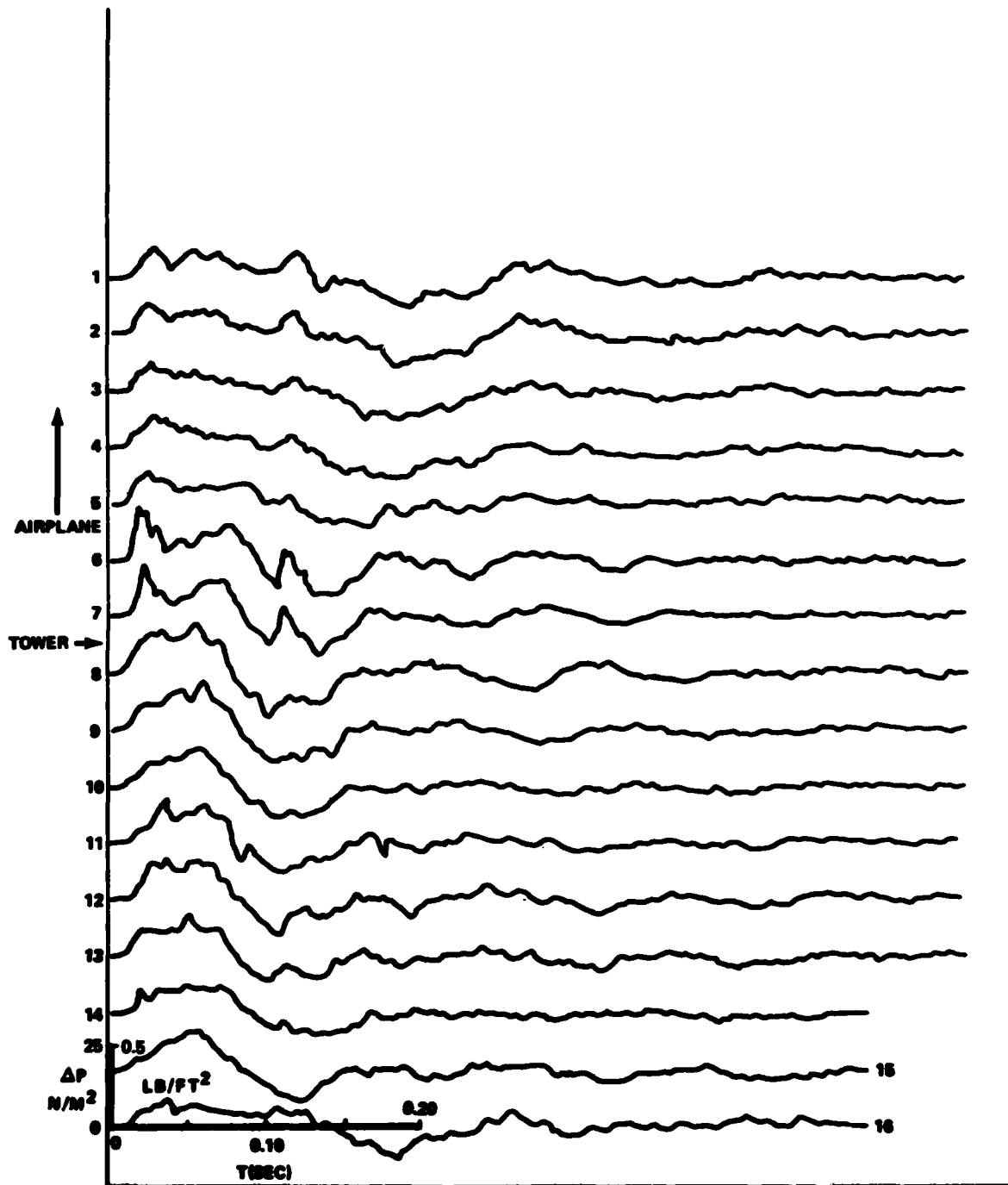


FIGURE 3.5 GROUND PRESSURE SIGNATURES BEFORE LATERAL CUTOFF—PASS 029, AUGUST 27, 1-1 -REF. 6

Table 3.6

Sound Levels in Decibels Measured at Ground
Positions Just Prior to Lateral Cutoff
Pass 029, Ref. 6

| Position | L_{pk} | L_E | L_{AE} | L_{CE} | $L_{pk} - L_E$ | $L_{pk} - L_{AE}$ | $L_{pk} - L_{CE}$ |
|----------|----------|-------|----------|----------|----------------|-------------------|-------------------|
| 1 | 112.8 | 102.1 | 86.7 | 90.9 | 10.7 | 26.1 | 22.0 |
| 2 | 111.8 | 101.8 | 83.9 | 88.6 | 10.1 | 28.0 | 23.3 |
| 3 | 111.2 | 101.9 | 81.2 | 85.6 | 10.1 | 30.0 | 25.6 |
| 4 | 113.4 | 102.3 | 79.4 | 86.5 | 11.1 | 34.0 | 26.9 |
| 5 | 113.3 | 100.8 | 59.4 | 86.6 | 12.6 | 54.0 | 26.7 |
| 6 | 118.1 | 103.5 | 90.0 | 94.0 | 14.6 | 28.1 | 24.1 |
| 7 | 116.7 | 102.5 | 87.8 | 92.8 | 14.6 | 28.9 | 23.9 |
| 8 | 117.4 | 104.6 | 82.0 | 89.5 | 12.9 | 35.5 | 27.9 |
| 9 | 117.7 | 103.7 | 78.5 | 88.1 | 14.0 | 39.2 | 29.6 |
| 10 | 115.2 | 102.4 | 52.3 | 85.2 | 12.7 | 62.9 | 30.0 |
| 11 | 115.9 | 101.7 | 88.8 | 91.1 | 14.2 | 27.0 | 24.7 |
| 12 | 115.4 | 102.7 | 89.3 | 91.8 | 12.7 | 26.1 | 23.6 |
| 13 | 115.0 | 101.6 | 87.5 | 90.2 | 13.4 | 27.5 | 24.7 |
| 14 | 111.6 | 100.1 | 84.3 | 86.9 | 11.5 | 27.3 | 24.8 |
| 15 | 115.1 | 101.4 | 85.8 | 87.9 | 13.7 | 29.3 | 27.2 |
| 16 | 111.0 | 101.1 | 58.8 | 84.7 | 9.9 | 52.3 | 26.3 |
| Avg. | 114.5 | 102.1 | 79.7 | 88.8 | 12.4 | 34.8 | 25.7 |
| Std.Dev. | 2.4 | 1.1 | 11.9 | 2.8 | 1.7 | 11.5 | 2.3 |

caustic is formed. Pressure-time traces are shown on Figure 3.6 and sound levels are listed in Table 3.7. Interestingly, peak sound level has an average of 109.4, almost 20 decibels below the N-wave prediction. Average CSEL and ASEL for this case, however, are almost the same as in the previous case. Obviously differences between peak sound level and CSEL are less here, and, characteristically, a wide range of ASEL's occurs for a narrow range of peak levels.

Pressure-time traces and sound levels for Passes 033 and 035 are shown in Figures 3.7 and 3.8, and Tables 3.8 and 3.9. These two cases have somewhat more caustic-like characteristics and higher peak sound levels than obtained during Passes 029 and 030. However, the high frequency "jitter" on these signals is almost gone, particularly on Pass 035. This feature shows up in the low average ASEL for 035, 59.1 decibels, even though it has the highest peak sound level average of the set, 119.0 decibels.

Despite the wide range of peak sound levels and ASEL's observed in these four cases, CSEL's are strikingly stable, having a range of 3 decibels for average CSEL as compared to more than 20 decibels for average ASEL, and 10 decibels for peak sound level. This stability is a valuable feature for use in predictive models. In this case, the CSEL average is 15.1 decibels below the CSEL that would be predicted for an N-wave not near cutoff.

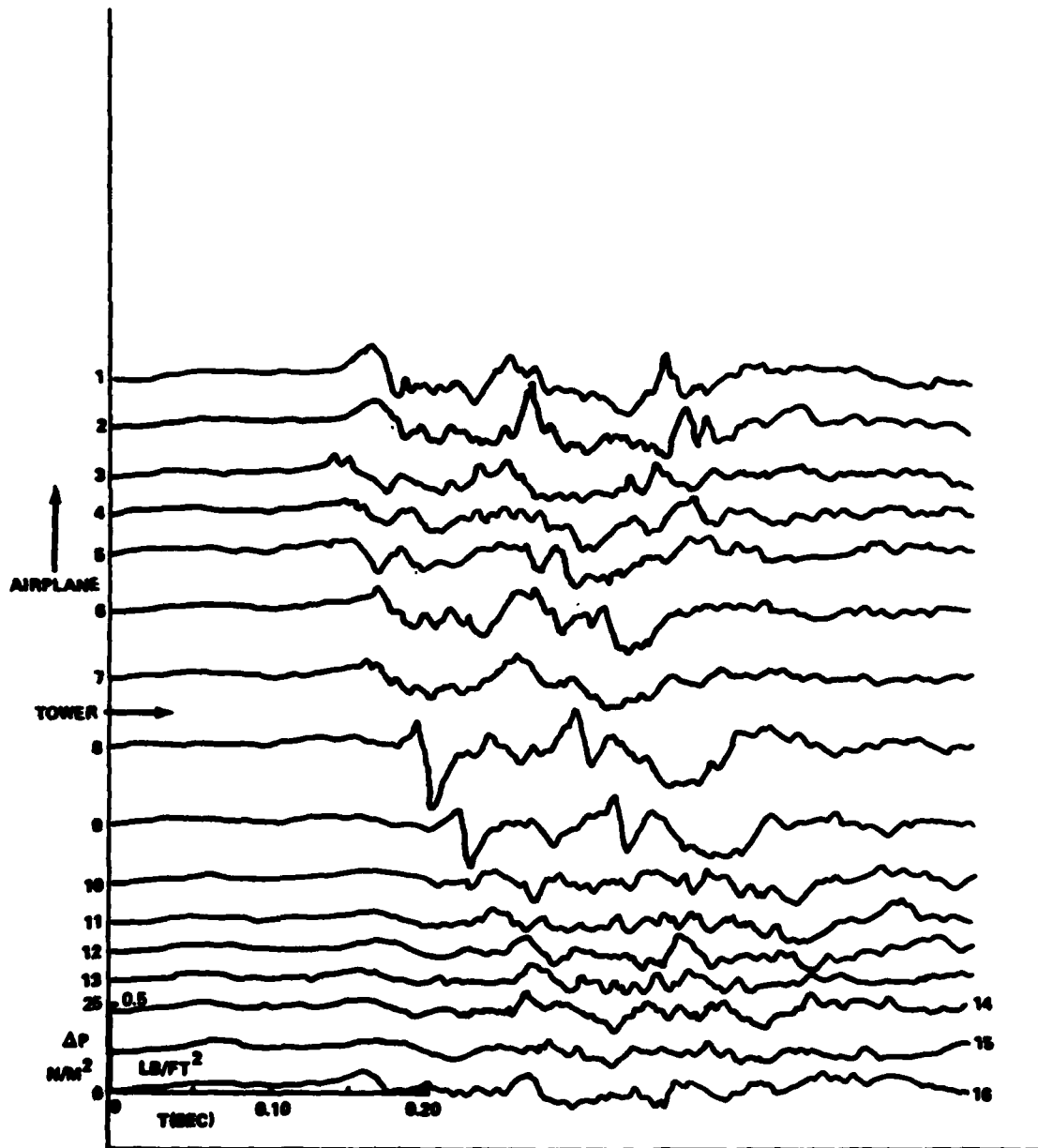


**FIGURE 3.6 GROUND PRESSURE SIGNATURES NEAR LATERAL CUTOFF
 -PASS 030, AUGUST 27, 1-2 -REF. 6**

Table 3.7

Sound Levels in Decibels Measured at Ground
Positions Near Lateral Cutoff
Pass 030, Ref. 6

| Position | L_{pk} | L_E | L_{AE} | L_{CE} | L_{pk}^- L_E | L_{pk}^- L_{AE} | L_{pk}^- L_{CE} |
|----------|----------|-------|----------|----------|---------------------|------------------------|------------------------|
| 1 | 114.3 | 100.0 | 85.8 | 90.6 | 14.1 | 28.3 | 21.9 |
| 2 | 114.3 | 100.2 | 86.0 | 92.4 | 14.1 | 28.3 | 21.9 |
| 3 | 107.9 | 97.8 | 83.1 | 87.5 | 10.1 | 24.8 | 20.4 |
| 4 | 109.4 | 98.2 | 75.8 | 86.7 | 11.2 | 33.6 | 22.7 |
| 5 | 107.9 | 98.2 | 87.5 | 61.7 | 9.7 | 46.1 | 20.3 |
| 6 | 108.8 | 99.0 | 90.0 | 92.0 | 10.3 | 18.8 | 16.8 |
| 7 | 109.5 | 98.4 | 90.2 | 91.3 | 11.1 | 19.4 | 18.2 |
| 8 | 113.3 | 102.2 | 86.5 | 94.7 | 11.2 | 26.9 | 18.6 |
| 9 | 108.8 | 98.9 | 82.1 | 91.8 | 9.9 | 26.7 | 17.0 |
| 10 | 106.6 | 94.9 | 67.5 | 86.0 | 11.6 | 39.0 | 20.6 |
| 11 | 109.6 | 95.2 | 84.6 | 87.1 | 14.4 | 25.0 | 22.5 |
| 12 | 108.2 | 94.2 | 83.9 | 88.1 | 13.3 | 24.3 | 20.1 |
| 13 | 109.7 | 94.7 | 81.3 | 87.0 | 15.0 | 28.4 | 22.7 |
| 14 | 108.1 | 93.8 | 77.1 | 85.3 | 14.3 | 31.0 | 22.8 |
| 15 | 104.1 | 90.6 | 75.0 | 79.7 | 13.5 | 29.1 | 24.4 |
| 16 | 108.1 | 96.4 | 68.3 | 86.2 | 11.7 | 39.8 | 21.9 |
| Avg. | 109.4 | 97.0 | 81.5 | 86.8 | 12.2 | 29.3 | 20.8 |
| Std.Dev. | 2.7 | 3.0 | 7.0 | 7.6 | 1.8 | 7.3 | 2.2 |

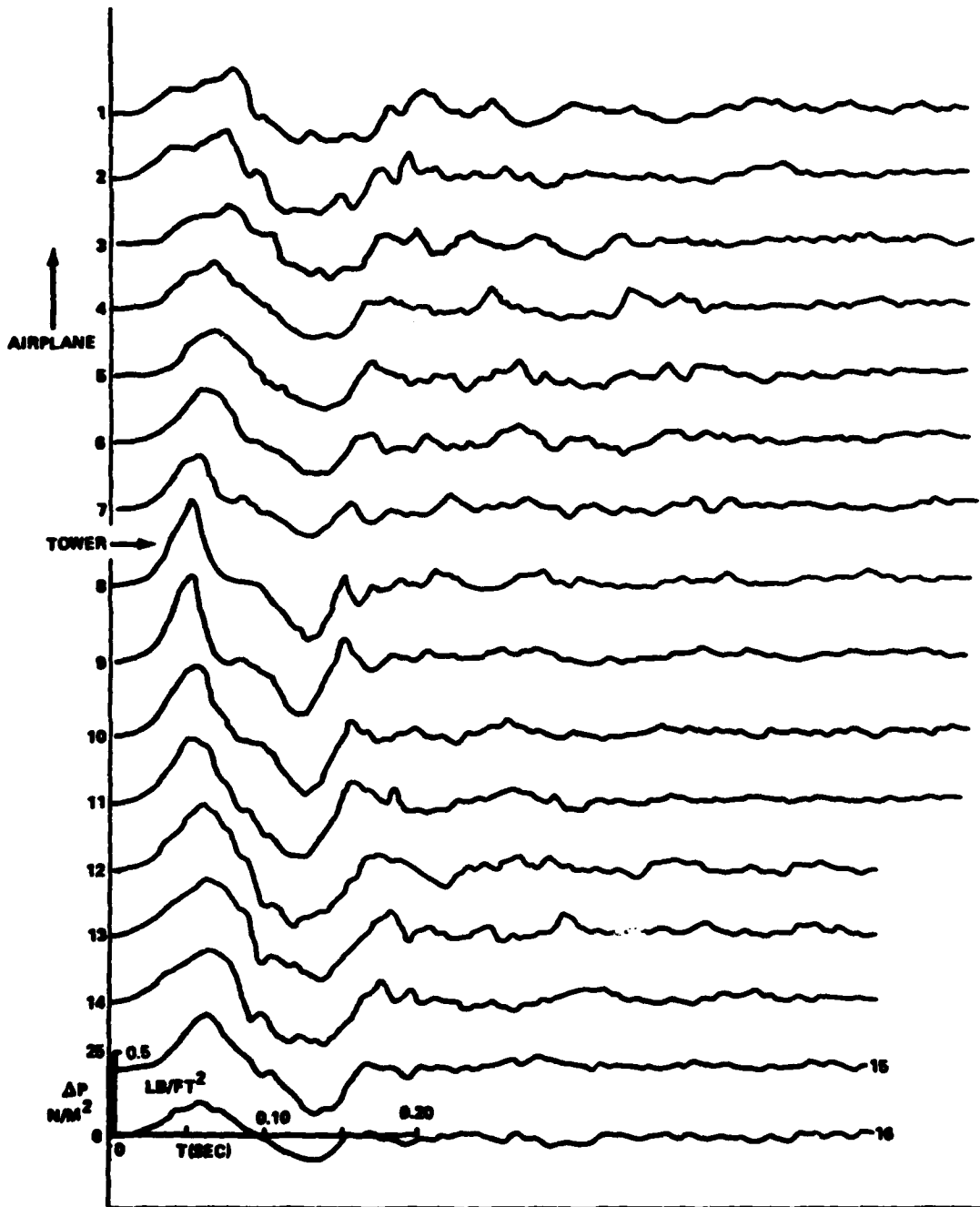


FIGURE 3.7 GROUND PRESSURE SIGNATURES NEAR LATERAL CUTOFF—PASS 033,
AUGUST 27, 2-2 - REF. 6

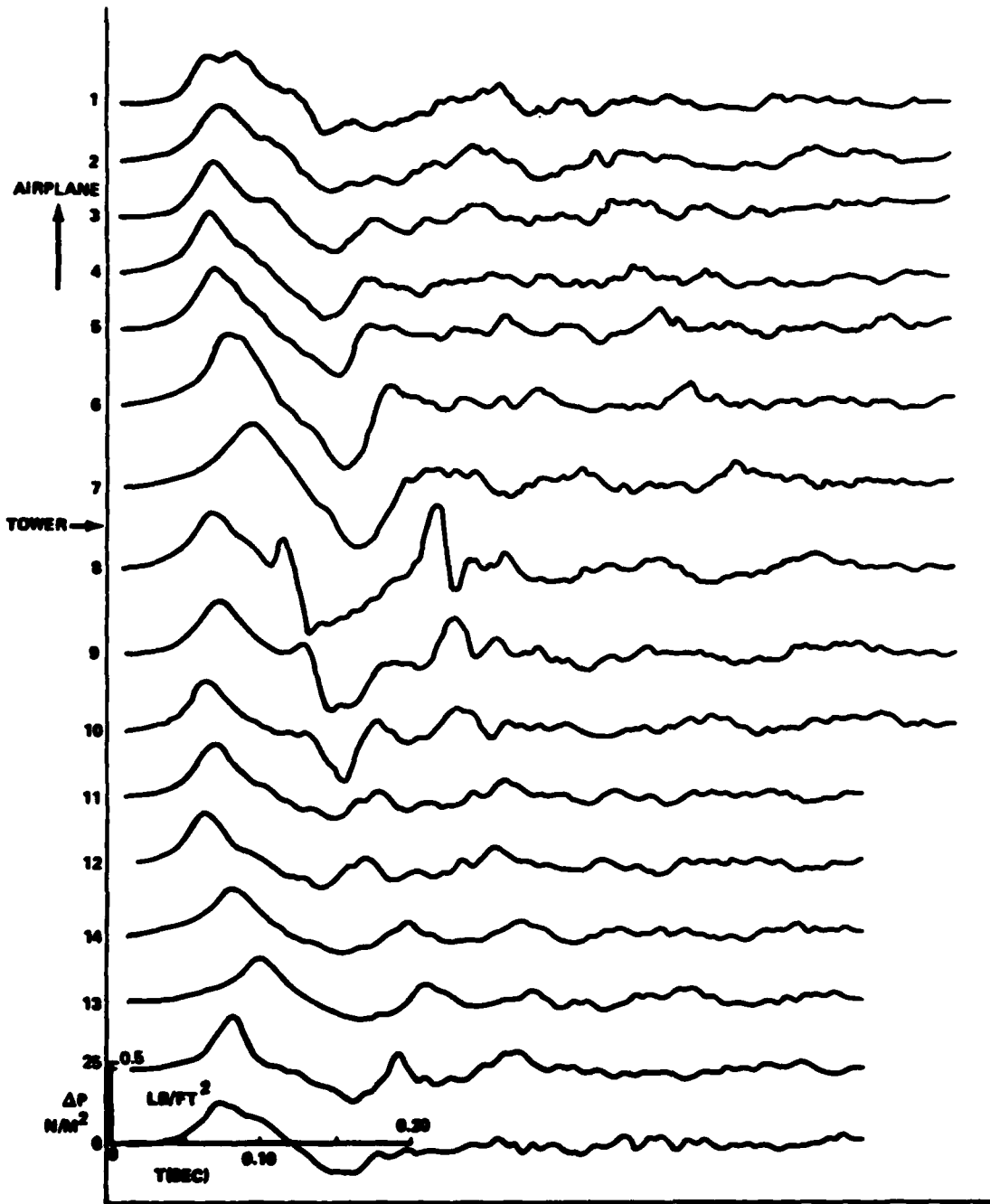


FIGURE 3.8 GROUND PRESSURE SIGNATURES NEAR LATERAL CUTOFF—PASS 035.
AUGUST 27, 3-1 - REF. 6

Table 3.8

Sound Levels in Decibels Measured at Ground
Positions Near Lateral Cutoff
Pass 033, Ref. 6

| Position | L_{pk} | L_E | L_{AE} | L_{CE} | L_{pk}^- L_E | L_{pk}^- L_{AE} | L_{pk}^- L_{CE} |
|----------|----------|-------|----------|----------|---------------------|------------------------|------------------------|
| 1 | 116.0 | 102.5 | 85.0 | 88.8 | 13.5 | 31.0 | 27.2 |
| 2 | 116.7 | 104.0 | 85.1 | 90.1 | 12.7 | 31.6 | 26.6 |
| 3 | 114.1 | 102.5 | 81.1 | 87.1 | 11.6 | 33.0 | 27.0 |
| 4 | 116.0 | 102.7 | 79.9 | 85.9 | 13.3 | 36.2 | 30.1 |
| 5 | 116.2 | 102.8 | 55.1 | 85.4 | 13.4 | 61.0 | 30.7 |
| 6 | 117.4 | 103.5 | 86.0 | 90.2 | 13.8 | 31.4 | 27.2 |
| 7 | 117.4 | 102.2 | 87.3 | 91.0 | 15.1 | 30.0 | 26.4 |
| 8 | 121.7 | 105.8 | 79.0 | 92.7 | 16.0 | 42.7 | 29.0 |
| 9 | 122.2 | 105.8 | 80.5 | 94.5 | 16.4 | 41.7 | 27.7 |
| 10 | 120.5 | 105.8 | 57.1 | 90.7 | 14.7 | 63.4 | 29.8 |
| 11 | 120.4 | 106.6 | 89.6 | 93.4 | 13.8 | 30.8 | 27.0 |
| 12 | 120.4 | 107.2 | 88.9 | 92.5 | 13.2 | 31.5 | 27.9 |
| 13 | 118.2 | 105.6 | 88.1 | 92.1 | 12.6 | 30.2 | 26.1 |
| 14 | 117.4 | 105.2 | 85.1 | 91.0 | 12.2 | 32.3 | 26.4 |
| 15 | 118.2 | 104.2 | 79.2 | 89.5 | 14.0 | 39.0 | 28.7 |
| 16 | 113.4 | 100.4 | 49.8 | 83.1 | 13.0 | 63.6 | 30.3 |
| Avg. | 117.9 | 104.2 | 78.6 | 89.9 | 13.7 | 39.3 | 28.0 |
| Std.Dev. | 2.6 | 1.9 | 12.7 | 3.1 | 1.3 | 12.2 | 1.5 |

Table 3.9

Sound Levels in Decibels Measured at Ground
Positions Near Lateral Cutoff
Pass 035, Ref. 6

| Position | L_{pk} | L_E | L_{AE} | L_{CE} | L_{pk}^- L_E | L_{pk}^- L_{AE} | L_{pk}^- L_{CE} |
|----------|----------|-------|----------|----------|---------------------|------------------------|------------------------|
| 1 | 117.9 | 104.5 | 56.6 | 87.6 | 13.4 | 61.3 | 30.3 |
| 2 | 118.9 | 105.2 | 56.2 | 86.5 | 13.7 | 62.7 | 32.4 |
| 3 | 118.4 | 103.3 | 54.8 | 88.0 | 15.0 | 63.6 | 30.3 |
| 4 | 119.5 | 104.7 | 59.3 | 89.2 | 14.9 | 60.2 | 30.4 |
| 5 | 119.9 | 105.3 | 61.1 | 90.1 | 14.6 | 58.7 | 29.7 |
| 6 | 121.1 | 107.5 | 58.1 | 91.1 | 13.5 | 63.0 | 30.0 |
| 7 | 120.2 | 107.5 | 54.3 | 89.7 | 12.7 | 66.0 | 30.5 |
| 8 | 119.7 | 107.6 | 65.4 | 96.7 | 12.1 | 54.3 | 23.0 |
| 9 | 118.3 | 105.7 | 62.5 | 92.7 | 12.5 | 55.8 | 25.6 |
| 10 | 118.0 | 103.4 | 61.3 | 90.3 | 14.6 | 56.7 | 27.8 |
| 11 | 118.1 | 102.0 | 55.5 | 86.7 | 16.2 | 62.6 | 31.4 |
| 12 | 117.7 | 102.3 | 55.8 | 87.8 | 15.5 | 62.0 | 30.0 |
| 13 | 117.0 | 101.0 | 49.0 | 83.2 | 15.5 | 67.5 | 33.4 |
| 14 | 125.2 | 112.3 | 84.9 | 96.6 | 12.9 | 40.3 | 28.6 |
| 15 | 118.5 | 102.4 | 59.2 | 90.0 | 16.1 | 59.3 | 28.5 |
| 16 | 116.1 | 102.6 | 51.5 | 84.5 | 13.5 | 64.6 | 31.5 |
| Avg. | 119.0 | 104.8 | 59.1 | 89.4 | 14.0 | 59.9 | 29.6 |
| Std.Dev. | 2.1 | 2.9 | 8.0 | 3.7 | 1.2 | 6.4 | 2.5 |

4.0 IMPROVED MODELS FOR ASSESSING ENVIRONMENTAL IMPACT OF SONIC BOOMS PRODUCED DURING AIR COMBAT MANEUVERING

The purpose of the work described in the previous sections of this report was either to substantiate the model of Ref. 1 from a broader data base, or to provide information which would permit development of an improved model. The data developed in this study support the conceptual aspects of the original model and provide the means for refining and broadening its applicability. These refinements are discussed in this section.

It should be noted that a key element in all the analyses considered here is the fundamental reliance on the Carlson [6] model to predict sonic boom parameters when airplane type, Mach number, pitch angle, and altitudes are known. None of the work reported here involved direct measurements to validate this model. Although increased confidence in the analysis concept is obtained from this study, validation through a measurement program still remains to be done.

The basic concept of the ACM sonic boom model of Ref. 1 is that, for any point within a specifiable geographic region on the ground, sonic booms will occur randomly in time, but with statistically definable properties. These properties include probabilities of receiving one or more booms per day, boom strength, and average (mean square) sound levels. These quantities, in turn, are dependent on airplane type, ground elevation, and number of sorties per day. It is convenient to consider the model as having three components:

- 1) Distribution of boom magnitudes,
- 2) Distribution of flight time per sortie during which a sonic boom reaches the ground,

3) Spatial distribution of sonic booms.

Each of these components is considered here.

4.1 Sonic Boom Magnitudes

Data obtained from ACMI at Luke and Nellis AFB's were described in Section 2 for each airplane type. Data were provided (in Tables 2.2 and 2.3, pages 14 and 15) to specify a single Mach number and effective height (for each airplane type) that can be used to calculate a value for CSEL (or other parameter) that is the root-mean-square (or "energy") average sound level for each airplane's distribution of flight conditions. These rms values, for points directly below the airplane flight path, will be used later in this report to obtain long term average sound levels, and are listed here in Table 4.1.

The rms CSEL's listed in Table 4.1 are specific to the two different ranges studied here. These sound levels may be different at other ranges due to several basic factors. Increases in rms airplane altitude above mean sea level, for the same effective height above ground, will reduce sound levels marginally. Increases in effective height due to increases in minimum terrain clearance requirements will reduce sound levels more rapidly than absolute altitude increases alone. Different mission characteristics may also increase effective height and absolute altitude. There is evidence for this in the differences between F-16 flights at Luke as compared to all other airplanes at Luke and F-16 flights at Nellis.

Adjustments to the rms sound levels listed in Table 4.1 for changes in any flight parameters may be made from the equations listed in Appendix A as long as the overall distribution function characteristics relative to the rms value of that distribution is assumed to remain constant.

Table 4.1
Parameters for Supersonic Flight That
Represent RMS Values of Distributions

| A/C | AFB | Rms No. Events per sortie $M > M_c$ | Rms Mach No. | Effective height - ft. | Rms CSEL - dB | $d_{y,c}$ -1000 ft. | Rms duration - sec. | Rms carpet length -1000 ft. | Rms area -sq.mi. | Space Average Rms CSEL - dB |
|------|--------|-------------------------------------|--------------|------------------------|---------------|---------------------|---------------------|-----------------------------|------------------|-----------------------------|
| P-4 | Nellis | 1.1 | 1.088 | 9,000 | 115.7 | 13.8 | 62.2 | 66.2 | 52.4 | 115.3 |
| P-4 | Luke | 3.1 | 1.110 | 17,000 | 111.0 | 22.1 | 71.7 | 74.8 | 94.9 | 110.2 |
| P-5 | Luke | 0.7 | 1.090 | 10,750 | 112.8 | 18.3 | 42.9 | 45.4 | 47.7 | 111.7 |
| P-14 | Luke | 0.4 | 1.04 | 2,500 | 124.9 | 6.7 | 28.5 | 30.9 | 11.9 | 123.0 |
| P-15 | Nellis | 0.8 | 1.167 | 15,000 | 112.4 | 29.3 | 50.2 | 52.1 | 87.6 | 111.1 |
| P-15 | Luke | 0.8 | 1.090 | 11,750 | 114.7 | 18.7 | 44.8 | 47.5 | 51.0 | 113.7 |
| P-16 | Nellis | 1.1 | 1.181 | 9,500 | 114.2 | 28.7 | 31.2 | 32.9 | 54.2 | 112.1 |
| P-16 | Luke | 0.6 | 1.212 | 27,000 | 105.4 | 43.4 | 52.9 | 52.6 | 131 | 104.3 |

4.2 Fractions of Flight Time When Sonic Booms Are Generated

Mach number, altitude, and effective height distributions as described above allow prediction of an rms sound level when a boom is produced that propagates to the ground. In order to determine the long-term average sound level for a series of flight missions it is necessary to know how often a propagating boom is produced during a typical sortie. It is also necessary to know how long the airplane flies at a Mach number above cutoff when it is supersonic in order to calculate the geographic extent of the sonic boom "carpet."

As shown earlier in Tables 2.2 and 2.3, there is a substantial difference in the number of supersonic events per sortie from one airplane type to another, and a wide range of supersonic durations from one event to another for each airplane type. Again, since long-term average sound level is the primary interest here, the effective durations of supersonic flight during which booms can be expected to reach the ground can be represented by the average number of events above cutoff Mach number per sortie, and the rms duration obtained from the distribution of durations observed for each airplane type. These data are summarized in Table 4.1.

4.3 Spatial Distribution of Sonic Booms

4.3.1 Rms Area and Sound Exposure Levels For Sonic Boom Carpets

Data have been developed, so far, to obtain CSEL (or other sound level measures) on the ground track of an airplane, and to obtain an rms duration of flight. In addition, Mach number, cutoff Mach number and airplane altitude determine the lateral cutoff distance, $d_{y,c}$, beyond which the boom is refracted

upwards and no longer intercepts the ground. If constant speed is assumed, the carpet boom produced on the ground will have an rms area that has a length equal to the airplane speed times the rms duration, and a width that is twice the lateral cutoff distance.

Rms areas for the observations at Luke and Nellis are listed in Table 4.1. Following Magleri [8], the essential area covered is truncated at lateral distances of 0.8 times the lateral cutoff distance, since the booms have disintegrated into low level events by that distance.

An important point to be aware of here is the sensitivity of lateral cutoff distance to airplane height. As height increases, cutoff Mach number increases (below 35,000 feet), and lateral cutoff distance decreases. In adapting the data from this report to different circumstances these features should be kept in mind. For example, at sea level, if airplane height above terrain remains the same as at Luke, the width of the boom carpet increases by 9 percent. On the other hand, if the terrain is at an elevation of 4000 feet, and airplane height above terrain is maintained constant, the width of the boom carpet shrinks to 68 percent of the width at Luke, or 63 percent of that at sea level.

The rms CSEL values listed in Table 4.1 apply to points on the ground directly below the airplane's flight path (i.e. on the flight track). At points off track boom overpressures, and sound exposure levels, decrease with increasing distance (overpressures decrease at $3/4$ power function of distance, for example). For ease of computation, it is useful to assign space average values for overpressures or sound levels to the rms carpet area defined above. The space average CSEL over the carpet may be closely approximated as the level directly under the flight path, minus one-third of the difference in CSEL

between the level under the flight path and the level at 0.8 times the lateral cutoff distance. Using equations 7 and 13 of Appendix A, the space average CSEL is thus:

$$\bar{L}_{CE} = L_{CE} - 5 \log \frac{[(0.8d_{y,c})^2 + h^2]^{\frac{1}{2}}}{h} \quad (4.1)$$

where L_{CE} is the rms value of CSEL underneath the flight path, h is effective height above ground, and $d_{y,c}$ is lateral cutoff distance. This may also be written as:

$$\bar{L}_{CE} = L_{CE} - 2.5 \log (1 + \Delta^2) \quad (4.2)$$

where

$$\Delta = 0.8 \left(\frac{1 + M_c}{M} \right) \left(\frac{M^2 - M_c^2}{M_c^2 - 1} \right)^{\frac{1}{2}} \quad (4.3)$$

M is flight Mach number and M_c is cutoff Mach number (as defined in Appendix A).

Values for space average rms CSEL are listed in Table 4.1 for the different airplanes observed at Luke and Nellis.

4.3.2 Spatial Distribution of Flight Tracks

Up to this stage of the data interpretation the analysis has followed the same line of reasoning as in the development of the model in Ref. 1. In the development of that model insufficient data were available to define the spatial distribution of flight tracks other than to circumscribe an ellipse around the flight tracks and to assume equal probability that an airplane could be anywhere within the ellipse. The data discussed in Section 2 of this report allow a significant refinement to the equal probability assumption.

Review of the Luke data for individual airplanes types indicated that the amount of data still appeared to be too small

to obtain sensible distributions of flight tracks, although the amount of F-15 data probably is adequate. A more satisfying data set was obtained by aggregating all flight tracks where Mach number was above cutoff, irrespective of airplane type. These are the data shown in Figure 2.2 on page 16.

As described in Section 2, the ACMI data for each flight were segregated into the number of seconds a flight intercepted a series of incremental "cells" of the variables of interest. Segregation of aircraft position, projected to the ground plane, was obtained by checkerboard-like cells in the X-Y coordinate plane. The data were segregated by computer into cells that are squares with dimension of one mile per side. In order to see patterns in the data a little more easily, the one mile squares were added together to form a grid of square cells whose sides were four miles long. Further, the distinctive alignment of flight tracks at an angle with the coordinate axes was accounted for by displacing successive cells in the vertical structure by one-half a cell per row. The resulting pattern is shown in Figure 4.1.

The number of seconds during which a flight track was contained within each 4 mile square cell are shown by the numerals within the squares on Figure 4.1. These numbers can be used to redefine the principal axes of the flight track distributions, and to develop a probability density estimate for fraction of flights intercepting individual cells. As can be seen almost by visual inspection of Figure 2.2, a new set of x,y axes, labelled x',y' on Figure 4.1 can be selected from the numerical data, with the origin displaced to the cell that has the highest density of tracks.

One can make the empirical assumption that the two new axes form the major and minor axes for a series of ellipses. (This assumption provides a convenient geometry for various

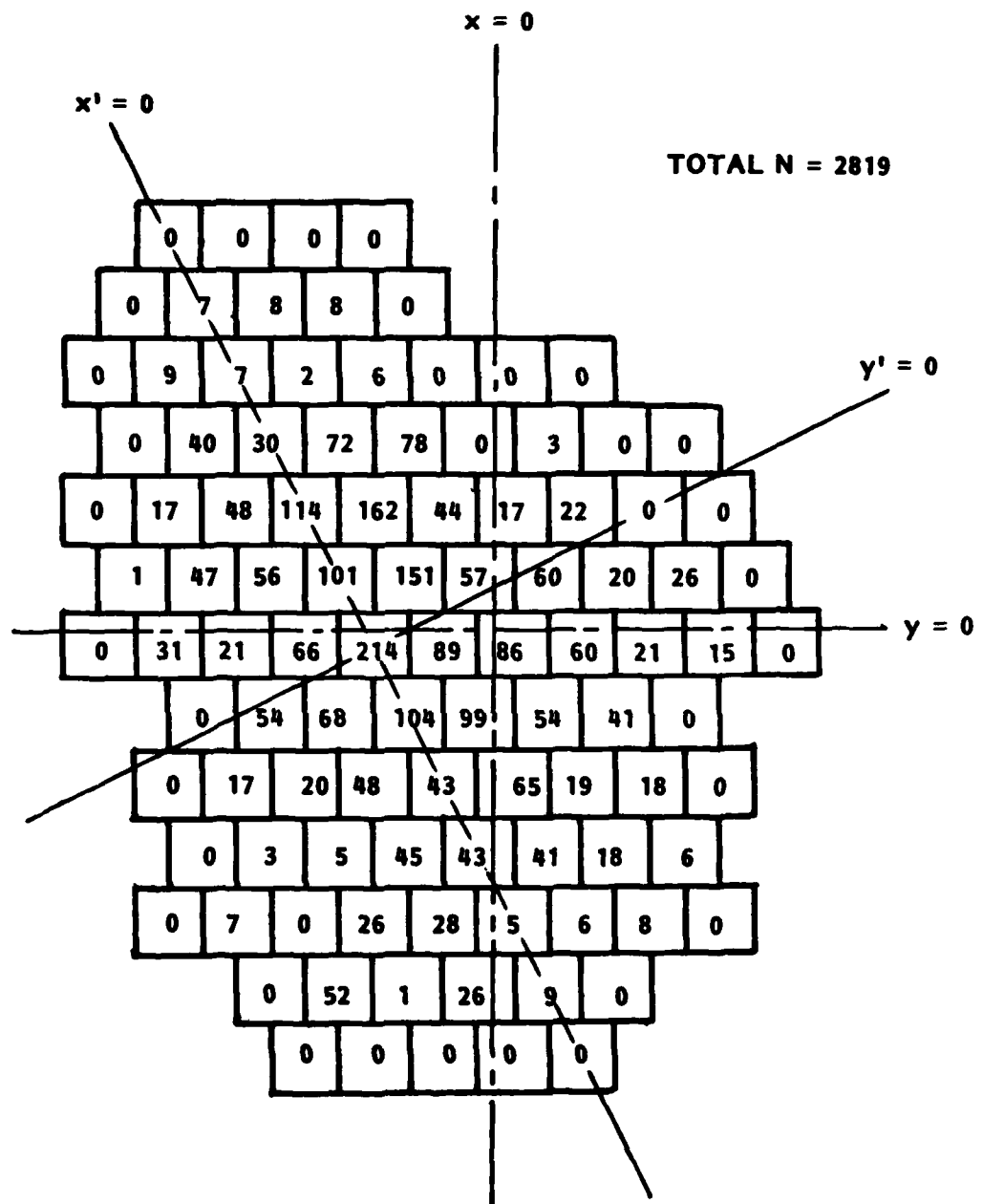


FIGURE 4.1 NUMBER OF SECONDS OF FLIGHT WITHIN 4 x 4 MILE CELLS - ALL AIRCRAFT WHERE $M > M_c$ - LUKE AFB

computations). A somewhat crude estimate of probability density functions along these axes can then be obtained from the cell counts. Because the cells are not exactly aligned properly for the axes chosen, some averaging is useful between some adjacent cells. The resulting distributions obtained in this manner are plotted in Figure 4.2 and designated as "observed distribution."

For computational purposes it is useful to approximate these empirical distributions with an analytic function that is easily integratable. Further, there is no reason to assume that the asymmetries observed in the data are due to other than finite sample sizes. With these points in mind, least squares fits of power functions were made to the data. The resulting functions are shown on Figure 4.2 as "estimated distribution." The equations used are:

$$x' = 1.126(x+18) \quad (4.4)$$

$$y' = 0.4279(x+24) \quad (4.5)$$

These estimated probability density functions were then integrated over a series of distance intervals along each axis to obtain cumulative distributions. With a moderate amount of rounding (to avoid implying unwarranted precision with arbitrary decimal values) the distances along each axis that incorporate various cumulative fractions of the data are listed in Table 4.2. Using these distances as semi-chords of ellipses yields the areas also listed in Table 4.2. The sizes and shapes of the ellipses are shown in Figure 4.3.

Table 4.2

Dimensions of Ellipses Enclosing Specified
 Cumulative Fractions of Flight Tracks -
 All Aircraft Where $M > M_c$, Luke AFB

| Cumulative Percent of Flights | Major Semi- Chord - statute miles | Minor Semi- Chord - statute miles | Area - square statute miles |
|-------------------------------------|---|---|--------------------------------------|
| 25 | 5 | 4 | 63 |
| 50 | 8 | 6.5 | 163 |
| 75 | 12 | 9.5 | 358 |
| 90 | 18 | 14 | 792 |
| 99 | 24 | 18 | 1357 |

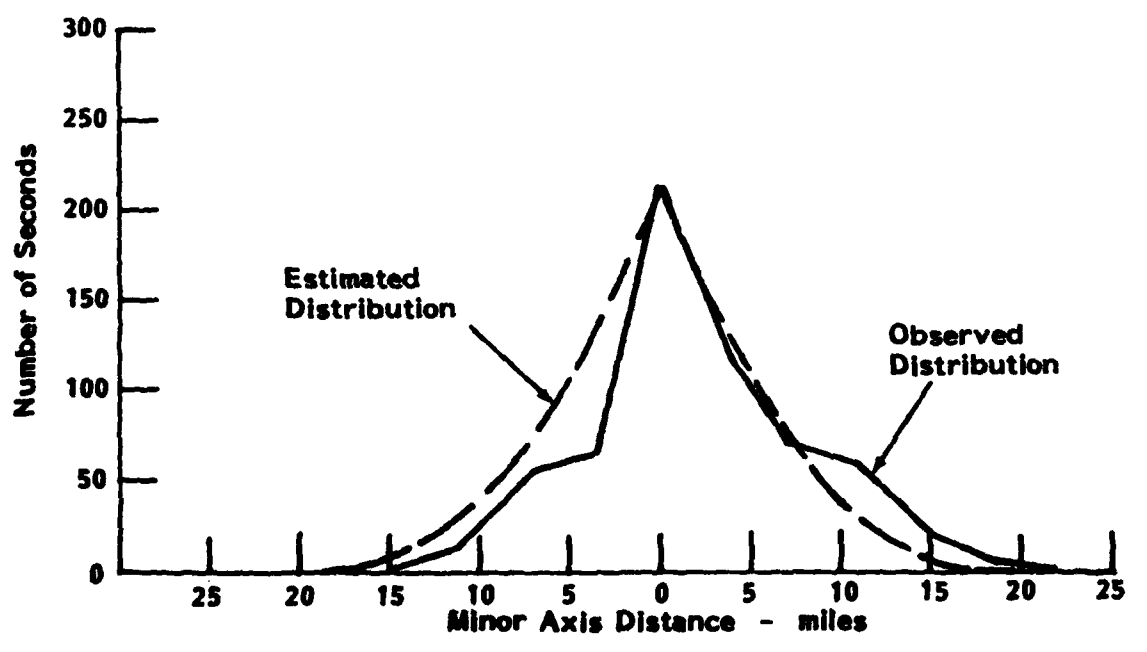
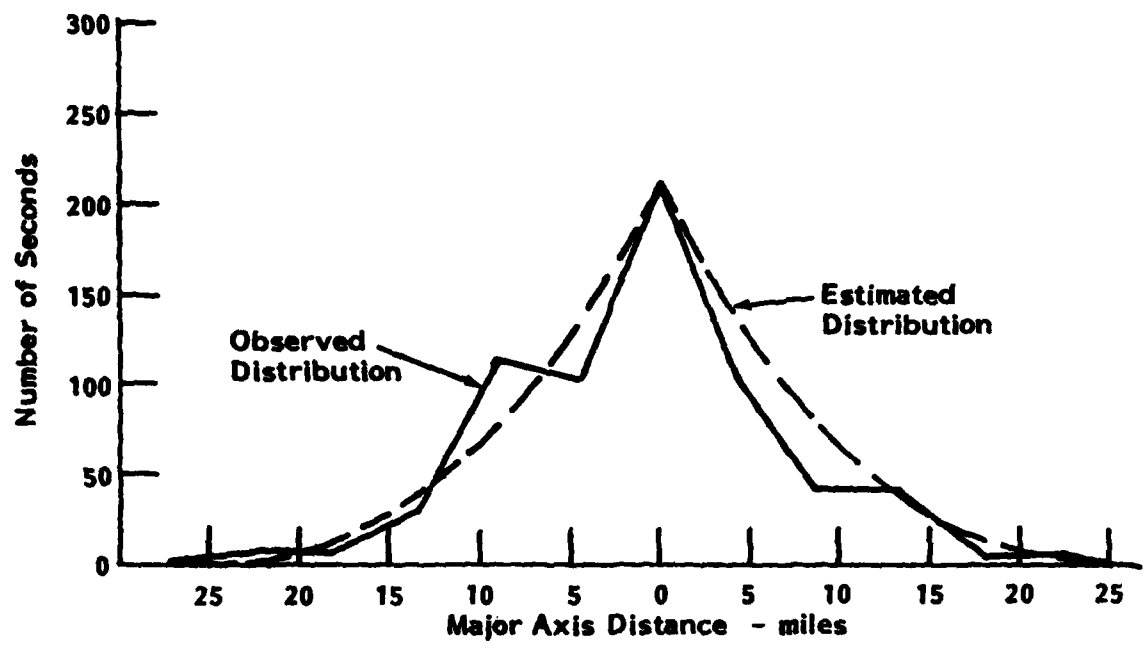


FIGURE 4.2 SPATIAL DENSITY DISTRIBUTIONS OF FLIGHT TRACKS FOR ALL AIRCRAFT WHERE $M > M_c$ - LUKE AFB

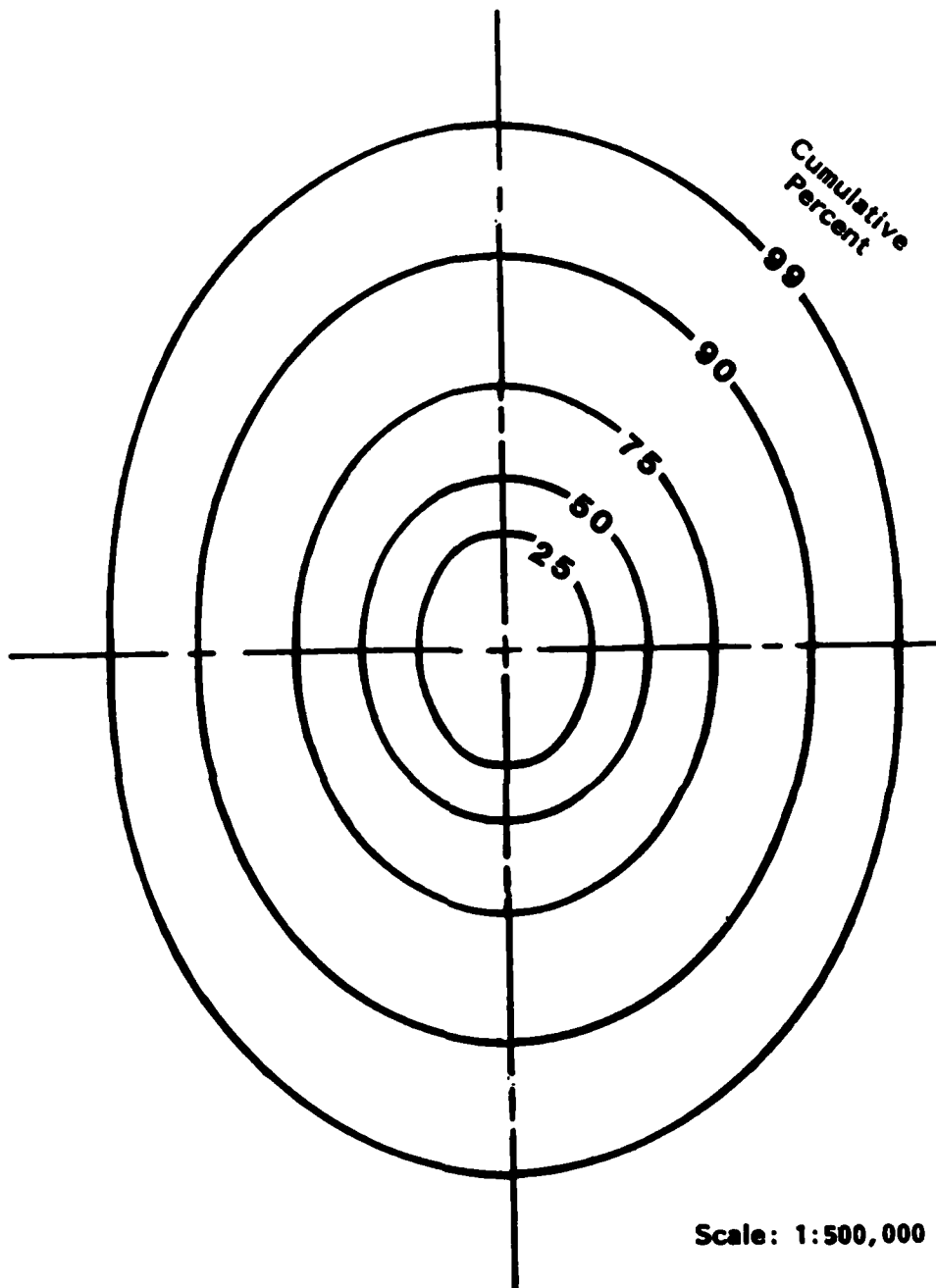


FIGURE 4.3 AREA ENCLOSING SPECIFIED PERCENT OF FLIGHT TRACKS FOR ALL AIRCRAFT WHERE $M > M_c$ - LUKE AFB

4.3.3 Spatial Distribution of Sonic Booms

All would be made more simple in these computations if an airplane would simply produce its sonic boom at points along the flight track directly below the airplane. As shown in Appendix A, this is not the way sonic booms propagate. At any instant where an airplane generates a sonic boom, the boom leaving the airplane at that time will not reach the ground until traveling a distance, d_x , along the flight track as measured from a point beneath the airplane. For the Luke data, an rms average d_x for the F-5 and F-15 airplanes is 5.4 statute miles.

Referring to Figure 4.3, if one assumes an airplane produces a boom while flying upward from the bottom of the 25 percent ellipse along the major axes, the boom produced at the instant the ellipse was crossed would not reach the ground until 0.4 miles beyond the origin. By the time the airplane reaches the top of the ellipse, the boom won't reach the ground until it is 2.4 miles into the annular area beyond the 50 percent ellipse.

If one assumes that within any elliptical annulus there is an equal probability that an airplane can fly in any direction, one can develop a spatial distribution of boom occurrence, weighted by the spatial distribution of flight tracks. This computation is shown graphically in Figure 4.4. The procedure used was to define the possible extent of boom coverage by an airplane flying anywhere within an annular area. This region is then multiplied by the fraction of the cumulative distribution of flight tracks within the annulus.

At any distance from the origin the cumulative fraction of booms expected is calculated by summing over all the annular areas. These sums are also shown in Figure 4.4. Obviously the steps in the distribution are produced solely by the simplicity

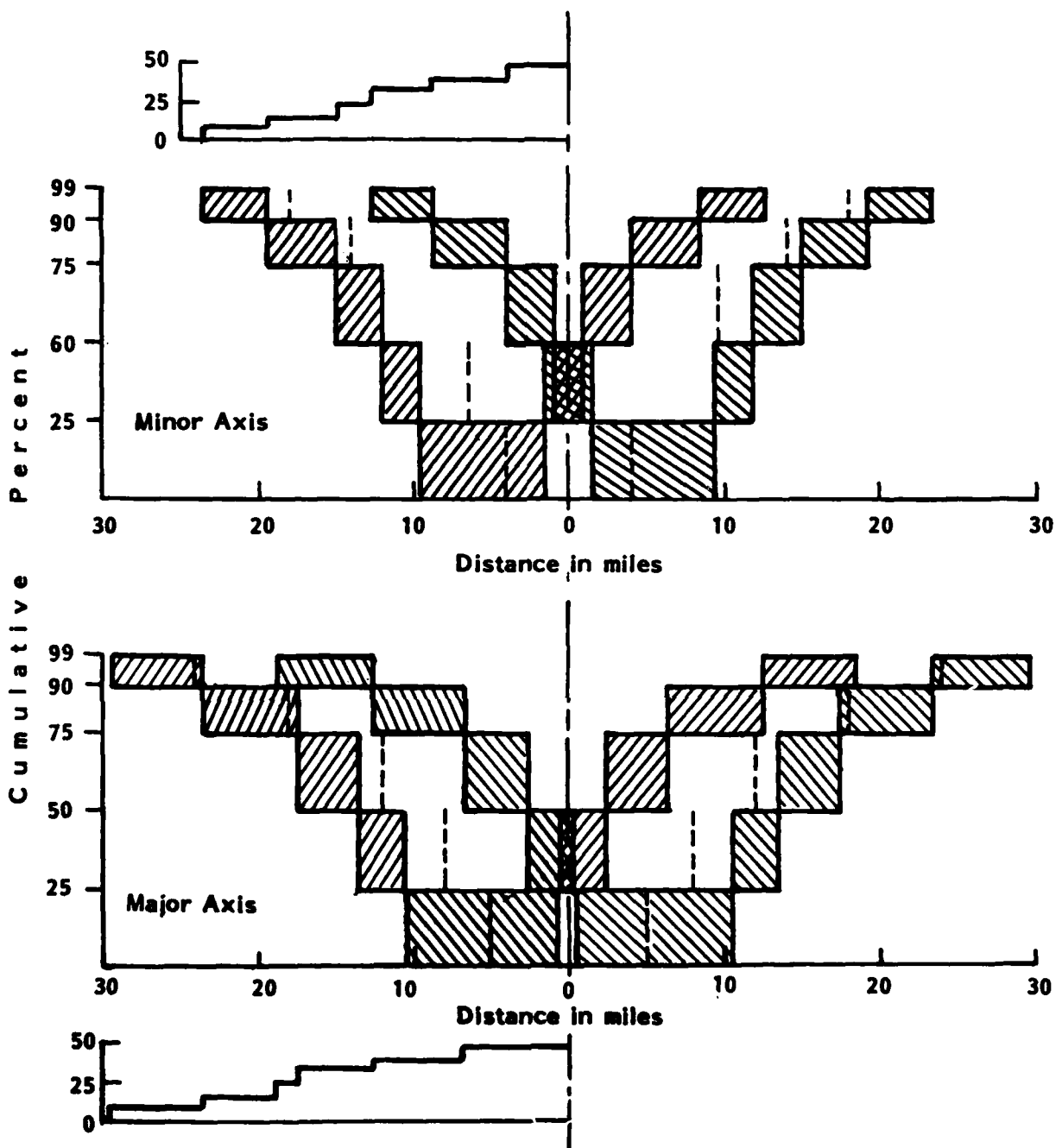


FIGURE 4.4 DISTRIBUTION OF REGIONS WHERE BOOMS COULD OCCUR WITH EQUAL PROBABILITY TO BE ANYWHERE WITHIN AN ANNULAR AREA

of the analysis. A more refined method would show the function to be smooth with continuous derivatives. Assuming this smoothing, one can restate the cumulative distribution in terms of decibels relative to the level of operations at the origin. In essence this provides a temporal/spatial distribution function, expressed in decibels.

The resulting distribution is reflected in several contours that will eventually have sound level values assigned to them. As a working tool, the contours are shown on a relative basis in Figure 4.5. The dimensions of the ellipses are listed in Table 4.3.

Table 4.3

Dimensions of Ellipses Used To
Determine Average Sound Level
For Air Combat Maneuvering

| Level in decibels re center of ellipse | Major Semi- Chord - statute miles | Minor Semi- Chord - statute miles | Area - square statute miles |
|--|---|---|--------------------------------------|
| - 1 | 7 | 4 | 88 |
| - 3 | 18 | 14 | 792 |
| - 6 | 22 | 18 | 1244 |
| - 10 | 27 | 22 | 1866 |

Center of ellipse is 2.2 decibels greater than space average from center to - 10 decibel contour

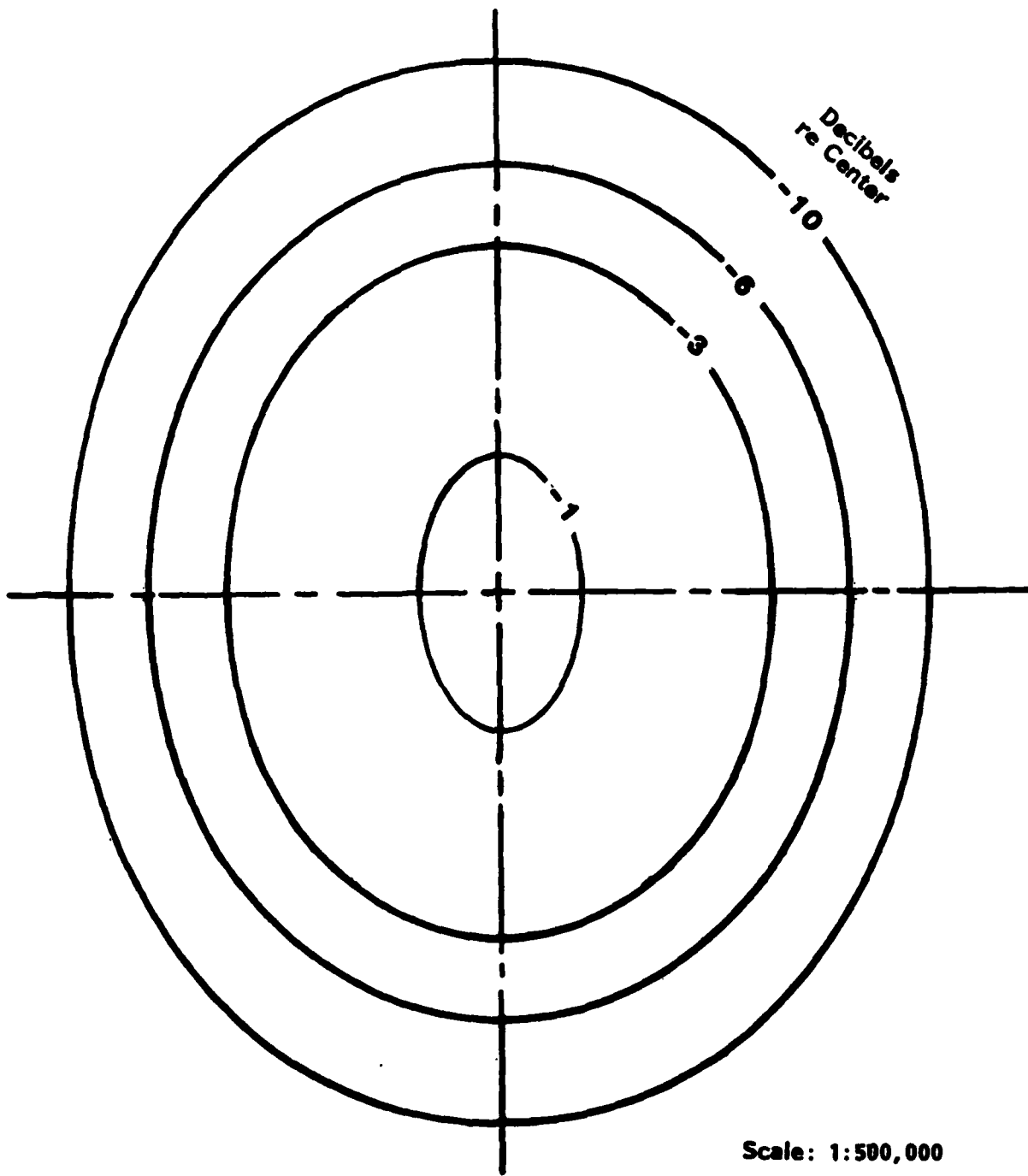


FIGURE 4.5 TEMPLATE FOR CALCULATING SOUND EXPOSURE LEVEL CONTOURS, LUKE AFB

4.3.4 Long-Term Average Sound Exposure Level

The data in Table 4.1 can now be used to assign a numerical value to the contours shown in Figure 4.5. Using the values for an F-15 at Luke, the space average rms CSEL for a single carpet boom is 113.7 decibels, with an rms carpet area of 51 square miles. The space average CSEL over the maneuvering area is simply the carpet boom rms CSEL, reduced by 10 times the logarithm of the ratio of the carpet boom area to the maneuvering regions area--taken to be the - 10 decibel area in Table 4.3. That is:

$$\langle \bar{L}_{CE} \rangle = 113.7 + 10 \log \frac{51}{1866} = 98.1 \quad (4.4)$$

As stated in Table 4.3, the CSEL at the origin of the ellipses is 2.2 decibels higher than the space average, thus in this example, the origin has a CSEL of $98.1 + 2.2 = 100.3$ decibels. CSEL for each of the contours in Figure 4.5 is now obtained by subtracting the contour offset numbers from 100.3. For example, the - 10 decibel contour on Figure 4.5 would be labeled as a CSEL of 90.3 decibels in this case.

4.3.5 Long-term Average Sound Level

The CSEL contours developed above may now be translated to C-weighted average sound levels (or day-night average sound levels) by appropriate restatement of the numerical values associated with the contours. Recall that a general statement for average sound level is:

$$L_T = \bar{L}_E + 10 \log N_{\text{eff}} + 10 \log \frac{1}{T} \quad (4.5)$$

where \bar{L}_E is mean-square average sound exposure level, N is the effective number of operations (which includes nighttime adjustments if applicable), and T is the time interval in seconds over which the averaging takes place.

When T is 86,400, or 24 hours, and L_E is C-weighted, the resulting L_T becomes C-weighted day-night average sound level (CDNL). If no night operations are involved, which is usually the case in a training situation, the resulting 24 hour average sound level is also called equivalent sound level.

Returning to the numerical example developed above, the CSEL contours are converted to CDNL by determining N_{eff} for a typical situation, and making the appropriate calculation to obtain the average. Two pieces of information are required. One needs to know how many sorties will take place in a 24-hour period, based on long-term averages, and again on a long-term average basis, how many propagating booms will be produced per sortie. This last number is listed in Table 4.1.

Continuing with an F-15 example, from the table one can expect 0.8 propagating booms per sortie. Typical usage might be 15 sorties per day, 5 days per week. For 24 hours, the constant $10 \log 1/T$ becomes - 49.4 decibels. The resulting expression becomes:

$$L_{Cdn} = \bar{L}_{CE} + 10 \log (15 \times \frac{5}{7} \times 0.8) - 49.4 \quad (4.6)$$
$$L_{Cdn} = L_{CE} - 40.1$$

The contours in Figure 4.5 may now be relabeled. In Section 4.3.5 it was found that the CSEL for the origin was 100.3 decibels. Subtracting 40.1, the origin would now be designated as a CDNL of 60.3 decibels, with the contours redesignated accordingly.

4.3.6 Comparison to Previous Model

The model developed in Ref. 1 was based on 21 sorties of F-15 airplanes at the offshore Oceana MOA. These flights were performed by experienced pilots from an operationally ready

fighter wing. The range is smaller in overall dimensions than either that of Luke or Nellis, and has an operational floor of 10,000 feet above sea level. Neither the Luke nor Nellis ranges has such a floor.

Despite these differences, the effective Mach number and effective heights for F-15 airplanes of all three ranges are quite similar, resulting in similar rms CSEL's: 112.7 at Nellis, 113.2 at Oceana, 114.7 at Luke. Average time on range per sortie is similar, and the 0.8 propagating booms per sortie obtained at Oceana is identical to that at both Luke and Nellis.

Major differences between the Oceana data and the new data occur in the areas covered by single carpet booms and the total areas covered by flight tracks during supersonic maneuvering. The first case, individual boom carpet areas, is primarily due to the difference in rms duration of supersonic flight while above cut-off Mach number. Examination of the Oceana data showed supersonic flight duration varied from 6 to 24 seconds with an average of 15 seconds. In contrast, the rms durations at Luke were 44.8 seconds and 50.2 at Nellis, three times as long as at Oceana. All other things equal, these booms thus cover three times the area.

The second major difference is in the extent of the supersonic maneuvering areas. At Oceana supersonic flight was contained within an ellipse that was 12 miles wide by 18 miles long. In contrast, at Nellis the overall extent of supersonic maneuvering was 30 miles wide by 36 miles long. At Luke an even greater area 36 miles wide and 48 miles long was covered. At Luke, approximately two-thirds of the sorties were contained within the area for all flights at Oceana, while one-third were dispersed over space of almost 8 times this area (1375 square miles versus 170 square miles).

Although one can speculate as to the reasons why these differences occur, insufficient information is really available to make a definite statement. The techniques used in this study, however, could readily be used to develop more discrimination between MOA characteristics and mission capabilities. Pragmatically, one can say that, for any specific boom, the most likely amplitude will be essentially the same for F-15 operations at all three sites. The CDNL, however, will be somewhat (2 to 4 decibels) higher in the central region of the Oceana areas than at the other two. Further, the areas over which some booms will occur at Nellis are about 5 times that at Oceana and at Luke the boom area is about 8 times that at Oceana.

5.0 RECOMMENDATIONS FOR FURTHER RESEARCH

5.1 Operational Characteristics of ACM

The results of this study indicate that Mach number and height distributions for fighter airplanes engaged in air combat maneuvering are in general well understood. There is evidence, however, from the comparison of F-16 data at Nellis with that at Luke, that either a peculiar sample was observed at Luke, or a definitely different type of mission is involved. Similarly, the F-15 operational data at Nellis agreed well with that at Oceana, but the Luke data showed the F-15's being flown differently there.

Other questions in operations come to mind. Is there a reason why the durations of average supersonic flights of F-15's at Nellis and Luke are 3 times longer than at Oceana? Why are supersonic F-4 flights half again as long in duration as other airplanes? What reasons exist for the large geographic dispersion of flight tracks at Luke and Nellis as compared to Oceana? Does Oceana represent the situation for an operationally ready wing as compared to Luke as representative of a transition training wing?

In order to improve the understanding of these and related questions it is recommended that the USAF obtain similar ACMI data from every available range and analyze them with the programs developed in this study. Based on the F-15 data at Luke, it appears that data on 40 to 50 sorties of each airplane type is about the minimum sample that should be considered.

It is also recommended that a better idea of the nature of the missions expected for ACM operations at each range be identified. What information exists in various training curricula that would help provide more identifiable statistics on expected operations? For example, how many sorties are planned as one versus one, two versus one, etc., missions? Does the use of

different armament systems affect the nature of the maneuvering altitudes and flight tracks? Judicious discussion with wing and squadron operations personnel, as well as review of TAC training requirements, would likely yield enlightenment in this area.

5.2 Sound Exposure Level Conversions

The data examined in this study support the nominal 26 decibel conversion between peak overpressures in decibels and C-weighted sound exposure level. This relation holds over a broad range of conditions, except at lateral cutoff. Under this circumstance, peak pressure prediction is also poor, with large variation in measured values over relatively short distances. On the other hand, CSEL appears quite stable, even under these close to cut-off situations.

A similar statement cannot be made for A-weighted sound exposure level. The relations between peak overpressure and ASEL vary by large, unpredictable amounts, both with absolute level and with type of boom. Whether or not CSEL or ASEL is a better psychoacoustic measure, ASEL is a poor second for prediction purposes. It is recommended that any future USAF sonic boom measurement program should concentrate on CSEL and peak flat sound level as primary measures for sonic booms.

5.3 Validation of Models

All the estimates of C-weighted day-night sound level discussed in this report, while certainly considered plausible by the

the author, are completely devoid of field validation. Inevitably, both applicability of the models to other situations as well as their validity when applied to the actual sites where operational data were originally obtained will be questioned. All of the best intentioned analyses that can be performed may well be set aside by opposing analyses, or spot acoustical measurements that may or may not be relevant.

There is no escaping the fact that the USAF should pursue an adequate measurement project to determine the actual CSEL and CDNL environments within the boundaries of operating areas where supersonic ACM takes place.

5.4 Development of Computer Programs

5.4.1 ACMI Data

Flight data obtained from ACMI records were analyzed for this study by the methods discussed in the text and Appendix B. Transferring ACMI data into these computer programs was done by key-punched cards prepared from printed records obtained from the ACMI. This was tedious and slow.

In order to implement the recommendation in 5.1 to examine more ACMI data in detail, it is recommended that a computer program be developed to screen the ACMI data recorded on magnetic tape for supersonic flight conditions. A second program should sort the screened data as described in this study to prepare input data files on magnetic tape for the flight data analysis programs.

5.4.2 Spatial Density Distributions

Shape and spacing between adjacent noise contours for sonic booms produced during air combat maneuvering are determined by

flight track distributions obtained from ACMI data. It is recommended that the concepts explored in this study be merged with the broader based analyses of ACMI data recommended above by a computer program designed to generate two-dimensional spatial distribution functions for flight path density.

5.4.3 Computer-Based Model For Predicting Noise Environments

The two program packages recommended above, in conjunction with those used in this study, form the major pieces necessary to provide a general case program package for sonic boom predictions in air combat maneuvering areas. It is recommended that the USAF integrate these programs into a modular system.

The combined programs should be considered primarily as development tools. It is not too likely that the operational analyses recommended above will generate uniquely different conditions at each range. If they do, the computer programs will allow such uniqueness to be reflected in the final production of noise level contours.

It is more likely that only a few operational environments will emerge. In this event a few sets of generic noise contours may be all that is necessary, along with a simple set of computational rules to adjust the numerical values attached to the contours for numbers of sorties and airplane types.

REFERENCES

1. W. J. Galloway, "Development of C-Weighted Day-Night Average Sound Level Contours for F-15 Air Combat Maneuvering Areas," BBN Report 4430, 1980.
2. "Assessment of Community Response to High-Energy Impulsive Noises," National Research Council, 1981. (Report of CHABA Working Group 84, W. J. Galloway, Chairman.)
3. American National Standard S1.4-1983, "Specifications For Sound Level Meters," Acoust. Soc. Am., 1983.
4. P. D. Schomer, "Growth Functions for Human Response to Large-Amplitude Impulse Noise," J. Acoust. Soc. Am., 64, 1627-1632, 1978.
5. R. W. Young, "Average Sound Levels Including Sonic Booms," J. Acoust. Soc. Am., 58, s69, 1975 (A).
6. H. W. Carlson, "Simplified Sonic Boom Predictions, NASA TP-1122, March 1978.
7. G. T. Haglund, E. J. Kane, "Flight Test Measurements and Analysis of Sonic Boom Phenomena Near the Shock Wave Extremity," NASA CR-2167, February 1973.
8. I. E. Garrick and D. J. Maglieri, "A Summary of Results on Sonic-Boom Pressure-Signature Variations Associated With Atmospheric Conditions," NASA TN D-4588, 1968.

APPENDIX A

PREDICTION OF SONIC BOOM CHARACTERISTICS

APPENDIX A

PREDICTION OF SONIC BOOM CHARACTERISTICS

Intensive studies of sonic boom phenomena during the 1960's and 1970's produced accurate procedures for predicting the characteristics of sonic booms [A1,A2]. Implementation of these prediction processes is performed with sophisticated computer programs that depend upon detailed knowledge of airplane configurations and aerodynamic properties as well as the wave propagation characteristics of real and ideal atmospheres. Utilizing these models is a complex, lengthy, and expensive process.

Sonic boom characteristics of interest in environmental impact analyses are peak overpressures, pulse durations, and weighted sound exposure levels of the boom. Carlson [A3] has been able to simplify the prediction process for peak overpressures and durations of sonic booms produced by airplanes in steady-state flight into an accurate procedure that does not require the detailed aerodynamic and configuration information of individual airplanes. This procedure is quite generally applicable to any arbitrarily shaped flight vehicle with any reasonable flight trajectory.

The Carlson procedure is provided in Reference 3 as a series of equations involving a substantial number of coefficients that are obtained from graphical representations in his report. Limiting use of the procedure to fighter airplanes, with Mach number and altitude ranges of interest for air combat maneuvering, allows the many graphical representations of parameters necessary for the computation to be expressed in analytical form. We have developed these analytic expressions from least-squares curve fits to Carlson's graphical data. The following equations result.

Before introducing the computational procedure, it is helpful to consider the geometrical relationships and terminology involved. Figure 1 depicts schematically the parameters used in computations for sonic booms produced along the flight track directly beneath the airplane. The airplane is assumed to be in steady flight at altitude h_a above mean sea level (MSL), flight Mach number M , along a flight path with angle γ relative to a horizontal plane. Ground level is at height h_g above MSL, and thus the airplane is height h above ground, where $h = h_a - h_g$.

The effect of flight path angle γ is to introduce a parameter called effective height, h_e , which is used to compute peak overpressure on the ground. For airplanes in level flight h_e is equal to h . In a climb γ is positive, with h_e greater than h , and boom strength is less than that for level flight at the same Mach number. In a dive γ is negative, h_e is less than h , and boom strength is greater than that for level flight at the same Mach number.

Sonic boom wave fronts emitted when the airplane is at each point along its flight will propagate along a series of curved ray paths. Curvature is caused by the change in the speed of sound that results from the decrease in atmospheric temperature with increasing altitude (up to about 35,000 feet above MSL). Booms which propagate to the ground will strike the earth at a distance d_x along the flight path, measured from a point directly below the airplane.

Under certain combinations of Mach number and altitude, refraction in the atmosphere will cause the curvature of the ray path to tilt the sonic boom wave front sufficiently to become perpendicular to the ground, or even to turn the wave front before it reaches the ground. The Mach number for the condition where the ray path is tangent to the ground is called cutoff Mach number, M_c . At flight conditions below M_c , no boom reaches the ground.

The lateral extent of a sonic boom is limited by a similar refraction process, even for booms that reach the ground directly beneath the flight path, where M is greater than M_c . The distance to the side where the wavefront is perpendicular to the ground is called lateral cutoff distance, $d_{y,c}$, as shown in Figure 2. Experimental data [4] show that, in practice, sonic boom signatures tend to distort dramatically at distances of approximately 0.8 times $d_{y,c}$ and to essentially disappear at $d_{y,c}$.

With these points in mind, sonic boom parameters are predicted from the following equations:

Sonic Boom Overpressure and Duration

1. Effective Mach number, M_e :

$$M_e = \frac{1}{\sin(\gamma + \cot^{-1} \sqrt{M^2 - 1})} \quad (1)$$

2. Cutoff Mach number, M_c :

$$M_c = e^{4.033 \times 10^{-6} h_a} \quad 0 \leq h_a \leq 35,300 \text{ ft} \quad (2)$$

$$M_c = 1.153 \quad 35,300 < h_a \leq 65,600 \text{ ft}$$

3. Horizontal propagation distance, d_x , in feet:

$$d_x = K_d \left(\frac{h}{\sqrt{M_e^2 - 1}} \right) \quad (3)$$

$$\text{where: } K_d = K_{d,c} + (1.04 - K_{d,c}) \left(\frac{M_e - M_c}{M_e - 1} \right)^{n_d} \quad (4)$$

$$K_{d,c} = 2 + (4.53 \times 10^{-6})h_a \quad h_c \leq 35,300 \text{ ft} \quad (5)$$

$$= 2.16 - (6.60 \times 10^{-6})h_a \quad h_a > 35,300 \text{ ft}$$

$$n_d = 0.22 + (1.6 \times 10^{-6})h_a \quad (6)$$

4. Lateral cutoff distance, $d_{y,c}$, in feet:

$$d_{y,c} = h \frac{(1 + M_c)}{M} \left(\frac{M^2 - M_c^2}{M_c^2 - 1} \right)^{1/2} \quad (7)$$

5. Effective height, h_e , in feet:

$$h_e = h \cos \gamma + d_x \sin \gamma \quad (8)$$

6. Peak sonic boom overpressure, Δp , in pounds-per-square-foot:

$$\Delta p = \frac{8.4 \times 10^3 (\delta_a \delta_g)^{1/2} (M^2 - 1)^{1/8}}{h_e^{3/4}} \quad (9)$$

where:

$$\delta_a = [1 - (6.8756 \times 10^{-6})h_a]^{5.2559} \quad (10)$$

$$\delta_g = [1 - (6.8756 \times 10^{-6})h_g]^{5.2559} \quad (11)$$

Note 1: At points lateral to the side of the flight path, distance d_y , such that $d_y \leq 0.8 d_{y,c}$, the effective slant distance to the flight path, s_e , should be used in equation (9) instead of h_e . The effective slant distance is approximately:

$$s_e = (d_y^2 + h_e^2)^{1/2} \quad (13)$$

Note 2: Equation (9) applies to F-14 and F-15 airplanes. To obtain Δp for other airplanes, or Δt from equation (13), apply the following multipliers:

| | |
|--------|------|
| F - 4 | 0.93 |
| F - 5 | 0.76 |
| F - 16 | 0.80 |
| F - 18 | 0.91 |

7. Sonic boom duration, Δt , in seconds:

$$\Delta t = 5.8 \times 10^{-3} \left[\frac{M}{(M^2 - 1)^{3/8}} \right] h_e^{1/4} \quad (13)$$

Sound Levels

Historically, the magnitudes of sonic booms have been expressed largely in terms of peak overpressures, Δp , or in terms of the time integral of overpressure during the positive phase of the boom, called the positive impulse, I_o . These quantities are generally used in assessing the effect of a boom on building structures. In order to assess the effects of sonic booms on people various sound levels in decibels are of more utility [5].

Three such measures are of use: peak flat sound pressure level, C-weighted sound exposure level, and A-weighted sound exposure level.

Peak flat sound pressure level, abbreviated as PKT, symbolized as L_{pk} , is the magnitude of the peak overpressure stated in terms of sound pressure level in decibels. It may be calculated as:

$$L_{pk} = 10 \log_{10} (\Delta p)^2 + 127.6 \quad (15)$$

C-weighted sound exposure level, abbreviated as CSEL, symbolized as L_{CE} , is recommended in Reference 5 and used by various Department of Defense agencies for describing the effect of individual sonic booms on human response. C-weighted sound exposure level is the time integral over the duration of the boom of C-weighted, squared sound pressure, expressed in decibels. C-weighting is a standardized frequency weighting specified for sound level meters [6].

Sonic booms from fighter aircraft operating in the Mach number and altitude ranges of interest for air combat maneuvering, have been found experimentally to have C-weighted sound exposure levels that are approximately 26 decibels lower than peak flat sound pressure level [7].

Thus:

$$L_{CE} = L_{pk} - 26 \quad (16)$$

A-weighted sound exposure level, abbreviated as ASEL and symbolized as L_{AE} , is the preferred measure for describing the magnitude of non-impulsive sounds as produced, for example, by the flyover of a subsonic airplane. Analogous to C-weighted sound exposure level, A-weighted sound exposure level is the

time integral over the duration of an event of the A-weighted, squared sound pressure expressed in decibels, where A-weighting is a frequency weighting standardized in Ref. 6. A-weighting significantly suppresses low frequencies which contain the predominant energy in a sonic boom, placing more emphasis on mid and high frequencies that are significant for human audibility.

Experimental measurements of ASEL have been reported by Young [8] for relatively short sonic booms produced by fighter airplanes. We have fit an analytic expression to his data to obtain the following equation:

$$L_{AE} = 188.7 \ln L_{pk} - 825.6 \quad (17)$$

This expression yields differences between peak flat sound pressure level and A-weighted sound exposure level of approximately 31 decibels for 10 psf booms and approximately 38 decibels for 1 psf boom. Ongoing research for the USAF indicates, for the same overpressures, that the range of difference between ASEL and P_{kt} may exceed 10 decibels, and that equation (17) may overpredict ASEL by as much as 10 to 15 decibels. Equation (17) must be regarded as quite tentative at this time.

Boom Strengths During Maneuvering

The above expressions apply only to constant speed flight, which produces so-called "carpet" booms. Maneuvers which involve acceleration can cause focusing effects that increase overpressures, relative to those of carpet booms, by factors of up to 3 or more. Supersonic maneuvers such as longitudinal acceleration, pushover from a climb, and turns are the principal sources of maneuvering booms.

REFERENCES

- A1. H. W. Carlson, D. J. Maglieri, "Review of Sonic-Boom Generation Theory and Prediction Methods," J. Acoust. Soc. Am., 51, 675-685, 1972.
- A2. W. D. Hayes, R. C. Haefeli, H. E. Kulsrud, "Sonic Boom Propagation in a Stratified Atmosphere, With Computer Program," NASA CR-1299, 1969.
- A3. H. W. Carlson, "Simplified Sonic-Boom Prediction," NASA Technical Paper 1122, March 1978.
- A4. H. H. Hubbard, D. J. Maglieri, V. Huckel, D. A. Hilton, "Ground Measurements of Sonic-Boom Pressures for the Altitude Range of 10,000 to 75,000 feet," NASA TR R-198, 1964.
- A5. W. J. Galloway, "Assessment of Community Response to High-Energy Impulsive Sounds," Report of CHABA Working Group 84, National Academy Press, 1981.
- A6. American National Standard S1.4-1982, "Specifications For Sound Level Meters," Acoust. Soc. Am., 1982.
- A7. P. D. Schomer, "Growth Functions for Human Response to Large-Amplitude Impulse Noise," J. Acoust. Soc. Am., 64, 1627-1632, 1978.
- A8. R. W. Young, "Average Sound Level Including Sonic Booms," (Abstract), J. Acoust. Soc. Am., 58, s69, 1975.

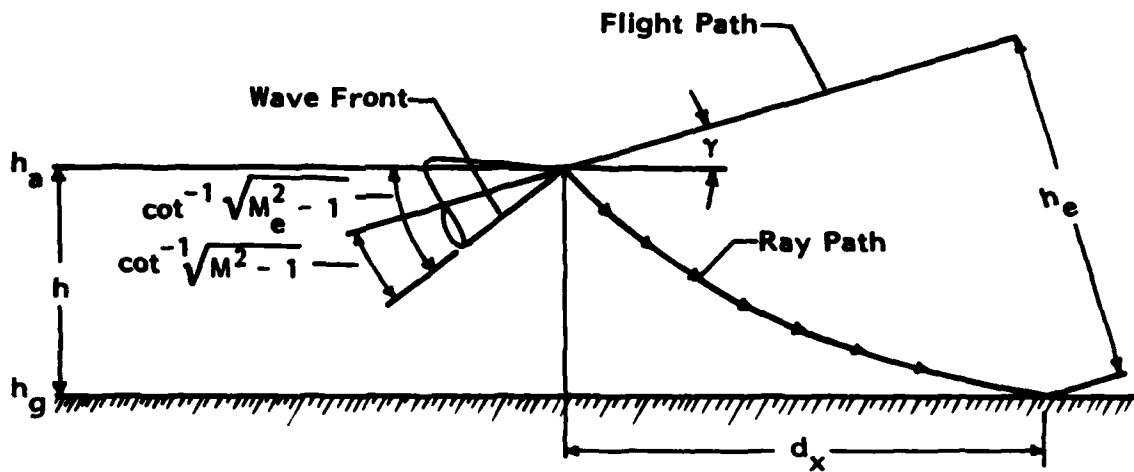


FIGURE A-1. SONIC BOOM GEOMETRY UNDERNEATH FLIGHT PATH

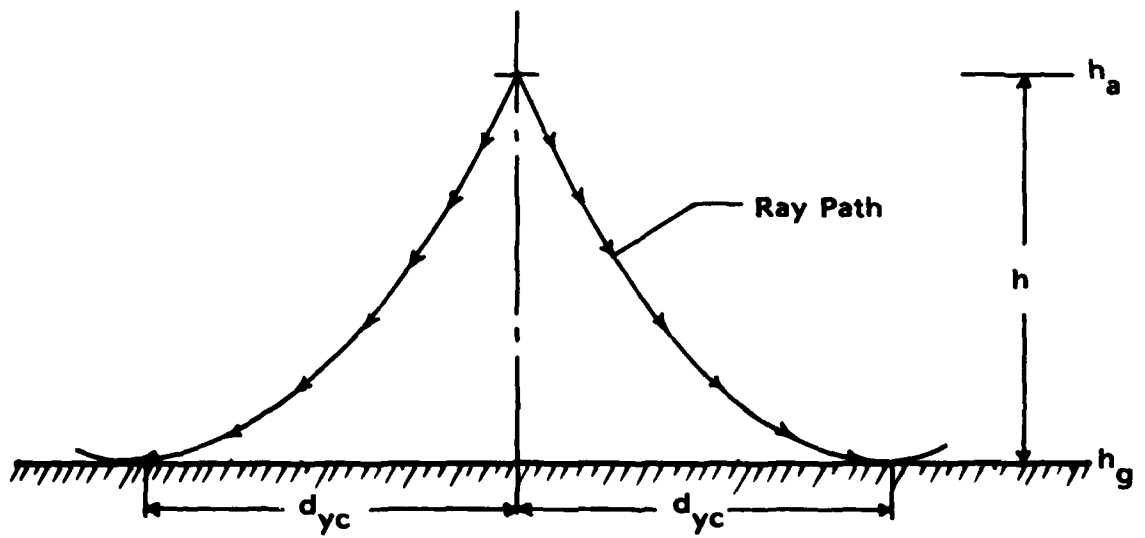


FIGURE A-2. SONIC BOOM GEOMETRY AT LATERAL CUT OFF

APPENDIX B

AIRCRAFT FLIGHT DATA HANDLING AND ANALYSIS

APPENDIX B

AIRCRAFT FLIGHT DATA HANDLING AND ANALYSIS

B1.0 INTRODUCTION

Aircraft flight and tracking data made available by the U.S. Air Force provided the basis for estimating propagating boom conditions and boom strengths and for determining the over-ground locations of aircraft flight tracks. These data are routinely acquired during aircrew training missions over instrumented air combat training ranges. The instrumentation consisted of a Tactical Aircrew Combat Training System/Air Combat Maneuvering Instrumentation (TACTS/ACMI) manufactured by Cubic Corporation. The purpose of the TACTS/ACMI system is to digitize various position and performance parameters of each aircraft on the range at frequent intervals (200 milliseconds) for later replay in graphical or tabular form during aircrew debriefings. The digitization of parameters for a single time interval represents a "snapshot" of aircraft activity at a given instant in time, analogous to a single frame of motion picture film. By concatenating a series of snapshots a time history of the various parameters may be produced. Parameters of particular interest in this study were x, y, z coordinates, Mach number, and climb/dive angle. Figure B1 shows the manufacturer supplied accuracy with which the system is capable of recording these variables.

The data acquired for this study were obtained in printed form from the TACTS/ACMI, keypunched on computer punch cards, and then processed by a Control Data Corporation (CDC) Cyber 176 digital computer. Output products included graphical presentations of aircraft flight tracks and statistical treatments of aircraft position, speed, and estimated boom strengths over the test range. All computer programs were written in Fortran IV.

TACTS /ACMI SPECIFICATIONS

TACTS /ACMI Parametric Data Specifications and Current Measured Values

| Parameter | Maximum Standard Deviation of Error | |
|--|-------------------------------------|-----------------|
| | Specification | Measured |
| ● Closing velocities between "fighters" and "targets" (VC) | 35 ft/sec | 3 ft/sec |
| ● Slant ranges from "targets" to "fighters" (AR) | 50 ft | 15 ft |
| ● Angle off the tail (AOT) | 2° | 1.3° |
| ● AOT in wing plane of target aircraft (AOT _h) | 2° | 1.3° |
| ● AOT in wing plane perpendicular to wing plane of target aircraft (AOT _v) | 2° | 1.3° |
| ● Aircraft dive or climb angle (D/CA) | 2° | 1.3° |
| ● Aircraft normal acceleration (N) | 0.5 g | 0.05 g |
| ● Antenna train angle (ATA) | 2° | 1.3° |
| ● Aircraft position components in respect to cartesian coordinates \hat{x} , \hat{y} , \hat{z} , with \hat{z} above mean sea level | X, Y = 25 ft Z = 25 ft | 8.7 ft 25 ft |
| ● Aircraft Mach number (M) | 0.02M | 0.02M |
| ● Aircraft attitude with respect to earth coordinates | 2° | 0.05° |
| ● Aircraft velocity components (\dot{x} , \dot{y} , \dot{z}) | 15 ft/sec | 5 ft/sec |

TACTS /ACMI Required Operational Environment Data

| Aircraft Function | Limitation | Aircraft Function | Limitation |
|-------------------|------------------------|---------------------|------------------------|
| ● Attitude | None | ● Roll Rate | 0 to 360°/sec |
| ● Acceleration | -2.5 to 8.5 g | ● Relative velocity | 0 to ± 4000 ft/sec |
| ● Airspeed | 100 ft/sec to Mach 1.6 | ● Altitudes | 5,000 to 50,000 ft |

FIGURE B-1. MANUFACTURER SPECIFICATIONS FOR AIRCRAFT TRACKING SYSTEM

B2.0 EXTRACTING THE RAW ACMI DATA

Site visits were made to both Nellis AFB, Nevada, and Luke AFB, Arizona, to obtain flight data for specific aircraft types from a number of different sorties. By entering a specific date and time into the Display and Debriefing Subsystem (DDS) of the TACTS/ACMI, a two-page report (shown in Figures B2 and B3) was produced. At the top of the page the mission, date, and time (to the nearest hundredth of a second) are identified. The report presents a numerical snapshot of all aircraft on the practice range at the specified time (one column for each aircraft) and the instantaneous values of a number of flight parameters for each aircraft. The arrows in Figures B2 and B3 indicate the six parameters of interest in this study.

- 1) aircraft id number
- 2) aircraft Mach number
- 3) aircraft climb (+) or dive (-) angle
- 4) range x-coordinate (in feet)
- 5) range y-coordinate (in feet)
- 6) range z-coordinate (in feet above MSL)

To minimize the volume of data to be handled, readouts were obtained only when at least one of the aircraft was supersonic (Mach number greater than or equal to 1.00) and at nominal 1-second intervals (rather than the 200-millisecond digitization interval).

2229-13

08/17/82

1310:06:27

CONSOLE MODE: REPLAY / ACTIVE / S

PK = 0

CONTROL CONSOLE: 28

R
BRNG
V_C(KTS)
AOT
ATA

| A/C | 1 | 2 | 3 | 4 | 5 | 6 | 7 | 8 |
|------|-------|-------|-------|-------|---|---|---|---|
| MACH | .92 | .92 | .96 | 1.05 | | | | |
| IAS | 372 | 382 | 364 | 398 | | | | |
| ALT | 30720 | 28261 | 33339 | 31855 | | | | |
| AOA | 10 | 10 | 1 | 0 | | | | |
| C | .8 | .9 | .8 | 1.3 | | | | |
| FILT | 20 | 20 | 0 | 0 | | | | |
| INT | 3 | 3 | 4 | 4 | | | | |

KEYBOARD INPUT:
OPERATOR MESSAGE:

EQUIPMENT STATUS CHANGE, SEE RANGE STATUS

FIGURE B-2. TYPICAL ACMI AIRCRAFT SNAPSHOT (PAGE 1 of 2)

2229-13

08/17/82

1310:06:27

| CONSOLE NODE: | REPLAY / ACTIVE / S | | | | PK = 0 | CONTROL CONSOLE: 28 | | |
|---|---------------------|----------|----------|----------|--------|---------------------|---|--|
| | 1 F-15/L02 | F-15/L03 | F-16/R 4 | F-16/R 5 | 6 | 7 | 8 | |
| G | .8 | .9 | .8 | 1.3 | | | | |
| -/AOA | 0/S | 0/S | 0/S | 0/S | | | | |
| D/CA | 2 D | 0 D | 6 D | 5 D | | | | |
| RC | - 23 | - 1 | - 57 | - 48 | | | | |
| P | 1 D | 2 U | 11 D | 6 D | | | | |
| R | 6 L | 1 R | 3 L | 28 L | | | | |
| H | 18 | 16 | 206 | 218 | | | | |
| CRAB | 1 L | 0 L | 1 R | 0 R | | | | |
| ASS | 0 | 1 | 0 | 0 | | | | |
| X | - 88241 | - 83684 | - 35234 | - 57123 | | | | |
| Y | - 55431 | - 61540 | 23436 | 38855 | | | | |
| Z | 30728 | 28261 | 33339 | 31855 | | | | |
| VX | 314/S | 274/S | - 428/S | - 582/S | | | | |
| VY | 993/S | 978/S | - 852/S | - 767/S | | | | |
| VZ | - 39/S | - 1/S | - 96/S | - 79/S | | | | |
| FILT | 20 | 20 | 0 | 0 | | | | |
| INT | 3 | 3 | 4 | 4 | | | | |
| _KEYBOARD_INPUT: _____ OPERATOR MESSAGE: EQUIPMENT STATUS CHANGE, SEE RANGE STATUS | | | | | | | | |

FIGURE B-3. TYPICAL ACMI AIRCRAFT SNAPSHOT (PAGE 2 of 2)

B3.0 KEYPUNCHING OF ACMI REPORTS

The reports shown in Figures B2 and B3 were screened for anomalous data before forwarding to a commercial data-processing house for keying onto computer punch cards. All data were verified after punching. To facilitate handling and minimize keypunch errors, data from the ACMI reports were punched row-wise, one report line per punch card. Thus, for a single time snapshot six cards were punched corresponding to the six variables of interest. The time of day was punched in the first field of every card. To further contain the amount of data to be keypunched, only the data for those aircraft which were supersonic at the time of the snapshot were punched.

The snapshots from each sortie were punched as separate decks, and header cards were added to label each sortie by its identification number, air base, and date. Additional cards identified each aircraft by type and pilot. The sortie identification number was obtained from the top left hand corner of the TACTS/ ACMI report, and the date from the top center. Aircraft types and pilot identification were obtained from separate forms (not shown).

B4.0 INITIAL DATA PROCESSING--REFORMATTING AND SORTING OF KEYPUNCHED DATA

The punch cards were entered into the computer for reformatting, sorting, and screening by an initial processing program (BOOM1). The program first reformatted the data from each sortie so that the time history for each aircraft was repunched as a separate mini-deck (essentially exchanging the columns and rows in the original data format). These mini-decks were then sorted by aircraft type to consolidate the flight activity for each type into a single deck of cards. The data were also screened for inconsistencies by calculating an approximate Mach number from

the position and time data and then comparing this approximation with actual Mach number. Any errors discovered were corrected in the reformatted deck. The new reformatted and consolidated card decks were then used for all subsequent data processing.

B5.0 GRAPHIC DATA PROCESSING

Flight track maps (plan views) of supersonic flight activity were generated on an X-Y plotter by software (BOOM2) which essentially connected the time series of x, y data points with straight line segments during those portions of the flight when the Mach number was equal to or greater than 1.0. Individual maps were produced depicting activity for each aircraft type. A composite map showing all aircraft activity was also produced. An example of a flight track map is shown in Figure B4.

Additional software (BOOM5) was prepared to depict those portions of the original flight tracks from which the propagation algorithms of Appendix C predicted the shock wave would reach the ground. These maps were produced by incrementally proceeding through the flight time history at 1-second intervals, performing the propagation calculations based on the instantaneous flight parameters, and tracing out only the propagating boom sections of the flight tracks. A typical track map, using the same input data as Figure B4, is shown in Figure B5.

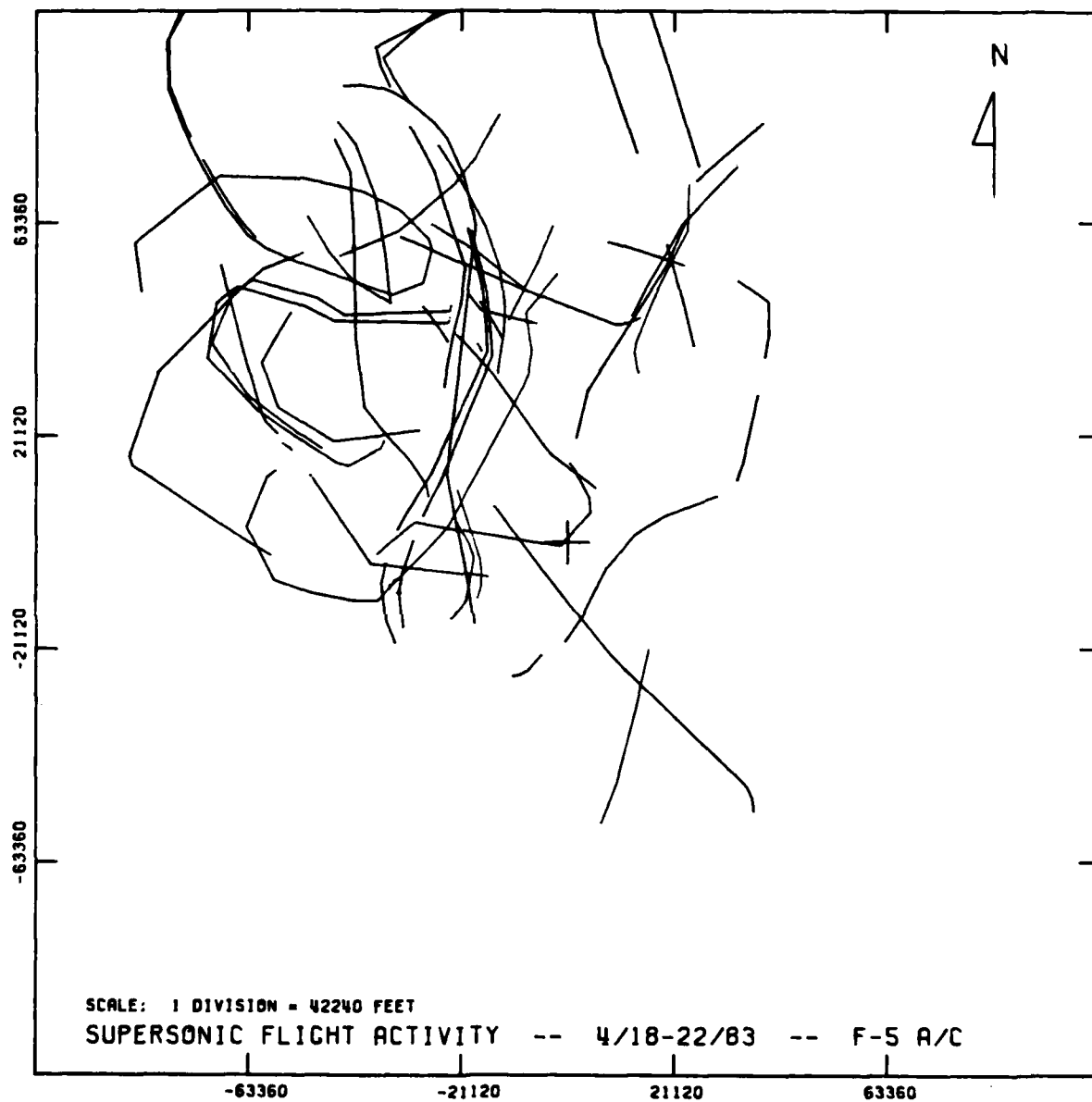


FIGURE B-4. TYPICAL COMPUTER GENERATED AIRCRAFT FLIGHT TRACK MAP SHOWING SUPERSONIC FLIGHT ACTIVITY

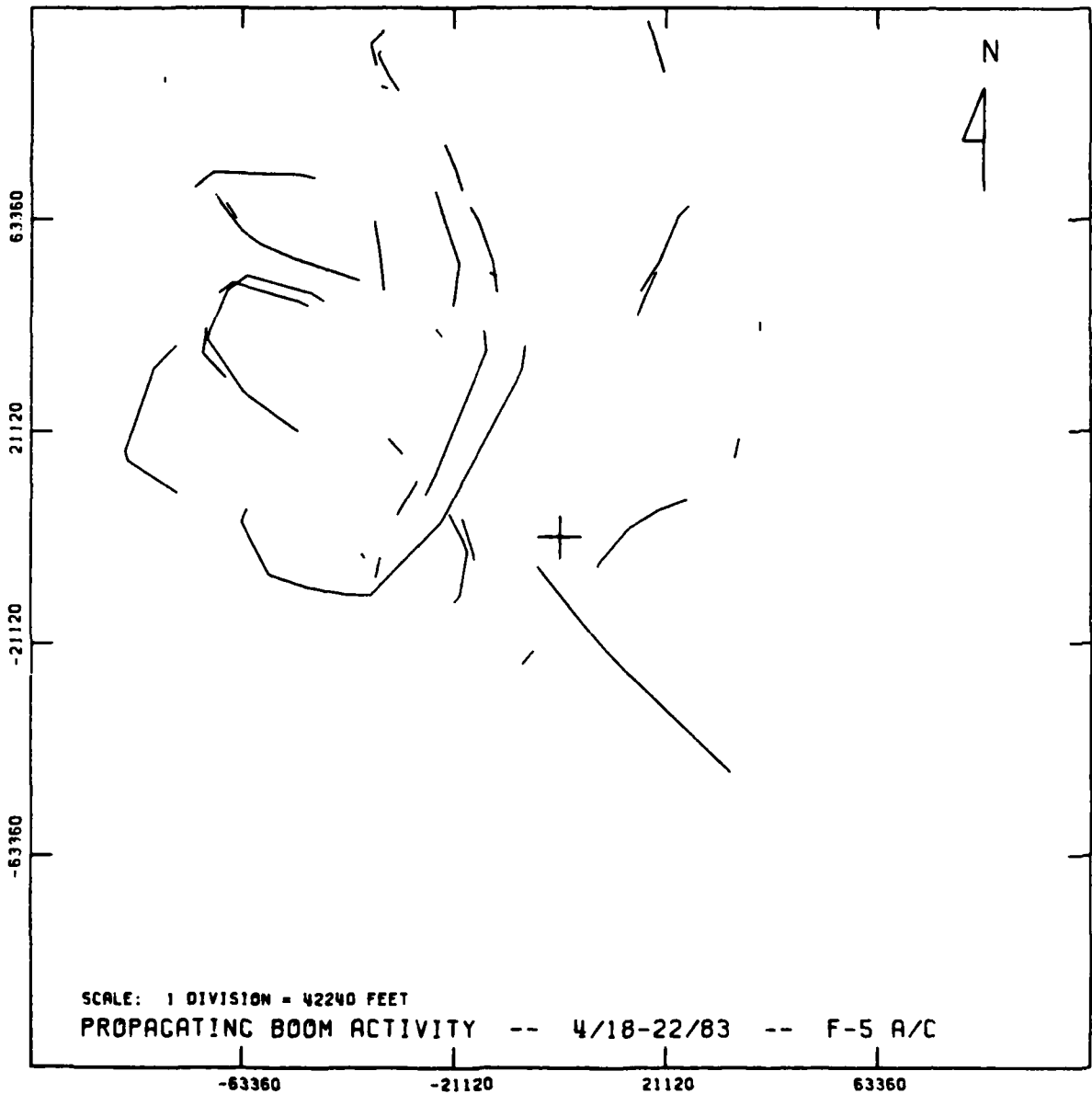


FIGURE B-5. TYPICAL COMPUTER GENERATED FLIGHT TRACK MAP SHOWING FLIGHT TRACKS FOR FLIGHTS WHICH WOULD GENERATE SONIC BOOMS

B6.0 STATISTICAL DATA PROCESSING

In another computer program (BOOM4) the statistics of the original flight parameters along with a number of computed parameters from the prediction model were generated to provide insight into the central tendencies and distributions of these variables. Frequency distributions were generated for x, y, and z position variables, Mach number, and estimated boom strengths by incrementing through the flight data at 1-second intervals and summing the variables of interest in selected incremental segments.

APPENDIX C

PROCEDURES FOR OBTAINING SPECTRAL ANALYSES
OF SONIC BOOM PRESSURE-TIME TRACES

APPENDIX C

PROCEDURES FOR OBTAINING SPECTRAL ANALYSES OF SONIC BOOM PRESSURE-TIME TRACES

C1.0 INTRODUCTION

The computer system techniques used to perform spectral analysis by Fourier Transform of aircraft sonic boom pressure time traces are described in this appendix. Flat, A-weighted, and C-weighted Sound Exposure Level were calculated for a number of such traces and compared to peak overpressure.

C2.0 SOFTWARE DEVELOPMENT

C2.1 Digitization

Pressure-time traces of test signals and sonic booms were digitized on a GTCO Model DIGI-PAD Digitizing Tablet in conjunction with an Apple III computer and a BASIC program developed for the purpose. This program stores identifying information and up to a maximum of 100 pressure-time coordinate pairs (appropriately scaled) for each run. The digitizing tablet has the capability of "continuous firing" of input coordinate pairs (at a 2 per second rate) as the mechanism is "pulled" along the trace or of selecting discrete input coordinate pairs for digitizing.

This digitized trace is then transmitted from the Apple III across a telephone modem interface into a CDC on-line tape storage file. From this point, analysis is completed using CDC system equipment.

The FORTRAN program processes the pressure-time pairs by performing a linear interpolation at intervals Δt . The selection of the Δt value, and its influence on the results are described in Section 1.2.2.

C2.2 Fast Fourier Transform and Integrated Noise Measure Development

The Fast Fourier Transform to be performed may be written:

$$P(f) = \int_0^T p(t)e^{-2\pi jft} dt \quad (1)$$

is used to obtain the coefficients for the Fourier series of fundamental period T . The square of the absolute values of the coefficient of each sinusoidal component constitutes a mean-square sound pressure during the time "window" T associated with the frequency bandwidth $\frac{1}{T}$ hertz.

$$\frac{2}{T} |P(f)|^2 = G_{xx}(f) \quad (2)$$

The integral of these components in the frequency domain is the (flat) sound exposure level, L_E :

$$L_E = \int_0^{f_c} G_{xx}(f) df \quad (3)$$

As opposed to filtering the input pressure signal to arrive at an A- or C-weighted pressure-time trace; the Fourier transform coefficients were frequency weighted in the following way:

$$\hat{G}_{xx} = G_{xx}(f) + A(f)[\text{or } C(f)] \quad (4)$$

and then integrated to obtain:

$$L_{AE} \text{ or } L_{CE} = \int_0^{f_c} \hat{G}_{xx}(f) df \quad (5)$$

The A and C frequency weightings were calculated from the following formulas for the steady-state relative magnitude

response level in decibels*:

$$C(f) = 10 \log \left[\frac{K_1 f^4}{(f^2 + f_1^2)(f^2 + f_4^2)^2} \right] \quad (6)$$

$$A(f) = 10 \log \left[\frac{K_3 f^4}{(f^2 + f_2^2)(f^2 + f_3^2)} \right] + C(f) \quad (7)$$

where f is frequency in hertz and K_1 and K_3 are scale factors chosen so that $C(f)$ and $A(f)$ are 0 dB at 1000 Hz. The values for the constants are given below:

$$\begin{aligned} f_1 &= 20.598997 & K_1 &= 2.242881 \times 10^{16} \\ f_2 &= 107.65265 \\ f_3 &= 737.86223 & K_3 &= 1.562339 \\ f_4 &= 12194.22 \end{aligned}$$

C3.0 ANALYSIS OF IDEALIZED SIGNALS

C3.1 Verification of Computer Routines

The FFT and integrating features of the computer routines developed were tested using an ideal single-cycle sinewave with known flat and A-weighted Sound Exposure Levels, following Young [C1]. A single-cycle sinewave (amplitude of zero at start of signal) of frequency 31.6 Hz (and 32 millisecond duration) with rms amplitude 1 volt (120 dB) was developed using the computer sine function. The analyzing parameters were set to duplicate Young's analyzer hardware as follows:

*Appendix C, ANSI S1.4 (1983), American National Standard Specification for Sound Level Meters.

$N_t = 1024$ (number of time points)
 $T = 2.0$ sec. (total analysis time window)
 $B = 200$ Hz (total analysis bandwidth)

Since the sinewave duration is only 32 msec, the input pressure values are set to zero from 0.032 sec. to 2.0 sec. The actual number of points analyzed from the non-zero portion of the trace is just $(\frac{.032}{2.0}) \times 1024 = 16$. The above constraints also give a frequency resolution of 0.5 Hz ($\Delta f = \frac{1}{T}$), so that the N_f (number of frequency points) parameter was set to 400 (the theoretical $f_c = 256$ Hz*) to arrive at a 200 Hz analysis band. The results of the computer run with these input parameters were:

$L_E = 105.0$
 $L_{AE} = 69.5$
 $L_{CE} = 101.1$
 $L_{pk} = 123.0$

These results for the single-cycle sinewave compare to Young's flat sound exposure level of 105.2 and A-weighted sound exposure level of 69.2 for the 200 Hz (total) analysis band (see Reference C1).

As a further check on the ability of the program to use the FFT to calculate integrated noise measures, the flat sound exposure level was calculated directly from the pressure versus time function and compared with the results from the FFT program using the relationship:

*The "folding" or cutoff frequency for the Fourier transform is $f_c = 1/(2\Delta t)$.

$$\int_0^T p^2(t)dt = \int_0^{f_c} G_{xx}(f)df \quad (8)$$

Exact agreement was found in the case of the single-cycle sinewave and N-wave. No differences greater than 0.2 dB were found for all sonic boom pressure-time traces analyzed).

The digitizing portion of the analysis procedure was first tested by sampling the graph of the single-cycle sinewave, Figure 2 of Reference C1. Ninety-three pressure-time coordinate pairs were digitized in the "continuous firing" mode* from the non-zero portion of the trace. Because of the "analyzer" constraints described above, only 16 of these values (developed by the interpolation described in Section 1.1.2) were actually transformed, as before. The results are:

$$\begin{aligned} L_E &= 104.6 \\ L_{AE} &= 69.6 \\ L_{CE} &= 100.5 \\ L_{pk} &= 122.8 \end{aligned}$$

The numerical results from the digitized graph of the single-cycle sinewave agree well with the computer-generated signal within the limitations of the input parameters, but agreement is far better when the number of input time-pressure points is increased, as described in the next section.

A more appropriate test signal for the study of sonic booms is an idealized N-wave. An N-wave with the same parameters as Young's 400 millisecond N-wave with a 9 msec rise time was analyzed using the following conditions:

*It was found that the "continuous firing" mode was more useful when digitizing smaller scale traces (because of the lower pen resolution) and the discrete point mode was more useful for the larger scale traces

$N_t = 1024$
 $T = 4.0 \text{ sec}$
 $B = 100 \text{ Hz}$

The number of non-zero pressure time points analyzed was 102, with a frequency resolution of 0.25 Hz. The N_f parameter was set at 400 to obtain the 100 Hz total analysis band, and the peak overpressure 125.1 decibels. The results were:

$L_E = 116.4$
 $L_{AE} = 67.4$
 $L_{CE} = 98.6$
 $L_{pk} = 125.1$

Young's results for the same pressure-time trace were a peak (flat) sound pressure level of 115.1 dB and a flat sound exposure level of 116.1 dB.

The pressure-time graph of the N-wave (Figure 1, Reference 2) was digitized and analyzed, with the input parameters set as above. The results were:

$L_E = 116.4$
 $L_{AE} = 68.7$
 $L_{CE} = 98.9$
 $L_{pk} = 125.0$

The increase in A and C-weighted sound exposure levels can be attributed to the higher frequency energy introduced by the "rounded" peaks of the electronically generated (and digitized) N-wave. Otherwise, agreement is quite good, substantiating the validity of the computer analysis procedures developed for the calculation of sound exposure levels.

C3.2 Parametric Study

In order to determine the most meaningful analysis bandwidth B (or cutoff frequency, f_c), and a compatible frequency resolution for sonic boom analyses, a sensitivity study of the input parameters N_t and T was performed for the single-cycle sinewave and N-wave inputs described earlier.

For the single-cycle sinewave ($f_0 = 31.6$ Hz), N_t was either 1024 (typical analyzer equipment value) or 2500 while T was varied from 2.0 to 0.5 seconds. For the ideal N-wave, T varied from 4.0 to 0.5 seconds. In the direction of decreasing T, the actual number of non-zero pressure/time points analyzed (N_{ta}) increases by the relationship,

$$N_{ta} = N_t \cdot T_e / T \quad (9)$$

where T_e = duration of signal in seconds. The total analysis bandwidth B was computed either by setting the total number of frequency points to 400* (typical analyzer equipment value), or by extending the frequency range to the upper limit of the FFT process,

$$f_c = \frac{1}{2\Delta t} = \frac{N_t}{2T} \quad (10)$$

Variation of flat and weighted sound exposure levels with these parameters is listed in Tables 1 and 2. These data show that the Flat SEL and C-weighted SEL are not very sensitive to the analysis bandwidth B or time window T, while the A-weighted SEL varies somewhat below about 1000 Hz cutoff. This is a result of two influences. First the shapes of the transformed frequency

*Since $\Delta f = \frac{1}{T}$, in these cases $B = 400 \times \Delta f$, or $B = \frac{400}{T}$ (hz).

spectra for both inputs are lobed, so that the upper frequency cutoff will either add or delete acoustical energy (from these lobes), depending on the exact value. Also, A-weighting corrections in this frequency range (100-1000 Hz) are much larger than the C-weighting, which acts in such a way as to magnify this effect. As a result, the values $N_t = 2500$ and $T = 0.5$ sec as well as the $f_c = \frac{1}{2\Delta t}$ were chosen for use in further analyses. These selections result in the following values for other parameters of interest:

$$\begin{aligned} B &= 2500 \text{ Hz} \\ t &= 0.2 \text{ msec} \\ f &= 2.0 \text{ Hz} \\ N_{ta} &= 500 \text{ (for 100 msec boom)} \end{aligned}$$

Sound pressure level spectra calculated for the single-cycle sine-wave and N-wave used for tests above are shown in Figures C-1 and C-2.

Table C1. Single-cycle Sinewave Parametric Study

| Input Signal Description | N_t | T (sec) | B (Hz) | N_{ta} | Δf (Hz) | FSEL | ASEL | CSEL |
|--------------------------|-------|------------|-----------|----------|--------------------|-------|------|-------|
| $f_o = 31.6$ Hz | 1024 | 2.0 | 200 | 16 | 0.5 | 105.0 | 69.5 | 101.1 |
| $T_e = 31.65$ msec | 1024 | 2.0 | 256 | 16 | 0.5 | 105.0 | 70.2 | 101.1 |
| Peak amplitude = 123 dB | 1024 | 1.0 | 400 | 32 | 1.0 | 105.0 | 69.8 | 101.1 |
| | 1024 | 1.0 | 512 | 32 | 1.0 | 105.0 | 70.0 | 101.1 |
| | 1024 | 0.5 | 800 | 64 | 2.0 | 105.0 | 70.0 | 101.1 |
| | 1024 | 0.5 | 1024 | 64 | 2.0 | 105.0 | 70.1 | 101.1 |
| | 2500 | 2.0 | 200 | 39 | 0.5 | 105.0 | 69.1 | 101.1 |
| | 2500 | 2.0 | 625 | 39 | 0.5 | 105.0 | 70.0 | 101.1 |
| | 2500 | 1.0 | 400 | 79 | 1.0 | 105.0 | 69.7 | 101.1 |
| | 2500 | 1.0 | 1250 | 79 | 1.0 | 105.0 | 70.1 | 101.1 |
| | 2500 | 0.5 | 800 | 158 | 2.0 | 105.0 | 69.9 | 101.1 |
| | 2500 | 0.5 | 2500 | 158 | 2.0 | 105.0 | 70.0 | 101.1 |

Table C2. N-Wave Parametric Study

| Input Signal Description | N_t | T (sec) | B (Hz) | N_{ta} | Δf (Hz) | FSEL | ASEL | CSEL |
|--------------------------|-------|------------|-----------|----------|--------------------|-------|------|------|
| $f_o = 2.5$ Hz | 1024 | 4.0 | 100 | 102 | 0.24 | 116.4 | 67.4 | 98.6 |
| $T_e = 400$ msec | 1024 | 4.0 | 128 | 102 | 0.25 | 116.4 | 68.1 | 98.6 |
| (9 sec rise time) | 1024 | 2.0 | 200 | 204 | 0.5 | 116.3 | 67.1 | 98.1 |
| | 1024 | 1.0 | 256 | 204 | 0.5 | 116.3 | 67.8 | 98.1 |
| Peak overpressure | 1024 | 1.0 | 400 | 409 | 1.0 | 116.3 | 68.2 | 98.1 |
| = 125 dB | 1024 | 1.0 | 512 | 409 | 1.0 | 116.3 | 68.6 | 98.0 |
| | 1024 | 0.5 | 800 | 819 | 2.0 | 116.3 | 68.0 | 98.0 |
| | 1024 | 0.5 | 1024 | 819 | 2.0 | 116.3 | 68.9 | 98.0 |
| | 2500 | 4.0 | 100 | 250 | 0.25 | 116.3 | 65.1 | 98.0 |
| | 2500 | 4.0 | 312.5 | 250 | 0.25 | 116.3 | 68.1 | 98.1 |
| | 2500 | 2.0 | 200 | 500 | 0.5 | 116.3 | 67.2 | 98.1 |
| | 2500 | 2.0 | 625 | 500 | 0.5 | 116.3 | 69.5 | 98.1 |
| | 2500 | 1.0 | 400 | 1000 | 1.0 | 116.3 | 67.8 | 98.1 |
| | 2500 | 1.0 | 1250 | 1000 | 1.0 | 116.3 | 68.6 | 98.0 |
| | 2500 | 0.5 | 800 | 2000 | 2.0 | 116.3 | 68.7 | 98.0 |
| | 2500 | 0.5 | 2500 | 2000 | 2.0 | 116.3 | 68.1 | 98.0 |

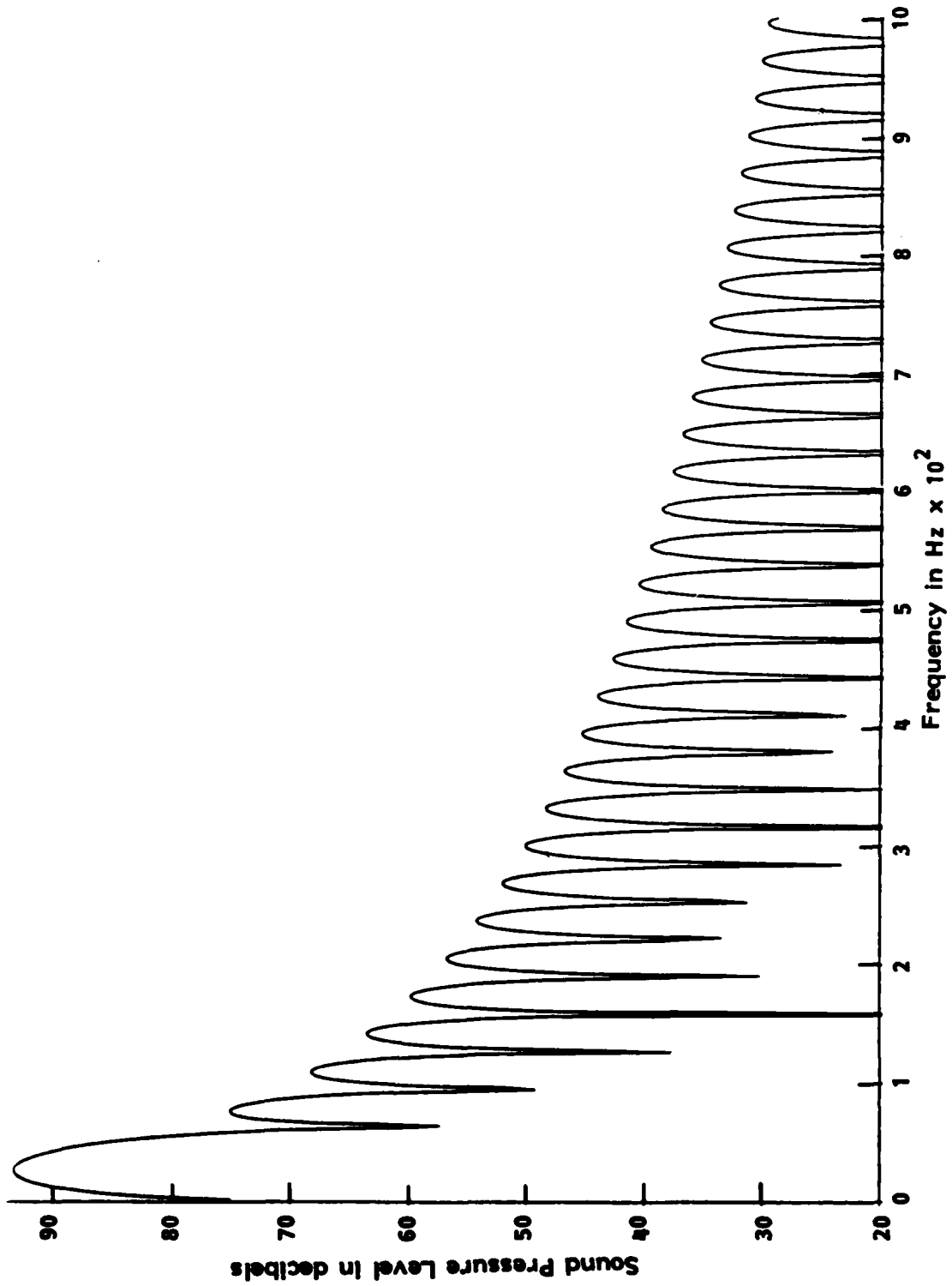


FIGURE C-1. SOUND PRESSURE LEVEL SPECTRUM OF A 31.6 HZ SINGLE-CYCLE SINE WAVE,
 $\Delta f \approx 2$ HZ, $\Delta t \approx 0.2$ MSEC, $B = 2500$ HZ

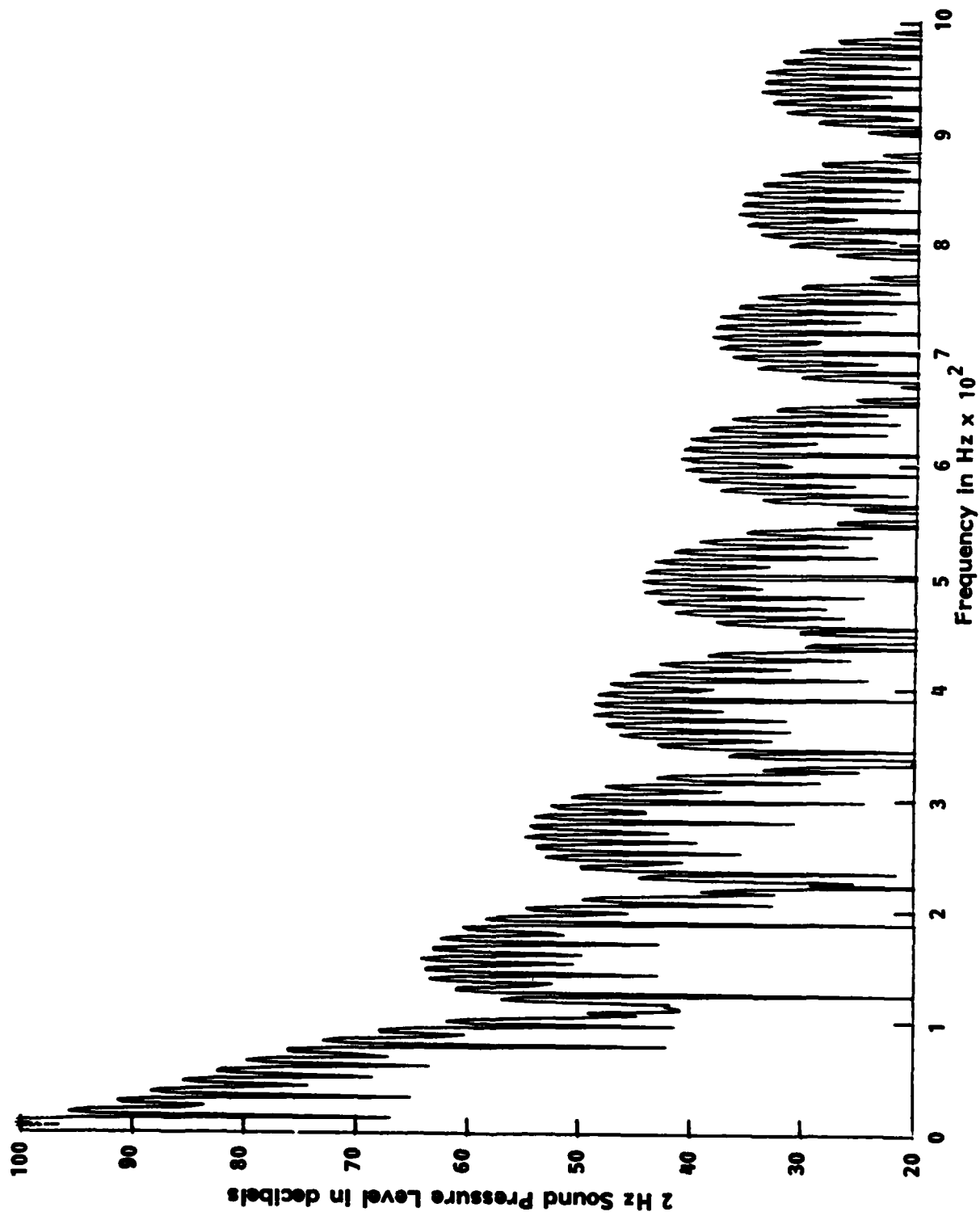


FIGURE C-2. SOUND PRESSURE LEVEL SPECTRUM, N-WAVE WITH 400 MSEC DURATION, 9 MSEC RISE TIME, $\Delta f = 2$ HZ, $\Delta t = 0.2$ MSEC, $B = 2500$ HZ

REFERENCES

- C1. R. W. Young, "Sound Exposure Level of a Sonic Boom From It's Discrete Fourier Transform," J. Acoust. Soc. Am. 69, S 28 (1981).
- C2. "Peak Flat South Pressure Level of a Sonic Boom, with Limited Frequency Response," J. Acoust. Soc. Am. 72, S 71 (1982).
- C3. G. T. Haglund, E. J. Kane, "Flight Test Measurements and Analysis of Sonic Boom Phenomena Near the Shock Wave Extremity," NASA CR-2167, Feb. 1973.

APPENDIX D

SUMMARY OF ANALYSES OF AIR COMBAT
MANEUVERING INSTRUMENTATION DATA

| | | | | |
|----------|------------|------------|---------|---------|
| LUKE AFB | 2323-3 | 10/18/73 | F-4C/RO | GILLMAN |
| 1 | 0816:30.89 | 0818:06.99 | 13 | |
| 2 | 0818:41.39 | 0818:51.59 | 3 | |
| 3 | 0818:55.29 | 0819:11.39 | 6 | |
| 4 | 0820:59.99 | 0821:41.09 | 7 | |
| 5 | 0824:59.59 | 0825:00.49 | 3 | |
| 6 | 0825:07.99 | 0825:57.29 | 4 | |
| 7 | 0826:27.09 | 0827:48.59 | 22 | |
| 8 | 0828:00.39 | 0829:27.79 | 14 | |
| 9 | 0829:35.49 | 0830:11.09 | 14 | |
| 10 | 0830:11.59 | 0830:34.19 | 11 | |

| | | | | |
|----------|------------|------------|---------|----------|
| LUKE AFB | 2323-3 | 10/18/73 | F-4C/RO | THOMPSON |
| 11 | 0817:17.89 | 0817:42.39 | 4 | |
| 12 | 0817:56.59 | 0818:27.79 | 12 | |
| 13 | 0818:34.79 | 0819:13.59 | 10 | |
| 14 | 0826:18.59 | 0827:23.99 | 20 | |
| 15 | 0829:21.49 | 0829:35.49 | 7 | |
| 16 | 0830:11.09 | 0831:21.59 | 17 | |
| 17 | 0833:04.79 | 0833:04.79 | 2 | |

| | | | | |
|----------|------------|------------|---------|---------|
| LUKE AFB | 2322-12 | 11/18/82 | F-4C/RI | MAHONEY |
| 18 | 1247:46.17 | 1248:45.67 | 20 | |
| 19 | 1249:11.27 | 1249:36.67 | 15 | |
| 20 | 1250:02.27 | 1250:37.77 | 24 | |
| 21 | 1253:57.87 | 1255:04.17 | 20 | |
| 22 | 1255:18.47 | 1255:50.17 | 17 | |
| 23 | 1255:52.67 | 1256:04.97 | 9 | |
| 24 | 1259:49.37 | 1300:43.77 | 13 | |
| 25 | 1301:11.37 | 1301:11.37 | 2 | |

| | | | | |
|----------|------------|------------|---------|---------|
| LUKE AFB | 2322-12 | 11/18/82 | F-4C/RO | GILLMAN |
| 26 | 1247:46.17 | 1248:36.27 | 16 | |
| 27 | 1249:11.27 | 1249:28.17 | 10 | |
| 28 | 1250:04.67 | 1250:31.07 | 18 | |
| 29 | 1254:13.67 | 1255:51.27 | 39 | |
| 30 | 1300:27.97 | 1301:08.17 | 9 | |

| | | | | |
|----------|------------|------------|---------|-----|
| LUKE AFB | 2323-4 | 11/19/82 | F-4C/RO | OPP |
| 31 | 0854:10.87 | 0854:16.87 | 3 | |
| 32 | 0854:36.17 | 0856:12.37 | 17 | |
| 33 | 0901:54.91 | 0903:39.81 | 11 | |
| 34 | 0907:03.21 | 0908:14.31 | 10 | |
| 35 | 0908:22.21 | 0908:41.31 | 8 | |

| | | | | |
|----------|------------|------------|---------|---------|
| LUKE AFB | 2323-4 | 11/19/82 | F-4C/RI | MAHONEY |
| 36 | 0854:49.47 | 0856:55.37 | 18 | |
| 37 | 0857:35.97 | 0857:53.57 | 7 | |
| 38 | 0901:54.91 | 0903:32.31 | 7 | |
| 39 | 0903:39.81 | 0904:35.01 | 18 | |
| 40 | 0907:03.21 | 0909:00.31 | 24 | |

| | | | | |
|----------|------------|------------|---------|---------|
| LUKE AFB | 2322-3 | 11/18/82 | F-4C/RO | GILLMAN |
| 41 | 0816:16.63 | 0818:11.03 | 31 | |
| 42 | 0823:33.53 | 0825:05.33 | 23 | |
| 43 | 0825:21.63 | 0826:49.63 | 16 | |
| 44 | 0828:10.13 | 0828:16.63 | 4 | |

| | | | | |
|----------|------------|------------|---------|---------|
| LUKE AFB | 2322-3 | 11/18/82 | F-4C/RI | MAHONEY |
| 45 | 0814:42.93 | 0818:34.83 | 51 | |
| 46 | 0823:19.63 | 0825:18.63 | 31 | |

| | | | | | |
|----------|------------|------------|----------|-------|-----------|
| LUKE AFB | 2235-11 | | 08/23/82 | F-5/L | CAZESSUS |
| 1 | 1234:46.23 | 1235:32.43 | | | 6 |
| LUKE AFB | 2235-11 | | 08/23/82 | F-5/L | MILLER |
| 2 | 1234:44.23 | 1235:16.23 | | | 6 |
| 3 | 1249:16.63 | 1249:43.73 | | | 8 |
| LUKE AFB | 2235-17 | | 08/23/82 | F-5/L | GRACE |
| 4 | 1553:31.05 | 1554:30.45 | | | 18 |
| LUKE AFB | 2235-11 | | 08/23/82 | F-5/L | BOMBERGER |
| 5 | 1249:16.63 | 1249:23.63 | | | 5 |
| LUKE AFB | 2237-17 | | 09/05/82 | F-5/L | MILLER |
| 6 | 1556:02.97 | 1557:08.97 | | | 7 |
| LUKE AFB | 2235-17 | | 08/23/82 | F-5/L | FAIN |
| 7 | 1553:29.55 | 1554:30.45 | | | 19 |
| 8 | 1600:16.35 | 1600:51.85 | | | 13 |
| LUKE AFB | 2237-17 | | 09/05/82 | F-5/L | GRACE |
| 9 | 1555:33.17 | 1556:02.97 | | | 6 |
| LUKE AFB | 2237-17 | | 09/05/82 | F-5/L | FAIN |
| 10 | 1554:47.87 | 1554:49.97 | | | 3 |
| LUKE AFB | 2307-11 | | 11/29/82 | F-5/L | TAN |
| 11 | 1216:02.09 | 1216:25.39 | | | 9 |
| 12 | 1216:28.59 | 1217:01.89 | | | 15 |
| LUKE AFB | 2307-11 | | 11/29/82 | F-5/L | TESKE |
| 13 | 1215:53.29 | 1217:22.29 | | | 27 |
| 14 | 1222:46.97 | 1223:03.17 | | | 8 |
| LUKE AFB | 2307-11 | | 11/29/82 | F-5/L | ZYVITSKI |
| 15 | 1214:11.79 | 1217:22.99 | | | 32 |
| 16 | 1217:36.69 | 1223:00.17 | | | 26 |
| LUKE AFB | 2307-11 | | 11/29/82 | F-5/L | GIMBORYS |
| 17 | 1214:11.79 | 1217:15.79 | | | 30 |
| LUKE AFB | 2307-4 | | 11/03/82 | F-5/L | PHILLIPS |
| 18 | 0843:21.09 | 0846:18.09 | | | 43 |
| LUKE AFB | 2307-4 | | 11/03/82 | F-5/L | EDWARDS |
| 19 | 0843:23.49 | 0844:24.89 | | | 32 |
| 20 | 0844:39.59 | 0844:49.29 | | | 4 |
| 21 | 0845:30.69 | 0845:53.69 | | | 7 |
| LUKE AFB | 2307-4 | | 11/03/82 | F-5/L | KALLMAN |
| 22 | 0843:01.09 | 0843:12.89 | | | 7 |
| 23 | 0843:17.39 | 0846:50.99 | | | 41 |
| LUKE AFB | 2307-4 | | 11/03/82 | F-5/L | SEVOY |
| 24 | 0843:01.09 | 0843:13.69 | | | 8 |
| 25 | 0843:17.39 | 0848:52.59 | | | 62 |
| LUKE AFB | 2307-20 | | 12/01/82 | F-5/L | PELOQUIN |
| 26 | 1627:29.39 | 1636:25.13 | | | 25 |
| LUKE AFB | 2307-20 | | 12/01/82 | F-5/L | GIMBORYS |

| | | | | | | |
|----------|------------|------------|---|----------|-------|---------|
| 27 | 1627:12.79 | 1627:29.39 | 4 | | | |
| 28 | 1629:35.49 | 1629:55.59 | 7 | | | |
| LUKE AFB | | 2307-20 | | | | |
| 29 | 1647:32.33 | 1647:39.33 | 4 | 12/01/82 | F-5/L | JACKSON |
| LUKE AFB | | 2307-20 | | | | |
| 30 | 1647:32.33 | 1647:39.33 | 4 | 12/01/82 | F-5/L | RICKMAN |

| | | | | | | | | | | | | | | | | | | | | | | | | | | | | | |
|--------------------|----|----|----|----|----|----|----|----|----|--------------------------------|-----|-----|----|----|----|----|----|----|----|----------------------|----|----|----|----|----|----|----|----|---|
| X-COORD | | | | | | | | | | LOWER BOUND CELL 2 = -132000.0 | | | | | | | | | | CELL SIZE = 5280.000 | | | | | | | | | |
| 0 | 0 | 0 | 0 | 0 | 0 | 0 | 0 | 0 | 0 | 0 | 0 | 0 | 0 | 0 | 0 | 0 | 0 | 0 | 0 | 2 | 11 | 31 | 24 | 37 | 21 | 27 | 21 | 0 | 0 |
| 32 | 5 | 3 | 13 | 17 | 3 | 0 | 0 | 0 | 0 | 5 | 18 | 16 | 24 | 5 | 1 | 0 | 0 | 0 | 0 | 1 | 0 | 0 | 0 | 0 | 0 | 0 | 0 | 0 | 0 |
| 0 | 0 | 0 | 0 | 0 | 0 | 0 | 0 | 0 | 0 | 0 | 0 | 0 | 0 | 0 | 0 | 0 | 0 | 0 | 0 | 0 | 0 | 0 | 0 | 0 | 0 | 0 | 0 | 0 | 0 |
| Y-COORD | | | | | | | | | | LOWER BOUND CELL 2 = -132000.0 | | | | | | | | | | CELL SIZE = 5280.000 | | | | | | | | | |
| 0 | 0 | 0 | 0 | 0 | 0 | 0 | 0 | 0 | 0 | 0 | 0 | 0 | 0 | 0 | 0 | 0 | 0 | 0 | 0 | 0 | 0 | 0 | 0 | 0 | 0 | 0 | 0 | 0 | 0 |
| 6 | 13 | 12 | 8 | 2 | 4 | 1 | 17 | 18 | 13 | 17 | 13 | 17 | 17 | 31 | 23 | 17 | 36 | 45 | 12 | 6 | 2 | 5 | 6 | 2 | 0 | 0 | 0 | 0 | 0 |
| 0 | 0 | 0 | 0 | 0 | 0 | 0 | 0 | 0 | 0 | 0 | 0 | 0 | 0 | 0 | 0 | 0 | 0 | 0 | 0 | 0 | 0 | 0 | 0 | 0 | 0 | 0 | 0 | 0 | 0 |
| Z-COORD | | | | | | | | | | LOWER BOUND CELL 2 = 1000.0 | | | | | | | | | | CELL SIZE = 1000.000 | | | | | | | | | |
| 0 | 0 | 0 | 0 | 0 | 0 | 0 | 0 | 0 | 0 | 0 | 1 | 25 | 35 | 48 | 19 | 0 | 0 | 0 | 0 | 14 | 15 | 24 | 24 | 45 | 57 | 33 | 14 | 3 | 0 |
| 2 | 3 | 4 | 3 | 0 | 0 | 0 | 0 | 0 | 0 | 0 | 0 | 0 | 0 | 0 | 0 | 0 | 0 | 0 | 0 | 0 | 0 | 0 | 0 | 0 | 0 | 0 | 0 | 0 | |
| 0 | 0 | 0 | 0 | 0 | 0 | 0 | 0 | 0 | 0 | 0 | 0 | 0 | 0 | 0 | 0 | 0 | 0 | 0 | 0 | 0 | 0 | 0 | 0 | 0 | 0 | 0 | 0 | 0 | |
| EFFECTIVE HEIGHT | | | | | | | | | | LOWER BOUND CELL 2 = 0.0 | | | | | | | | | | CELL SIZE = 1000.000 | | | | | | | | | |
| 0 | 0 | 0 | 0 | 0 | 0 | 0 | 0 | 0 | 0 | 0 | 30 | 60 | 35 | 33 | 9 | 56 | 0 | 0 | 26 | 33 | 25 | 28 | 2 | 14 | 13 | 1 | 2 | 0 | |
| 0 | 0 | 0 | 0 | 0 | 0 | 0 | 0 | 0 | 0 | 0 | 0 | 0 | 0 | 0 | 0 | 0 | 0 | 0 | 0 | 0 | 0 | 0 | 0 | 0 | 0 | 0 | 0 | 0 | |
| 0 | 0 | 0 | 0 | 0 | 0 | 0 | 0 | 0 | 0 | 0 | 0 | 0 | 0 | 0 | 0 | 0 | 0 | 0 | 0 | 0 | 0 | 0 | 0 | 0 | 0 | 0 | 0 | 0 | |
| MACH NO. | | | | | | | | | | LOWER BOUND CELL 2 = 1.0 | | | | | | | | | | CELL SIZE = .020 | | | | | | | | | |
| 0 | 0 | 0 | 0 | 0 | 0 | 0 | 0 | 0 | 0 | 0 | 134 | 176 | 10 | 1 | 0 | 0 | 0 | 0 | 0 | 0 | 0 | 0 | 0 | 0 | 0 | 0 | 0 | 0 | |
| 0 | 0 | 0 | 0 | 0 | 0 | 0 | 0 | 0 | 0 | 0 | 0 | 0 | 0 | 0 | 0 | 0 | 0 | 0 | 0 | 0 | 0 | 0 | 0 | 0 | 0 | 0 | 0 | 0 | |
| 0 | 0 | 0 | 0 | 0 | 0 | 0 | 0 | 0 | 0 | 0 | 0 | 0 | 0 | 0 | 0 | 0 | 0 | 0 | 0 | 0 | 0 | 0 | 0 | 0 | 0 | 0 | 0 | 0 | |
| CUTOFF MACH NO. | | | | | | | | | | LOWER BOUND CELL 2 = 1.0 | | | | | | | | | | CELL SIZE = .020 | | | | | | | | | |
| 0 | 0 | 0 | 0 | 0 | 0 | 0 | 0 | 0 | 0 | 0 | 166 | 14 | 0 | 0 | 0 | 0 | 0 | 0 | 0 | 0 | 0 | 0 | 0 | 0 | 0 | 0 | 0 | 0 | |
| 0 | 0 | 0 | 0 | 0 | 0 | 0 | 0 | 0 | 0 | 0 | 0 | 0 | 0 | 0 | 0 | 0 | 0 | 0 | 0 | 0 | 0 | 0 | 0 | 0 | 0 | 0 | 0 | 0 | |
| 0 | 0 | 0 | 0 | 0 | 0 | 0 | 0 | 0 | 0 | 0 | 0 | 0 | 0 | 0 | 0 | 0 | 0 | 0 | 0 | 0 | 0 | 0 | 0 | 0 | 0 | 0 | 0 | 0 | |
| EFFECTIVE MACH NO. | | | | | | | | | | LOWER BOUND CELL 2 = 1.0 | | | | | | | | | | CELL SIZE = .020 | | | | | | | | | |
| 0 | 0 | 0 | 0 | 0 | 0 | 0 | 0 | 0 | 0 | 0 | 33 | 60 | 42 | 32 | 31 | 27 | 19 | 10 | 8 | 7 | 11 | 4 | 0 | 0 | 0 | 0 | 0 | 0 | |
| 7 | 7 | 4 | 1 | 0 | 0 | 0 | 0 | 0 | 0 | 0 | 0 | 0 | 0 | 0 | 0 | 0 | 0 | 1 | 0 | 0 | 1 | 1 | 1 | 0 | 0 | 0 | 1 | 1 | |
| 1 | 1 | 0 | 1 | 0 | 0 | 0 | 0 | 0 | 0 | 0 | 0 | 0 | 0 | 0 | 0 | 0 | 0 | 0 | 0 | 0 | 0 | 0 | 0 | 0 | 0 | 0 | 0 | 0 | |
| OVERPRESSURE (PSI) | | | | | | | | | | LOWER BOUND CELL 2 = 0.0 | | | | | | | | | | CELL SIZE = .250 | | | | | | | | | |
| 0 | 0 | 0 | 0 | 0 | 0 | 0 | 0 | 0 | 0 | 0 | 0 | 0 | 0 | 0 | 0 | 0 | 0 | 0 | 39 | 40 | 19 | 17 | 2 | 6 | 2 | 5 | 29 | 0 | |
| 14 | 17 | 22 | 9 | 10 | 9 | 19 | 6 | 4 | 0 | 2 | 0 | 0 | 0 | 0 | 0 | 0 | 0 | 0 | 0 | 0 | 0 | 0 | 0 | 0 | 0 | 0 | 0 | 0 | |
| 0 | 0 | 0 | 0 | 0 | 0 | 0 | 0 | 0 | 0 | 0 | 0 | 0 | 0 | 0 | 0 | 0 | 0 | 0 | 0 | 0 | 0 | 0 | 0 | 0 | 0 | 0 | 0 | 0 | |
| PEAK LEVEL | | | | | | | | | | LOWER BOUND CELL 2 = 115.0 | | | | | | | | | | CELL SIZE = .500 | | | | | | | | | |
| 0 | 0 | 0 | 0 | 0 | 0 | 0 | 0 | 0 | 0 | 0 | 0 | 0 | 0 | 0 | 0 | 0 | 0 | 0 | 0 | 0 | 0 | 0 | 0 | 0 | 0 | 0 | 0 | 0 | |
| 0 | 0 | 0 | 0 | 0 | 0 | 0 | 0 | 0 | 0 | 0 | 0 | 0 | 0 | 0 | 0 | 0 | 0 | 2 | 0 | 0 | 4 | 0 | 2 | 18 | 7 | 13 | 0 | 0 | |
| 17 | 32 | 30 | 16 | 33 | 13 | 14 | 12 | 2 | 0 | 6 | 2 | 4 | 11 | 32 | 18 | 25 | 11 | 14 | 22 | 7 | 11 | 14 | 22 | 7 | 2 | 0 | 0 | 0 | |
| 2 | 0 | 0 | 0 | 0 | 0 | 0 | 0 | 0 | 0 | 0 | 0 | 0 | 0 | 0 | 0 | 0 | 0 | 0 | 0 | 0 | 0 | 0 | 0 | 0 | 0 | 0 | 0 | 0 | |
| C-LEVEL | | | | | | | | | | LOWER BOUND CELL 2 = 90.0 | | | | | | | | | | CELL SIZE = .500 | | | | | | | | | |
| 0 | 0 | 0 | 0 | 0 | 0 | 0 | 0 | 0 | 0 | 0 | 0 | 0 | 0 | 0 | 0 | 0 | 0 | 0 | 0 | 0 | 0 | 0 | 0 | 0 | 0 | 0 | 0 | 0 | |
| 0 | 0 | 0 | 0 | 0 | 0 | 0 | 0 | 0 | 0 | 0 | 0 | 0 | 0 | 0 | 0 | 0 | 0 | 2 | 0 | 4 | 0 | 2 | 18 | 7 | 13 | 32 | 0 | 0 | |
| 30 | 16 | 33 | 13 | 14 | 12 | 2 | 6 | 2 | 0 | 4 | 11 | 32 | 18 | 25 | 11 | 14 | 22 | 7 | 2 | 0 | 0 | 0 | 0 | 0 | 0 | 0 | 0 | 0 | |
| 0 | 0 | 0 | 0 | 0 | 0 | 0 | 0 | 0 | 0 | 0 | 0 | 0 | 0 | 0 | 0 | 0 | 0 | 0 | 0 | 0 | 0 | 0 | 0 | 0 | 0 | 0 | 0 | 0 | |
| A-LEVEL | | | | | | | | | | LOWER BOUND CELL 2 = 80.0 | | | | | | | | | | CELL SIZE = .500 | | | | | | | | | |
| 0 | 0 | 0 | 0 | 0 | 0 | 0 | 0 | 0 | 0 | 0 | 0 | 0 | 0 | 0 | 0 | 0 | 0 | 0 | 0 | 0 | 0 | 0 | 0 | 0 | 0 | 0 | 0 | 0 | |
| 0 | 0 | 0 | 0 | 0 | 0 | 0 | 0 | 0 | 0 | 0 | 0 | 0 | 0 | 0 | 0 | 0 | 0 | 2 | 0 | 0 | 0 | 0 | 0 | 5 | 16 | 4 | 4 | 13 | |
| 14 | 23 | 23 | 17 | 14 | 18 | 20 | 10 | 9 | 0 | 9 | 9 | 1 | 3 | 4 | 1 | 3 | 8 | 29 | 8 | 13 | 0 | 0 | 0 | 0 | 0 | 0 | 0 | 0 | |
| 22 | 11 | 11 | 6 | 20 | 7 | 5 | 1 | 0 | 0 | 0 | 0 | 0 | 0 | 0 | 0 | 0 | 0 | 0 | 0 | 0 | 0 | 0 | 0 | 0 | 0 | 0 | 0 | 0 | |

TIME GREATER THAN MACH 1.0 (1SEC) = 1203 TIME GREATER THAN CUTOFF MACH NO (SEC) = 369

LUKE AFB 2307-11
1 1222:59.17 1223:03.17 *

11/29/82 F-14/L DEGRAY

LUKE AFB 2307-20
2 1629:30.19 1629:34.19 *
3 1630:03.89 1630:47.99 *

12/01/82 F-14/L STUFFLEBEE

LUKE AFB 2307-20
4 1630:15.09 1630:47.99 *

12/01/82 F-14/L LEE

| | | | | | |
|----------|------------|------------|----------|---------|------------|
| LUKE AFB | 2235-17 | | 08/23/82 | F-15/LO | CARSON |
| 1 | 1553:37.85 | 1553:45.25 | | | 6 |
| LUKE AFB | 2201-1 | | 08/16/82 | F-15/RO | GRANLAUND |
| 2 | 1007:35.01 | 1007:51.91 | | | 7 |
| LUKE AFB | 2235-11 | | 08/23/82 | F-15/RO | THOMPSON |
| 3 | 1245:27.43 | 1247:01.63 | | | 11 |
| 4 | 1247:56.43 | 1249:54.03 | | | 16 |
| LUKE AFB | 2229-13 | | 08/17/82 | F-15/LO | CORSON |
| 5 | 1310:38.27 | 1312:15.27 | | | 21 |
| 6 | 1313:01.97 | 1313:08.17 | | | 4 |
| 7 | 1316:46.57 | 1317:07.37 | | | 5 |
| 8 | 1319:21.07 | 1321:35.77 | | | 34 |
| 9 | 1322:40.37 | 1323:03.07 | | | 5 |
| 10 | 1323:52.67 | 1324:32.67 | | | 12 |
| LUKE AFB | 2235-17 | | 08/23/82 | F-15/LO | WOOD |
| 11 | 1553:29.55 | 1553:33.55 | | | 5 |
| 12 | 1554:46.15 | 1556:17.45 | | | 9 |
| 13 | 1600:30.65 | 1600:46.95 | | | 5 |
| 14 | 1601:58.25 | 1602:30.05 | | | 6 |
| LUKE AFB | 2236-11 | | 08/24/82 | F-15/RO | HANDLEY |
| 15 | 1502:18.85 | 1503:04.55 | | | 4 |
| 16 | 1504:13.25 | 1504:56.75 | | | 6 |
| LUKE AFB | 2235-11 | | 08/23/82 | F-15/RO | ONEAL |
| 17 | 1245:43.33 | 1246:51.83 | | | 9 |
| 18 | 1248:21.83 | 1249:28.53 | | | 13 |
| LUKE AFB | 2229-13 | | 08/17/82 | F-15/LO | SMITH |
| 19 | 1317:24.87 | 1317:26.87 | | | 3 |
| 20 | 1318:55.27 | 1321:39.77 | | | 41 |
| LUKE AFB | 2237-17 | | 09/05/82 | F-15/LI | SITTON |
| 21 | 1557:13.67 | 1557:48.37 | | | 5 |
| LUKE AFB | 2228-17 | | 08/16/82 | F-15/LO | BRISON |
| 22 | 1543:49.35 | 1545:03.95 | | | 7 |
| 23 | 1546:23.55 | 1546:37.85 | | | 3 |
| LUKE AFB | 2235-17 | | 08/23/82 | F-15/RO | THOMPSON |
| 24 | 1554:10.05 | 1555:00.05 | | | 10 |
| 25 | 1600:21.85 | 1601:48.75 | | | 29 |
| 26 | 1602:04.65 | 1602:11.65 | | | 3 |
| 27 | 1610:14.75 | 1610:51.25 | | | 6 |
| LUKE AFB | 2237-17 | | 09/05/82 | F-15/RO | KACENA |
| 28 | 1555:33.17 | 1555:41.07 | | | 4 |
| LUKE AFB | 2235-17 | | 08/23/82 | F-15/RO | CANTABERRY |
| 29 | 1554:01.05 | 1554:47.95 | | | 13 |
| 30 | 1600:02.05 | 1601:52.15 | | | 26 |
| 31 | 1609:46.35 | 1611:21.55 | | | 11 |
| LUKE AFB | 2237-17 | | 09/05/82 | F-15/LO | NAMKE |
| 32 | 1538:05.37 | 1538:38.97 | | | 4 |
| 33 | 1557:38.77 | 1557:41.77 | | | 5 |

| | | | | |
|----------|-----------------------|----------|---------|-----------|
| LUKE AFB | 2231-20 | 08/19/82 | F-15/RO | NICHOLL |
| 34 | 1648:52.51 1649:12.91 | 5 | | |
| LUKE AFB | 2228-14 | 08/16/82 | F-15/LO | HALE |
| 35 | 1357:20.75 1357:42.65 | 5 | | |
| 36 | 1401:31.55 1401:36.15 | 4 | | |
| LUKE AFB | 2231-14 | 08/19/82 | F-15/LO | HOURON |
| 37 | 1350:53.83 1351:20.93 | 9 | | |
| 38 | 1358:56.03 1359:19.63 | 4 | | |
| LUKE AFB | 2228-13 | 08/22/82 | F-15/RO | CAMPBELL |
| 39 | 1313:45.57 1314:03.97 | 6 | | |
| 40 | 1314:42.47 1314:56.17 | 5 | | |
| 41 | 1320:03.97 1321:26.77 | 9 | | |
| 42 | 1321:43.17 1321:54.57 | 3 | | |
| LUKE AFB | 2231-20 | 08/19/82 | F-15/LO | POPE |
| 43 | 1641:34.21 1641:54.01 | 4 | | |
| LUKE AFB | 2228-14 | 08/16/82 | F-15/LO | GEESAMAN |
| 44 | 1356:11.85 1357:32.15 | 8 | | |
| LUKE AFB | 2231-14 | 08/19/82 | F-15/RO | LEVERSON |
| 45 | 1351:08.33 1351:18.93 | 6 | | |
| 46 | 1400:00.33 1400:29.03 | 6 | | |
| LUKE AFB | 2228-13 | 08/22/82 | F-15/RO | LITTLE |
| 47 | 1313:21.77 1315:03.27 | 12 | | |
| 48 | 1320:15.67 1321:14.07 | 6 | | |
| LUKE AFB | 2231-9 | 08/19/82 | F-15/RI | MCKEEFIN |
| 49 | 1131:04.07 1131:43.07 | 6 | | |
| 50 | 1139:41.47 1139:53.97 | 4 | | |
| LUKE AFB | 2323-3 | 10/18/73 | F-15/RO | ROLLINS |
| 51 | 0815:11.59 0815:31.19 | 3 | | |
| 52 | 0816:00.69 0816:30.89 | 6 | | |
| 53 | 0825:57.29 0827:01.29 | 19 | | |
| 54 | 0829:15.99 0829:33.89 | 7 | | |
| 55 | 0829:56.49 0830:21.49 | 17 | | |
| 56 | 0831:20.09 0831:29.89 | 6 | | |
| LUKE AFB | 2323-3 | 10/18/73 | F-15/RO | MARKLAND |
| 57 | 0817:56.59 0818:03.09 | 5 | | |
| 58 | 0826:36.29 0827:06.09 | 13 | | |
| 59 | 0828:42.09 0829:15.99 | 8 | | |
| 60 | 0829:52.39 0830:21.49 | 19 | | |
| LUKE AFB | 2322-12 | 11/18/82 | F-15/LO | MATTINGLY |
| 61 | 1245:59.17 1246:14.37 | 5 | | |
| 62 | 1247:53.57 1249:11.27 | 6 | | |
| 63 | 1250:02.27 1250:22.97 | 16 | | |
| 64 | 1252:53.17 1253:32.27 | 4 | | |
| 65 | 1253:34.87 1254:52.37 | 19 | | |
| 66 | 1255:11.17 1255:26.87 | 13 | | |
| 67 | 1257:08.67 1257:13.97 | 3 | | |
| 68 | 1259:17.87 1259:30.67 | 9 | | |
| 69 | 1259:49.37 1300:04.27 | 7 | | |
| LUKE AFB | 2324-17 | 11/20/82 | F-15/LI | LORRAINE |
| 70 | 1531:13.03 1531:44.63 | 4 | | |
| 71 | 1531:50.43 1532:42.93 | 11 | | |

| | | | | |
|----------|------------|------------|---------|-----------|
| LUKE AFB | 2324-4 | 11/20/82 | F-15/LO | HEIMAN |
| 72 | 0843:28.67 | 0844:14.97 | 7 | |
| 73 | 0845:44.87 | 0846:17.67 | 9 | |
| 74 | 0846:44.37 | 0847:04.07 | 5 | |
| 75 | 0847:34.67 | 0848:18.47 | 8 | |
| 76 | 0850:46.07 | 0851:04.67 | 4 | |
| 77 | 0901:04.67 | 0901:10.97 | 5 | |
| 78 | 0901:13.37 | 0901:25.67 | 4 | |
| 79 | 0901:27.87 | 0901:48.07 | 6 | |
| 80 | 0902:12.57 | 0902:33.77 | 8 | |
| LUKE AFB | 2323-4 | 11/19/82 | F-15/LO | MCALISTER |
| 81 | 0904:22.31 | 0905:11.91 | 10 | |
| 82 | 0906:50.81 | 0907:03.21 | 5 | |
| LUKE AFB | 2307-20 | 12/01/82 | F-15/RI | WILLENS |
| 83 | 1647:04.13 | 1647:18.73 | 7 | |
| 84 | 1647:21.83 | 1647:32.33 | 7 | |
| 85 | 1647:36.33 | 1647:39.33 | 3 | |
| LUKE AFB | 2324-17 | 11/20/82 | F-15/LO | PECK |
| 86 | 1525:00.13 | 1525:21.73 | 5 | |
| 87 | 1530:58.83 | 1532:28.83 | 12 | |
| LUKE AFB | 2323-4 | 11/19/82 | F-15/RO | MATTINGLY |
| 88 | 0856:55.37 | 0857:51.97 | 8 | |
| 89 | 0858:17.37 | 0858:59.57 | 5 | |
| 90 | 0903:32.31 | 0903:39.81 | 6 | |
| 91 | 0903:51.91 | 0904:25.01 | 13 | |
| 92 | 0908:51.61 | 0909:29.11 | 11 | |
| 93 | 0910:14.31 | 0910:17.51 | 3 | |
| LUKE AFB | 2307-20 | 12/01/82 | F-15/RO | BURGE |
| 94 | 1641:49.03 | 1642:14.63 | 5 | |
| 95 | 1647:18.73 | 1647:39.33 | 10 | |
| LUKE AFB | 2324-17 | 11/20/82 | F-15/LO | MERCY |
| 96 | 1511:32.53 | 1511:45.03 | 5 | |
| 97 | 1525:21.73 | 1525:54.93 | 6 | |
| 98 | 1532:42.93 | 1533:00.03 | 6 | |
| 99 | 1539:37.73 | 1539:48.13 | 7 | |
| LUKE AFB | 2324-4 | 11/20/82 | F-15/LO | CURRY |
| 100 | 0845:44.87 | 0845:55.57 | 6 | |
| 101 | 0847:34.67 | 0847:57.87 | 6 | |
| 102 | 0848:18.47 | 0850:38.47 | 5 | |
| 103 | 0850:40.87 | 0852:24.47 | 8 | |
| 104 | 0901:48.07 | 0902:28.67 | 7 | |
| LUKE AFB | 2324-17 | 11/20/82 | F-15/LO | BEECHUM |
| 105 | 1539:32.73 | 1539:42.03 | 7 | |
| LUKE AFB | 2322-3 | 11/18/82 | F-15/LO | TKACS |
| 106 | 0817:33.43 | 0817:44.83 | 6 | |
| 107 | 0824:26.13 | 0824:31.43 | 4 | |
| 108 | 0824:41.83 | 0824:45.53 | 4 | |
| 109 | 0826:30.83 | 0826:41.93 | 4 | |
| 110 | 0827:58.53 | 0828:10.13 | 3 | |
| LUKE AFB | 2324-12 | 11/20/82 | F-15/RI | HART |
| 111 | 1247:26.71 | 1247:42.11 | 5 | |
| 112 | 1247:53.21 | 1247:56.01 | 3 | |
| 113 | 1248:02.11 | 1248:10.21 | 6 | |

| | | | |
|-----|------------|------------|----|
| 114 | 1248:46.01 | 1248:57.11 | 4 |
| 115 | 1249:10.31 | 1250:41.61 | 7 |
| 116 | 1250:52.51 | 1252:24.71 | 25 |
| 117 | 1252:41.11 | 1253:23.61 | 18 |
| 118 | 1253:59.71 | 1254:03.71 | 3 |
| 119 | 1301:29.91 | 1302:09.41 | 10 |

| | | | |
|----------|------------|------------|----|
| LUKE AFB | | 2322-3 | |
| 120 | 0815:30.33 | 0817:14.03 | 26 |
| 121 | 0817:44.43 | 0817:54.03 | 5 |
| 122 | 0820:30.03 | 0820:42.93 | 5 |
| 123 | 0821:12.63 | 0821:54.23 | 7 |
| 124 | 0824:21.53 | 0824:50.43 | 13 |
| 125 | 0825:43.33 | 0825:54.83 | 7 |
| 126 | 0826:27.53 | 0826:32.03 | 4 |

11/18/82 F-15/RO MULLHARE

| | | | |
|----------|------------|------------|----|
| LUKE AFB | | 2324-12 | |
| 127 | 1251:29.31 | 1252:01.11 | 14 |
| 128 | 1253:09.91 | 1253:31.31 | 13 |
| 129 | 1254:03.71 | 1254:15.71 | 8 |
| 130 | 1256:26.71 | 1256:29.21 | 3 |
| 131 | 1257:25.61 | 1257:45.91 | 11 |
| 132 | 1258:23.91 | 1258:34.71 | 5 |

11/20/82 F-15/LO LOPRT

LUKE AFB 2228-21
1 1729:21.47 1729:33.87 5

08/16/82 F-16/R CAREY

LUKE AFB 2229-13
2 1309:26.87 1310:55.17 13
3 1317:17.87 1318:40.57 12
4 1319:37.17 1319:58.37 8
5 1320:30.17 1322:01.57 17
6 1322:47.87 1323:10.67 6
7 1323:47.17 1324:29.47 15

08/17/82 F-16/R CORRIGAN

LUKE AFB 2229-13
8 1309:55.27 1311:00.27 11
9 1311:38.77 1312:43.57 19
10 1313:40.97 1314:13.67 6
11 1316:21.07 1316:23.17 4
12 1318:15.37 1318:37.37 5
13 1319:28.27 1320:22.07 18
14 1321:16.07 1321:23.67 4
15 1324:09.07 1324:18.47 5

08/17/82 F-16/R CAREY

LUKE AFB 2231-20
16 1638:37.31 1640:18.21 27
17 1641:01.91 1641:20.41 4
18 1647:40.81 1648:54.61 12

08/19/82 F-16/R RAYBURN

LUKE AFB 2228-13
19 1318:57.87 1319:18.17 5
20 1321:43.17 1322:06.07 4
21 1327:59.17 1329:30.67 11

08/22/82 F-16/R ALLAIN

LUKE AFB 2231-20
22 1639:12.31 1640:02.91 17
23 1641:11.11 1641:54.01 3
24 1647:45.21 1648:21.91 8
25 1650:41.81 1651:44.31 9

08/19/82 F-16/L ALLAIN

| | | | | |
|------------|-----------------------|----------|---------|----------|
| NELLIS AFB | 2231-MG-1200 | 08/19/82 | F-16N/L | ALBIN |
| 1 | 1225:20.65 1225:23.85 | | | 3 |
| NELLIS AFB | 2230-MG-1100 | 08/18/82 | F-16N/L | PHILLIPS |
| 2 | 1102:42.08 1102:55.88 | | | 4 |
| 3 | 1112:18.39 1113:39.38 | | | 19 |
| 4 | 1119:46.69 1119:50.49 | | | 3 |
| NELLIS AFB | 2228-TD+E-1000-1 | 08/16/82 | F-16N/R | PHILLIPS |
| 5 | 1006:46.60 1007:00.51 | | | 4 |
| 6 | 1018:42.31 1019:03.80 | | | 5 |
| NELLIS AFB | 2237-MG-1100-1 | 08/25/82 | F-16N/L | PHILLIPS |
| 7 | 1119:33.25 1119:47.25 | | | 5 |
| NELLIS AFB | 2237-MG-1100-1 | 08/25/82 | F-16N/L | ALBIN |
| 8 | 1106:58.65 1107:26.04 | | | 6 |
| 9 | 1124:02.85 1124:17.55 | | | 6 |
| NELLIS AFB | 2221-TOVE-1130-1 | 08/09/82 | F-16/R | |
| 10 | 1135:30.89 1136:35.58 | | | 9 |
| 11 | 1142:59.99 1143:46.49 | | | 3 |

NELLIS AFB 2221-TDYE-1130-1 08/09/82 F-15/LI
1 1139:08.99 1140:19.09 16
2 1145:23.89 1146:15.89 9
3 1149:58.18 1149:58.18 2

NELLIS AFB 2221-TDYE-1130-1 08/09/82 F-15/LI
4 1137:22.18 1137:30.38 4
5 1138:09.99 1139:05.09 8
6 1139:33.48 1139:50.78 7
7 1149:35.18 1149:39.59 3
8 1150:33.19 1152:28.59 14

NELLIS AFB 2230-MG-1100 08/18/82 F-15/LI BROWN
9 1112:26.28 1113:15.48 11

| | | | | |
|------------|------------------|------------|--------|--------|
| NELLIS AFB | 2237-HG-1100-1 | 08/25/82 | F-4E/R | BARRY |
| 1 | 1106:26.55 | 1106:44.25 | 5 | |
| 2 | 1117:42.15 | 1118:37.05 | 4 | |
| NELLIS AFB | 2228-TD+E-1000-1 | 08/16/82 | F-4E/R | BARRY |
| 3 | 1028:09.61 | 1028:26.51 | 6 | |
| 4 | 1032:41.41 | 1033:30.31 | 6 | |
| NELLIS AFB | 2237-HG-1100-1 | 08/25/82 | F-4E/R | WRIGHT |
| 5 | 1108:13.35 | 1108:18.05 | 3 | |
| 6 | 1123:55.25 | 1126:08.45 | 20 | |
| NELLIS AFB | 2231-HG-1200 | 08/19/82 | F-4E/R | WRIGHT |
| 7 | 1225:12.55 | 1225:28.25 | 6 | |
| 8 | 1226:30.65 | 1226:40.35 | 4 | |
| NELLIS AFB | 2228-TD+E-1000-1 | 08/16/82 | F-4E/R | WRIGHT |
| 9 | 1031:12.31 | 1033:10.51 | 14 | |
| NELLIS AFB | 2231-HG-1200 | 08/19/82 | F-4E/R | FRENCH |
| 10 | 1226:40.35 | 1227:05.15 | 4 | |

